University of Stavanger

Faculty of Science and Technology

Master's Thesis

Study program/ Specialization: Offshore Technology/ Subsea Technology	Spring semester, 2015 Open / ~~Confidential~~
Author: Michael Berhe Awotahegn	(Writer's signature)
Faculty supervisor: Dr. Ljiljana.D.Oosterkamp External supervisor : Per Nystrøm- IKM Ocean Design	
Title of thesis: Experimental investigation of accidental drops of drill pipes and containers during offshore operations.	
Credits (ECTS): 30	
Key words: Drop objects, trajectory, cylindrical objects, dynamics in water, free fall in water, model test.	Pages: 67 + Appendix /Others: 36

MASTER THESIS SPRING 2015
For

Master Student Michael Awotahegn

Experimental investigation of accidental drops of drill pipes and containers during offshore operations.

Figuren under viser hvordan drillpipe har landet på bunnen etter å ha blitt sluppet fra origo (småskala tester fra Aanesland OTC-5497, 1987 "Numerical and Experimental Investigation of Accidentally Falling Drilling Pipes"). Dette indikerer at største treff-sannsynlighet ikke ligger under dropp punktet men i sirkler rundt dropp-punktet og der dropp vinkel styrer hvor langt ut høyeste treff-sannsynlighet. DNV RP-F107 Risk Assessment of Pipeline Protection referer mye til Aanesland sitt arbeid fra 1986-1987.

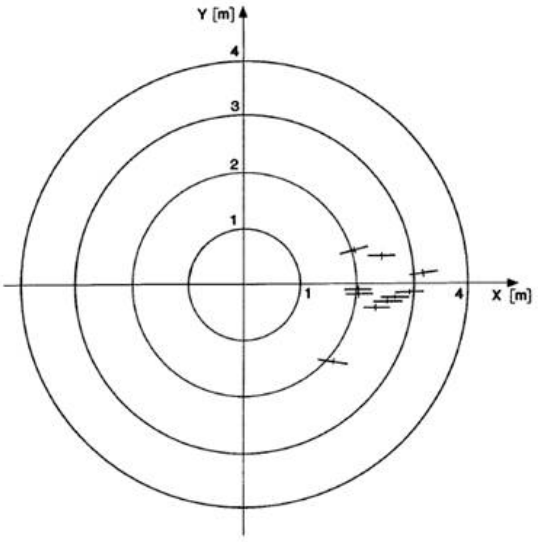

Fig. 3—Touchdowns on the bottom, α = 60°, h = 1.48 m and d = 2.46 m.

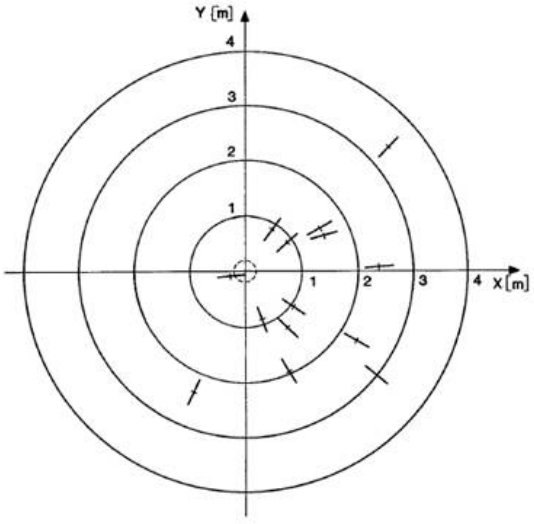

Fig. 4—Touchdowns on the bottom, α = 90°, h = 1.48 m, and d = 4.92 m.

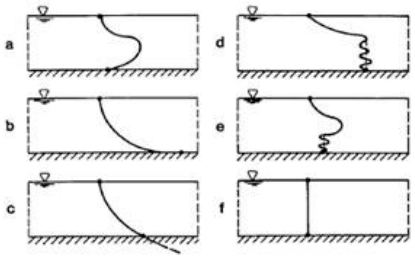

Fig. 5—Sketches of paths observed.

I praksis og iht regelverk så antas treff-sannsynligheten til å være størst rett under dropp-punktet -> gjengitt av normalfordelingen vist under.

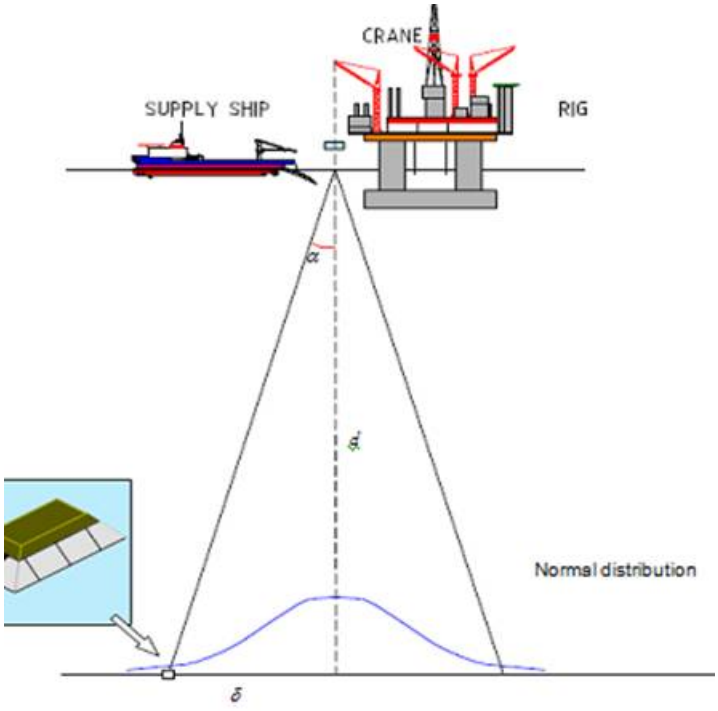

Object Excursion and Hit Probability

Hele Dropped Object metodikken i DNV virker uklar og konservativ (og i en del tilfeller kanskje ikke konservativ) og det virker som om det er behov for bedre forståelse av bakgrunnsdata, metodikk og optimaliserings

Basert på dette foreslår IKM Ocean Design en masteroppgave som involverer følgende elementer:

Litteraturstudie spesielt med å oversikt over metodikk i dagens DNV RP-F207, hva som er gjeldende praksis i IKM Ocean Design og andre brukere av RP, studere datagrunnlaget for gjeldende regelverk og metodikk:

DNV RP-F107 Risk Assessment of Pipeline Protection

SINTEF (1986), “Experimental and Numerical Investigation if Accidental Drops of Drilling Tubes”, Report no. 53-520075-01-86, V. Aanesland

Aanesland OTC-5497, 1987 ”Numerical and Experimental Investigation of Accidentally Falling Drilling Pipes”)

In-house rapporter I IKM Ocean Design

Offentlig tilgjengelige rapporter, artikler osv

Skala-tester i UiS sin nye tank (med basis i skala-tester utført av Aanesland i 1986)

Typer fallende gjenstand (drill pipe, container osv)

Størrelse på fallende gjenstand (lengde, diameter, vekt, vannfyllingsgrad for container osv)

Fallvinkel (0, 15, 30, 45, 60, 75, 90)

Vanndyp

Fallhøyde (dvs høyde over vannoverflaten)

Effekt av sideveis strøm? (dersom dette er mulig i test tank – men dette er ikke så viktig)

Sammenstilling av test-resultater, presentasjon osv

Vurdering av test-resultater opp mot eksisterende data og metodikk i DNV RP-F107

Komme med forslag til endring av nåværende formelverk, praksis osv for drillpipe

Komme med forslag til praksis for fall av container til sjøbunnen (inkludert se på statistikk for hvor mange av containere som faktisk blir vannfyllt og faller til bunn og avstand på disse fra drop-punkt osv)

Undersøke optimaliseringsmåter i metodikk:

Vurdere potensialet for å differensiere mellom forskjellige fallbane modeller (se figur med 6 fallbaner over)

ABSTRACT

The dynamic motion of falling pipes in water is treated theoretically using slender body theory at present time. This thesis focuses on the experimental investigation of accidentally falling drill pipes and to some extent containers in order to see the distribution on the sea bed and observe the trajectory for different drop angles.

The model test results are presented using tables and sea bed distribution contours. Although full scale results are included to have an insight, the discussion converges to the model scale mainly. A comparison between a simplified method and model scale results is outlined. Illustrative parametric study has been carried out to identify the significant parameters which affect the motion dynamics of the pipe under water. A case study has been conducted to show the difference of the test result with the present DNV methodology. Finally, based on the key findings of the experment conclusion has been drown and practical recommendation for further work is presented

ACKNOWLEDGEMENTS

Looking back to the first meeting we had at IKM office in Sandnes , were things are unclear and blurry , I was sure that doing the experment and getting some result requires an extra effort.

I would like to express my deep gratitude to my external adviser Per Nystrøm, from whom I learn a lot throughout the work. My professor at the university, Dr.Ljiljana.D.Oosterkamp for selecting me to work on the thesis and her guidance throughout the work – I say thanks to both of you.

I would like to tank IKM Ocean Design and the employee's for giving me an office access, financial support for the project, and for there continues motivation.

Very special thanks to John Grønli who made the experment possible. My appreciation goes to UiS subsea team for their support during the experment. To name few: Stefan Solberg, martin, and Haakon. My thanks go to the following persons and companies too:

Technip Norge for providing me subsea light system

A special thanks to Jarle håland from Technip Norge for his kind support.

Norwegian electronic supply As for there under water cameras

My friend Endeshaw for his support during the experment

Finally, my son Adam, from whom I get the aspiration and the courage to go forward, thanks a million.

CONTENTS

LIST OF FIGURES

LIST OF TABLES

ABBREVIATIONS

ASME: American society of mechanical engineers

ANSI : American national standard institute

DNV : Det Norske Veritas

DORIS : Dropped Objects Register of Incidents & Statistics

ISO : International organization for standardization


EXPERIMENTAL INVESTIGATION
OF
ACCIDENTALLY FALLING PIPES

Chapter 1 INTRODUCTION

1.1 BACKGROUND

The Oil and Gas sector is constantly evolving, and adapting into new environments involving deeper water depths. In recent years, deep water exploration and production activities have increased drastically, and new fields are discovered in deeper and deeper waters. As the water depth increases, marine operational challenges also increase leading to a higher safety standard request by regulators and operators to minimize the risk. Accident due to free falling objects occurs during offshore operation, some of them leading to high fatality to personnel or release of hydrocarbons which damage the environment. In order to cope with this challenges understanding the motion and dynamics of this objects is crucial to the standards we setting.

A dropped object is: '' any object, with the potential to cause death, injury or equipment / environmental damage, that falls from its previous static position under its own weight. Although the term is popular in many areas of operations, I use this term on my paper to specifically refer to marine operations. Dropped objects are regularly the principal causes of incidents in the oil and gas industry and contribute to the total risk level for offshore and onshore facilities.

With the increase of numerical tools, models, and a lot of applications, validation of this with an experment to update the procedures, planning, and execution is necessary. However, due to the complexity of fluid mechanics and parameters which govern the flow, application of model scale tests and numerical tools for deep water should be dealt with greater care.

1.2 SCOPE

Chapter 2 reviews the literature about drop objects according to type, frequency, and trajectory. In addition it gives an insight in to the theoretical treatment of the problem in predicting trajectories of falling drill pipes.

Chapter 3 describes how the experment is conducted and explain the basis of model testing.

Chapter 4 Describes method of extracting data and bases of analysis

Chapter 5 shows result from the experment

Chapter 6 discusses the results, by taking case study for 8'' and 12'' pipe.

Chapter 7 gives conclusion and recommendation.

Chapter 2 LITERATURE REVIEW

2.1 ACCIDENTALLY DROP OBJECTS

Drop object are defined as any object that fall under its own weight from a previously static position or fell due to an applied force from equipment or a moving object. Object that fall due to its own weight are called Static drop objects, where as object that falls due to an applied force called Dynamic drop object. The treatments of both cases are different.

Small objects such as scaffolding, cable trays and tools may be dropped often during offshore operation with small or no consequence at all. The consequence related to larger objects such as drill pipe, containers and even BOP is higher because of the impact energy involved in it. In order to avoid the risk, understanding the dynamics of a rigid body falling through the air, the splash zone, and through the water is useful. Shape, weight, and drop angle of the object are very important parameters as excursion on the sea bed is extremely dependant on these factors.

According to DORIS (*Dropped Objects Register of Incidents & Statistics*), Drop objects are among the top 10 causes of fatality and serious injury in oil and gas industry [1]. Tools and equipment falling during an operation on the deck are the main causes of incidents based on the statistics. Dropped objects during lifting or any other offshore operation to the sea are often the main interest to the oil and gas industry due to HSE and the associated risk related to it. A risk free zone is needed on the sea bed layout for lifting operation based on the possible hit points, hit frequency, and dynamics of the dropped objects.

Although the causes for dropped objects are many, here are the Top five:

- Inadequate securing
- Failed fixtures and fittings
- Poor house keeping
- Corrosion
- Operator error

Dropped objects in offshore operation generally can be categorized as based on the activity:

- Drilling operations
- Well service operations
- Lifting operations
- Maintenance operations

- Scaffolding
- Vessel operations
- Quayside operations
- Road transport
- Other operations

Dropping of larger objects such as pipes are significantly minimized by the safety procedure the industry follows and with the help of technology we have today. Nevertheless, understanding the dynamics and distribution on the sea bed is vital for offshore operation.

2.2 Drop Frequency

A registered drop frequency from the UK department of energy covering the period 1980—1986 is available for reference [2]. During this period, 81 incidents with dropped objects and 825 crane years are reported. The number of lifts in the period was estimated to be 3.7 million, which corresponds to 4.500 lifts to/from vessel per crane per year. This gives a dropped object probability of $2.2 \cdot 10^{-5}$ per lift. For lifts above 20 tonnes the drop probability has been estimated to $3.0 \cdot 10^{-5}$ per lift. The frequency is further split between fall onto deck (~70%) or into the sea (~30%). Lifts performed using the drilling derrick are assumed to fall only in the sea, and with a dropped loads frequency as for ordinary lifts with the platform cranes, i.e. $2.2 \cdot 10^{-5}$ per lift [2].

According to DNV detailed dropped object data are available for this period and no more recent data is available in sufficient detail to process. A database recording all the incidents is important to know failure rate, reliability, and risk. Unfortunately the industry is not transparent when it comes to exposing all the incidents occurred during operations, unless it hits the head line on major news papers. In order to assess the pipeline/umbilical risk from accidental loading, it is necessary to establish the frequency of such event [2].
The industry have made an improvement in collaborating to share and register incidents by founding a global work group represented by more than 100 operators, contactors, service companies and industry bodies . This is very useful depending on probity and commitment of this group for drop object prevention. The proposed dropped object frequency where the industry using is shown below.

Table 1 DNV Frequency table

Type of Lift	Frequency of dropped object in to the sea (Per lift)
Ordinary lift to/from supply vessel with platform crane < 20 tonnes	$1.2 \cdot 10^{-5}$
Heavy lift to/from supply vessel with the platform crane > 20 tonnes	$1.6 \cdot 10^{-5}$
Handling of load < 100 tonnes with the lifting system in the drilling derrick	$2.2 \cdot 10^{-5}$
Handling of BOP/load > 100 tonnes with the lifting system in the drilling derrick	$1.5 \cdot 10^{-3}$

An interesting finding by DORIS, is that environmental condition play little role on the drop frequency, however no sufficient data is available to concrete this statement [1].

2.3 TRAJECTORY OF DROP DRILL PIPES

Understanding the dynamics of a three dimensional rigid body in water is practical importance for marine engineering. There are a number of suggestions how to treat a falling drill pipe theoretically. However, this paper doesn't cover the numerical approach and the detail is not included.

Some experiments have been performed both in full scale and in model scale to compare and contrast the results with theoretical approach. Some in house programs which are not commercial to use have been developed by some companies promising to predict the maximum velocity, momentum, impact energy, and drop distribution of a falling object in deep water. However, the complexity of choosing drag and friction coefficients in different flow regime, the influence of tail effects, vortex shading, and pressure distribution made it difficult for application in deep water.

Hence, more experment and data needed in order to develop a more accurate numerical simulation for deep water application. So far, the dynamic motion of a free falling drill pipes in water is treated numerically by using slender body theory with some limitation. Model scale experment and observation is needed to understand the dynamics which support the numerical computation by the proposed theory.

Ånsland in his published report ''experimental and numerical investigations of accidental falling drilling tubes'' has adopted Newman's ship maneuvering equations corrected by viscous effects for his numerical computation [3, 4]. On his model test, he has used two different water depths, corresponding to 50m and 100m in full scale. His experment has reveled different paths followed by the cylinder (pipe) as shown in Fig 1. In addition he has documented distribution of the dropped pipes on the sea bed.

DNV and many other papers refer to this particular experment for calculation of drop object hit probability.

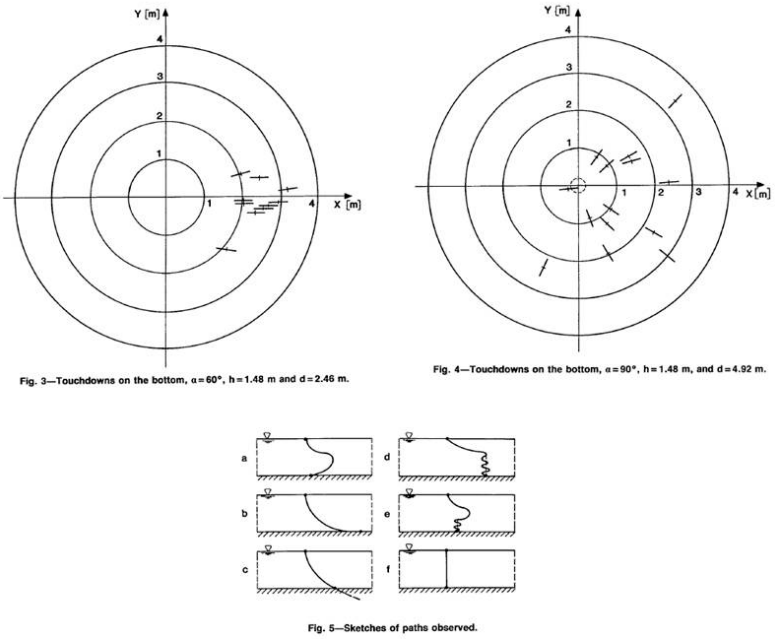

Figur 1 Observed path and seabed distributions of drill pipes

2.4 METHOD OF MOTION PROJECTION

For an object dropped from a certain height above the water surface, there are three phases of the falling motion.

(a) Falling in air

(b) Transient phase where part of the body is submerged in water

(c) Fully submerged in water

2.4.1 FREE FALL IN THE AIR

The subject of object falling in the air is well understood and particularly easy to find the velocity with or without air resistance.

Variables: time t, velocity v

Newton's 2nd Law: F = m.a = $m\left(\frac{dv}{dt}\right)$ ←net force

Force of gravity: F = m.g ←downward force

Force of air resistance: F = γv ←upward force, γ- coefficient of air friction

$m\left(\frac{dv}{dt}\right)$= mg- γv ,

Ignoring air resistance however,

$\left(\frac{dv}{dt}\right)$ = g → the velocity at impact of water → V = √2gh

h- Height of fall, g – acceleration due to gravity

2.4.2 IMPACT WITH THE WATER SURFACE

The water entry of falling objects is a very complicated phenomenon involving four separate phases. The shake phase, the flow forming phase, the open cavity phase, and the closed cavity phase. And it's beyond the scope of this paper to go to details.

2.4.3 FREE FALL IN WATER

A slender object falling through water is subjected to the following:

- A down ward gravitational force
- An upward jet force due to change in momentum of the water relative to the falling object. This force is proportional to the projected area.
- An upward frictional force due to the flow of water over the surface of the object. This force is related to the surface area, Reynolds number, and relative surface roughness.
- An upward buoyancy force equal to the weight of the displaced water [5].

The velocity of the dropped object is found by numerical integration of the equation of motion. The terminal velocity is given by expression:

$(V_T)^2 = 2.\left(\frac{(m-\rho I).g}{Cd.A.\rho}\right)$

ρ- Density of water

I – Immersed volume body

A- Frontal area

C_D – Drag coefficient

Terminal velocity is the velocity at which upward forces equals down ward forces, the objects stops accelerating and moves with constant speed v. When the net force = zero → $m\left(\frac{dv}{dt}\right)$ = 0, the gravitational force matches the force of buoyancy.

2.5 MOTION DYNAMICS OF A 3D BODY FALLING THROUGH WATER

For marine engineers it is vital to understand the dynamics of free falling of three-dimensional objects through water. The motion is dependent on several conditions like body geometry, potential flow effects, environmental conditions etc. Hence predicting accurate trajectory is a great deal of challenge for engineers.

A direct numerical scheme can be developed for a time-domain analysis of six degree of freedom of motion for three-dimensional bodies dropping in water. Building a mathematical model depend upon the objectives for studying a particular problem [6].

For a freely falling object in water, distance covered, time travel, trajectory, buoyancy force, drag ,shape of the object, and weight of the object are the most important parameters to be considered. In addition, initial body orientation, body aspect ratio and mass distribution are the key parameters for the characteristics of the body motion [7].

2.5.1 COORDINATE SYSTEM

Two coordinate systems can be selected to define the motion trajectory

- A fixed global system with its origin set at the center of gravity of the object at the instant of drop.
- A moving local system with its origin at the moving center of gravity of the dropped object. It also rotates with the object.

2.5.2 BASIC ASSUMPTIONS AND DEFINITIONS

A slender cylinder in this discussion implies to a body diameter is small relative to the length. The cylinder diameter, D, should be much less than the length, $\frac{D}{\lambda} << 1$

- Rigid body
- calm water
- uniform mass distributed body
- The in plane motion of the dropped object has three degrees of freedom.(Two translational, and one rotational)

For most dropped objects, the aerodynamic effect is relatively small and the falling trajectory is dominated by the gravity force. So this section focuses on absolute submergence phase.

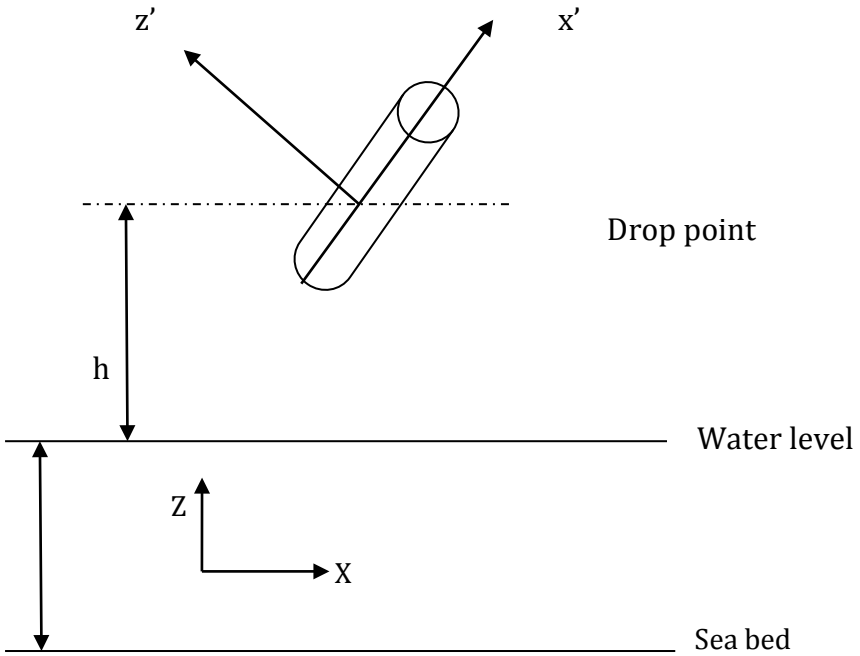

Figur 2 Coordinate systems

Generally speaking, flow field in space and time is expressed by several physical parameters such as velocity of fluid particles, pressure, density, and temperature, which are functions of space and time. These physical parameters are derived from mass conservation law, momentum conservation law, energy conservation law, and equations of state.
As to the dynamics, the density and temperature can be assumed as constant in space and time. Therefore, what we need to know is the velocity field and pressure field in the fluid domain. The fundamental equations can be derived from mass conservation law and momentum conservation law, which are represented by equations of motion of fluid.

2.5.3 Drag Forces and Moments

Drag loads are the hydrodynamic loads that are proportional to the square of fluid velocity relative to the cylinder. The drag forces are calculated on the cylinder using the "cross flow" assumption. That is, the relative velocity of the sea past the cylinder is split into its normal and axial components and these components are used, together with the specified drag areas and coefficients, to calculate the normal and axial components of the drag force.

The drag forces are specified by giving separate drag area and drag coefficient values for flow in the normal direction (local x and y directions) and in the axial direction (local z direction). The Drag Area is a reference area that is multiplied by the drag coefficient in the drag force formula. The drag moments are specified and calculated in a similar way

to the drag forces, except that the reference drag area is replaced by a reference area moment.

There are two alternative methods that you can adopt when specifying the drag data. The first method is to set data to get best possible match with real measured results for the pipe (e.g. from model tests or full scale measurements). This is the most accurate method.

The second method is to set the drag data using theoretical values or given in the literature. It is less accurate but can be used if you cannot get any real pipe results against which to compare.

2.5.4 SLAM/WATER EXIT FORCE

The slam force, as the pipe enters or exits the water, can be modeled by specifying non-zero slam data. Separate slam data are specified for water entry and water exit, and each can be set either to a constant slam coefficient value or else to be variable with submergence relative to the surface.

2.5.5 EQUATIONS OF MOTION

The equations of motions of a rigid body in a space fixed co-ordinate system follow from Newton's second law. The vector equations for the translations of and the rotations about the centre of gravity are given respectively by:

$$\overrightarrow{F} = \frac{d}{dt}\left(m.\vec{U}\right) \qquad \overrightarrow{M} = \frac{d}{dt}\left(\vec{H}\right)$$

$\overrightarrow{F}$ Resulting external force acting in the centre of gravity
m mass of the rigid body
$\vec{U}$ Instantaneous velocity of the centre of gravity
$\overrightarrow{M}$ Resulting external moment acting about the centre of gravity
$\vec{H}$ Instantaneous angular momentum about the centre of gravity
t time

In the Global system,

The free falling motion can be modeled by the following differential equations [8]:

$$M_{VX}\frac{d^2x}{dt^2} = F_X\left\{t, x, z, \theta, \dot{x}, \dot{z}, \dot{\theta}\right\} \qquad (1)$$

$$M_{VZ}\frac{d^2z}{dt^2} = F_Z\left\{t, x, z, \theta, \dot{x}, \dot{z}, \dot{\theta}\right\} \qquad (2)$$

$$I_V\frac{d^2\theta}{dt^2} = M_{XZ}\left\{t, x, z, \theta, \dot{x}, \dot{z}, \dot{\theta}\right\} \qquad (3)$$

M_{VX} Virtual mass in the global X-direction

M_{VZ} Virtual mass in the global Z direction

I_V Virtual rotational inertia

F_x External force at the X direction

F_Z External force at the Z direction

M_{XZ} External rotational moment

t Time

X,Z Global coordinate of body center of gravity

θ Angle with a horizontal which specify the body orientation

$\dot{X}$ Translational velocity = $\frac{dx}{dt}$

$\dot{Z}$ Translational velocity = $\frac{dz}{dt}$

$\dot{\theta}$ – $Rotetionalvelocity = \frac{d\theta}{dt}$

In the Local moving coordinate system,

The hydrodynamic forces and moment due to fluid drag are computed using the Morrison equation. For a slender body where turbulent flow is induced by relatively high surface roughness, we can assume that the incident flow upon the object can be split into orthogonal components, and that these orthogonal flow regimes are independent of each other [9].

$F_t = 0{,}5\ \rho\ C_{dt}\ A_t\ |V_t|V_t$ (4)

$F_n = 0{,}5 \int \rho . C_{dn} . D|V_n|V_n\ dx'$ (5)

$M_d = 0{,}5 \int \rho . C_{dn} . D|V_n|V_n\ x' dx'$ (6)

Where:

F_t Tangential drag

F_n Normal drag force

M_d Drag moment

ρ Density of the fluid

C_{dt} Tangential drag coefficient (including skin drag)

C_{dn} Normal drag coefficient

V_t Tangential relative velocity

A_t Tangential drag area

V_n Noramal relative velocity

x' X- Coordinate at the local system

F_n is dominated by pressure drag, whereas F_t has a considerable amount of skin friction drag. The forces and moment computed in the local system are transferred to global system using the following relation,

$F_x = F_t \cos\varphi + F_n \sin\varphi$ (7)

$F_z = -F_t \sin\varphi + F_n \cos\varphi$ (8)

$M_{xz} = M_d + M_m$ (9)

When the external forces\moments on the right hand side in equation (1), (2), (3) are computed, we will get 3 equations.

The global equations are solved using the Runge-Kutta 4th order method in the time domain. Where the forces and moments are time and spatial dependent and should be updated every time step.

$$M_{VX}\frac{d^2X}{dt^2} = 0{,}5\,\rho\, C_{Dt} A_t / V_t / V_t (\cos\varphi) + 0{,}5 \int \rho.\, C_{Dn}.D./V_n/ V_n\, dx' (\sin\varphi) \quad (*)$$

$$M_{VZ}\frac{d^2Z}{dt^2} = -0{,}5\,\rho\, C_{Dt} A_t / V_t / V_t (\sin\varphi) + 0{,}5 \int \rho.\, C_{Dn}.D./V_n/ V_n\, dx' (\cos\varphi) \quad (**)$$

$$I_V\frac{d^2\theta}{dt^2} = 0{,}5 \int \rho.C_{dn}.D./V_n/ V_n\, x'dx' \quad (***)$$

M_m – Munk moment= I x U; I-momentum vector, U-relative velocity vector. Slender bodies in near-axial flow experience a destabilizing moment called the Munk moment.

Chapter 3 EXPERMENT

3.1 HYDRODYNAMIC MODEL TESTING:

3.1.1 INTRODUCTION

A small scale model testing is a base tool for validation of theoretical hydrodynamic model, and estimation of related coefficients [2]. Superficial bathtub observation might reveal the flow of water around the model rationally similar to the large ship with certain velocity, but if we closely look in to the viscous flow close to the hull and the wake behind the stern, huge difference would be apparent between the model scale and full scale [4]. The weight might be determined using Archimedes principle in the bathtub, but the speed and power are very complex parameters to define. A proper scaling which accounts the variation is needed. By using dimensional analysis we much better understand the situation.

3.1.2 DIMENSIONAL ANALYSIS

Let's consider a physical quantity Q (it can be, a drag, acceleration...), the parameters that affect Q should be listed from the qualitative point of view (length, velocity, density, viscosity, etc.)

By using these parameters we can non dimensionalised Q, and we assert that the event in question will not be affected by the choice of units of measurements. The three fundamental units are mass [M], length [L], and time [T]. Hence, the unknown Q and its significant parameters upon which it depend can be expressed in terms of these units.

If Q depends on N-1 significant parameters → there will be a total of N interrelated dimensional quantities, including Q. since there are three fundamental units, the number of independent non dimensional parameters is reduced by the same number, leading to a total of N-3 non dimensional interrelated quantities. The end result of this statement is known as pi theorem.

Here is a simple illustration,

The drag force *F* per unit length on a long smooth cylinder is a function of speed *U*, density ρ, diameter *D* and viscosity μ. However, instead of having to draw hundreds of graphs portraying its variation with all combinations of these parameters, dimensional analysis tells us, the problem can be reduced to a single dimensionless relationship

$C_d = f(R_e)$; Where C_d is the drag coefficient and R_e is the Reynolds number

We can see that dimensional analysis reduced the number of variables from five (F, U, ρ, D, μ) to two (C_d, R_e), Hence N-3.

3.1.3 PHYSICAL MODELING

If a dimensional analysis indicates that a problem is described by a functional relationship between non-dimensional parameters Π1, Π2, Π3, then full similarity requires that these parameters be the same at both full ("*prototype*") scale and model scale.

$(\Pi 1)_m = (\Pi 1)_p$

$(\Pi 2)_m = (\Pi 2)_p$ and so forth.

For a multi-parameter problem it is often not possible to achieve full similarity. In particular, it is rare to be able to achieve full Reynolds-number scaling when other dimensionless parameters are also involved. For hydraulic modeling of flows with a free surface the most important requirement is Froude-number scaling [9].

It is common to distinguish three levels of similarity.

Geometric similarity – the ratio of all corresponding lengths in model and prototype are the same (i.e. they have the same shape).

Kinematic similarity – the ratio of all corresponding lengths and times (and hence the ratios of all corresponding velocities) in model and prototype are the same.

Dynamic similarity – the ratio of all forces in model and prototype are the same; e.g. Re = (inertial force) / (viscous force) is the same in both.

Achieving full similarity is particularly a problem with the Reynolds number $Re = UL/\nu$, as this lead to impractically large velocity in model scale. Whereas velocity scale fixed by, the Froude number ($Fr = U/\sqrt{gL}$) means that the only way to maintain the same Reynolds number is to adjust the kinematic viscosity. In practice, Reynolds-number similarity is unimportant if flows in both model and prototype are fully turbulent.

A very important parameter to preserve in hydrodynamic modeling of free-surface flows driven by gravity is the Froude number,

$Fr = U/\sqrt{gL}$

Preserving this parameter between model (*m*) and prototype (*p*) dictates the scaling of other variables in terms of the length scale ratio.

Some of the parameters expressed by Froude's number are as follows:

Velocity;

$(Fr)_m = (Fr)_p$,

Where m- model scale, and p – prototype full scale

$(U/\sqrt{gL})_m = (U/\sqrt{gL})_p \rightarrow \frac{Um}{Up} = \left(\frac{Lm}{Lp}\right)^{1/2}$, Lp/Lm – scaling factor λ (Geometric similarity)

Time;

t= Length/ velocity;

$\rightarrow \frac{tm}{tp} = \left(\frac{Lm}{Lp}\right)^{1/2}$

Force = pressure X area

$\rightarrow \frac{Fm}{Fp} = \left(\frac{Lm}{Lp}\right)^{3}$

Dynamic similarity requires that the ratio of all forces be the same. The ratio of different forces in full scale should be the same to the ratio of force in model scale. If we have dynamic and geometric similarity, it means we have kinematic similarity [10].

The following force contributions are of importance:

Inertia Forces (Fi),Viscous forces (Fv) ,Gravitational forces(Fg),Pressure forces(Fp),

Elastic forces in the fluid (compressibility) (Fe).

Table 2 Froud Scale table

Physical parameter	Unit	Scale factor (λ)
Length	[m]	λ
Structural mass	[Kg]	$\lambda^3.\rho_P/\rho_M$
Force	[N]	$\lambda^3.\rho_P/\rho_M$
moment	[Nm]	$\lambda^4.\rho_P/\rho_M$
Acceleration	[m/s²]	$a_P = a_M$
Time	[s]	$\sqrt{\lambda}$
Pressure	[P_a =N/m²]	$\lambda.\rho_P/\rho_M$

3.2 EXPERMENT DATA

3.2.1 INTRODUCTION:

The main objective of the experment is to investigate and document the motion, sea bed distribution, and the dynamics of a freely falling drill pipe in water. A typical 5'' drill pipe at first is considered. The pool used in the University of Stavanger is only 3m depth; hence scaling a 5'' drill pipe for a 100 m water depth was not practicable. So I decided to use 8'' and 12'' pipes for the study.

3.2.2 TEST MATERIAL PIPE

1. 8'' pipe
2. 12'' pipe

Data Based on ANSI/ASME specification of steel pipe, and ISO General Purpose stainless steel tube (weight tube) [11, 12].

Table 3 pipe data

Type	Nominal size	OD	Length	Mass\Length (W_{DP})	Wall Thickness	Material Grade	Amount needed
pipe	12’	0,324[m]	8,96 [m]	240 [Kg\m]	0,0286 [m]	Carbon steel seamless	10
pipe	8’	0,2191 [m]	8,96 [m]	90,44 [Kg\m]	0,0183 [m]	XS 120	10

12'' pipe have been updated according to ISO 4200

Scale: - **1: λ**

The geometric scaling is based on Froud scaling table.

Length – Linear relation (the Depth, OD, t) = (1\λ) *L, since all linear dimension scale the same. mass\Length = Density * volume \ Length = Density* Area, assuming the same material property. If we use 1\λ scale, the mass\Length = 1\λ^2 (W_{DP})

W_{DP} : Mass length ratio of drill pipe

$L_p / L_m = \lambda$, L_P = Length in full scale, L_m = Length in model scale.

For geometric similarity the scale is taken based on water depth, and all other parameters are scaled according to the scale law shown on table 2. This gives us two scales for two different water depths.

Scale 1: 50m water depth full scale, 3m model scale – 1:16.67

Scale 2: 100m water depth full scale, 3m model scale – 1:33.3

Table 4 Model Scale 1 :- 1:16.67

Type	OD	Length	Mass\Length	Wall Thickness	Material Grade
Pipe 12"	19,4 [mm]	537.4 [mm]	0,864 [Kg\m]	1,72 [mm]	Carbon steel seamless
Pipe 8''	13,2 [mm]	537.4 [mm]	0.325 [Kg\m]	1 [mm]	XS 120

Table 5 Model Scale 2:- 1:33.3

Type	OD	Length	Mass\Length	Wall Thickness	Material Grade
Pipe 12''	10 [mm]	269 [mm]	0,216 [Kg\m]	0,858 [mm]	Carbon steel seamless
Drill Tube	6,6 [mm]	269 [mm]	0,082 [Kg\m]	1,65 [mm]	XS 120

3.2.3 TEST MATERIAL CONTAINER

The external dimensions of the containers are specified in ISO 668, with the maximum allowable dimensional tolerances being ± 10 mm. The internal dimensions are stated as minimum values. The current internal container dimensions are dependent on the structural material used and the container type selected. 40' Container is selected for this test. The specified external and internal dimensions .*Table 6,7,8*

Table 6 External:

Type	Length	width	Height
40’ Container	12192 [mm]	2438 [mm]	2591 [mm]

Table 7 Internal:

Type	Length	width	Height	
40’ Container	11998 [mm]	2330 [mm]	2350 [mm]	

Table 8 Gross weight and Tare

Container size	Maximum gross weight	Tare
40’	32000 [Kg]	3880 [Kg]

Model Scale 1:- 1:16.67

Table 9 External

Type	Length	width	Height
40’ Container	731.4 [mm]	146,3 [mm]	155,4 [mm]

Table 10 Internal

Type	Length	width	Height
40’ Container	720 [mm]	140 [mm]	141 [mm]

Table 11 Gross weight

Container size	Maximum gross weight	Scale 1:33.3	Scale 1:16.67
40’	32000 [Kg]	0,87 [Kg]	7 [Kg]

Model Scale 2: - 1:33.3

Table 12 External

Type	Length	width	Height
40' Container	366 [mm]	73 [mm]	78 [mm]

Table 13 Internal

Type	Length	width	Height
40' Container	360 [mm]	70 [mm]	70,6 [mm]

3.3 EXPERMENT LAYOUT

The concrete lab at UiS is used to perform the test. The pool is basically 3m depth, 3m wide and about 25m long. In order to use the pool for this particular test substantial amount work has been done. The idea is to recorded each test with underwater camera both video and picture and to digitized such data afterwards for analysis. To achieve this preparing the rig by itself has taken enormous amount of time and energy.

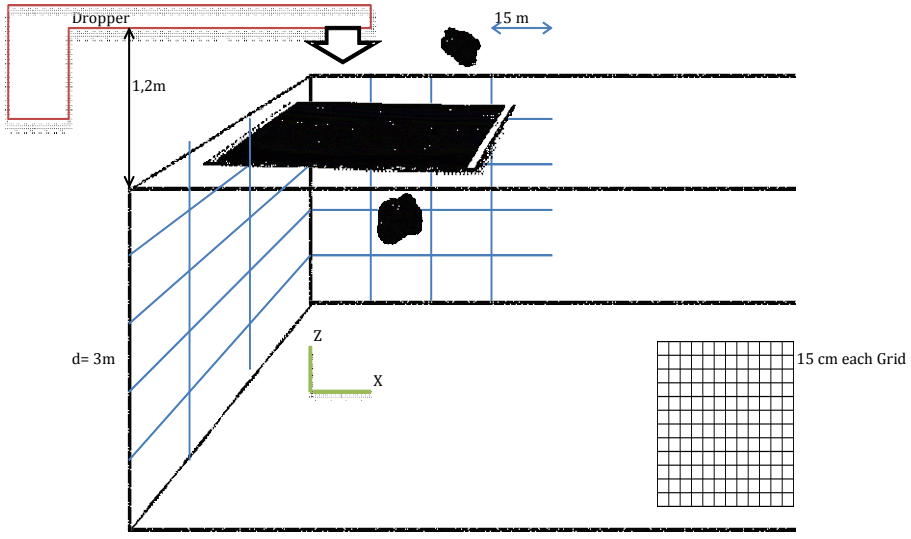

Figur 3 Sketch of rig layout.

3.3.1 EQUIPMENTS USED:

- 15cm x 15cm armoring net (grid), 300m^3 volume

-Tuvek water proof background

- 8 subsea lights

- 4 Gopro action cameras

- Custom made pipe dropper

- Water proof marker

- 6 water proof paint

- 8'' pipe with proper scale

- 12'' pipe with proper scale

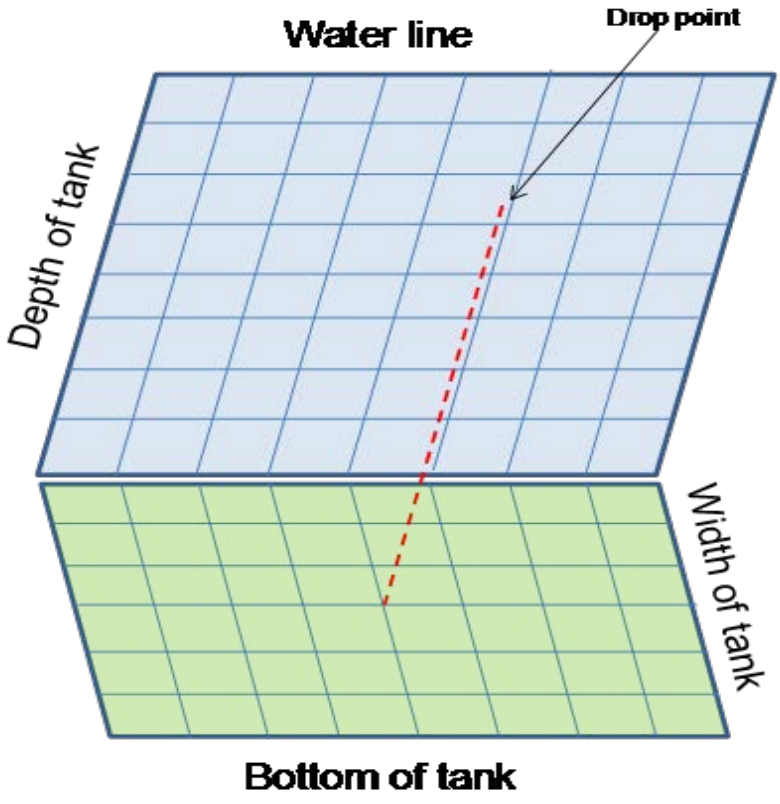

Figur 4 Concept

Figur 5 Pool under construction

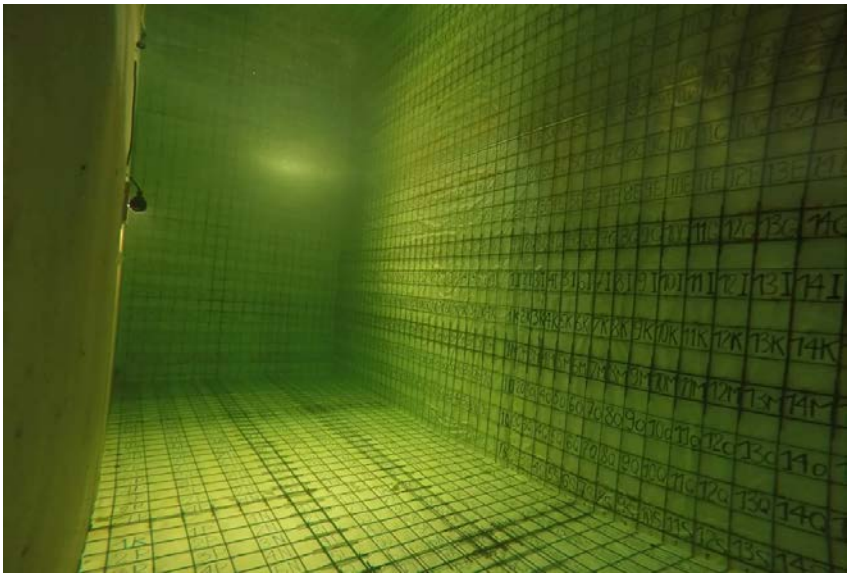

Figur 6 Pool after completion

3.4 EXPERMENT PROCEDURE

3.4.1 INTRODUCTION

The procedure followed by this experment is updated through a step by step discussion with the external adviser in combination with workshop manager at UiS. Test facility limitation, equipment shortage, availability, schedule etc. have been considered.

3.4.2 STEPS FOLLOWED

1- Pipe data is acquired according to ANSI/ASME specification of steel pipe, and ISO General Purpose stainless steel tube

2- Proper scaling has been set using the scale law *Fraud's law* , for geometrical similarities

3- Rig preparation has been done

- ❖ Rig Layout sketched (see section 3.3)
- ❖ Cleaning the pool
- ❖ Painting the armoring net (each grid)
- ❖ Building the grid on the concrete wall
- ❖ Marking each grid
- ❖ Setting up of the drop area
- ❖ Putting the subsea lights on the concrete wall
- ❖ Adjusting the custom made pipe dropper
- ❖ Filling the tank with water

4- Cutting and painting of the pipes, making container according to the scale in the workshop.

5- Preparing the camera for the right depth and view angle

- ❖ The camera used is a Gopro action camera, with its limitation- due to its low battery life and no Wi-Fi under water, the camera need to be taken out to stop and record after each test.

6- Dropping the pipes

- ❖ Start the test by dropping pipes as shown in the set up (Fig.7)

- Starting from 12" , Scale 1:33.3

  0^0,30^0,45^0,60^0,90^0

- Continue the work 12" , scale 1:16.67

  0^0,30^0,45^0,60^0,90^0

- 10 pipes dropped at each angle and retrieved after each test , this has been done several times to get a good data

  One test = dropping of 10 pipes of the same diameter at one angle and retrieve

- Similar procedure has been followed for 8'' pipes.

- Gathering of all the data, sorting out the video's and pictures etc.

7- Data analysis :- this is explained in detail in section (4)

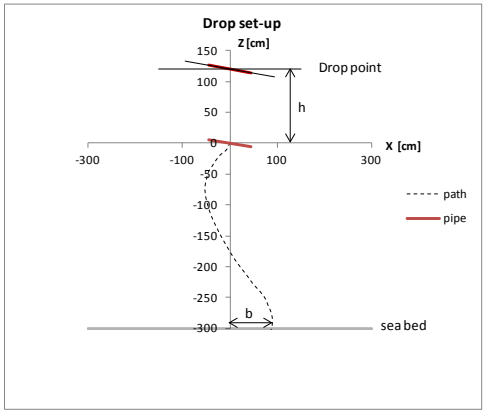

Figur 7 Test set-up

Figure 7, shows the set –up where the pipe is mounted on a clip, at a height h above a still water surface. A realistic drop from a platform or drop during lifting. By varying the dropping angel and assuming there is no rotation in the air when dropping, we can study the motion dynamics in water. The impact zone giving a rotation to the cylinder is very important and should not be under estimated by dropping the cylinder under the still water with no impact energy.

Chapter 4 ANALYSIS

4.1 INTRODUCTION

From the test enormous amount of data is collected through, manual observation, video recording, and picture data. The objective of the grid is to identify the path of each dropped pipe in X-Y-Z coordinate system. The drop point is set to a fixed coordinate (0, 0, 0) and the idea is to record the trajectory in a visual manner and to digitize the recorded data. A tool is needed to change the visual data in to coordinates. Luckily a free program on the internet is found for such purpose. An interface called web plot digitizer is used to digitize all the video and picture data in to x,y,z local coordinates. Examples are given in Fig 8, 9, and 10.

4.2 VIDEO DATA

The data recorded on the Gopro action camera is sorted, edited, and watched, using various available editing programs. Each video is registered for each test using test ID. Three cameras are used to record from Top view, side view, and 3D view at a time. More than 50 video files has been edited and changed to a sequence of picture data. The Data from the side camera is used to trace the trajectory of the drop pipes and containers. The top camera has recorded all the distribution of the pipes on sea bed.

4.3 PICTURE DATA

In addition of picture taken after each test, a sequential picture is extracted from the videos. These large numbers of data plotted as data points on the picture need to be extracted as numerical values. This was a very tedious process.

4.4 WEB PLOT DIGITIZER

Web Plot Digitizer was developed to facilitate easy and accurate data extraction from a variety of plot types. This program has been built using HTML5 which allows it to run within most popular web browsers and does not require an installation process that is performed by the user. This is distributed free of charge as an open source software [13]. The sequential pictures are used as input in this program.

The data points which are extracted from each picture have been exported as excel files for further analysis. The result shows how accurate this program is by comparing the original picture with the data points extracted from the picture. The outcome is satisfactory with very negligible error.

4.5 EXCEL

Microsoft excel is used to create calculation sheets, based on the data extracted from web plot digitizer, a lengthy process is followed for each data points to draw the plots.

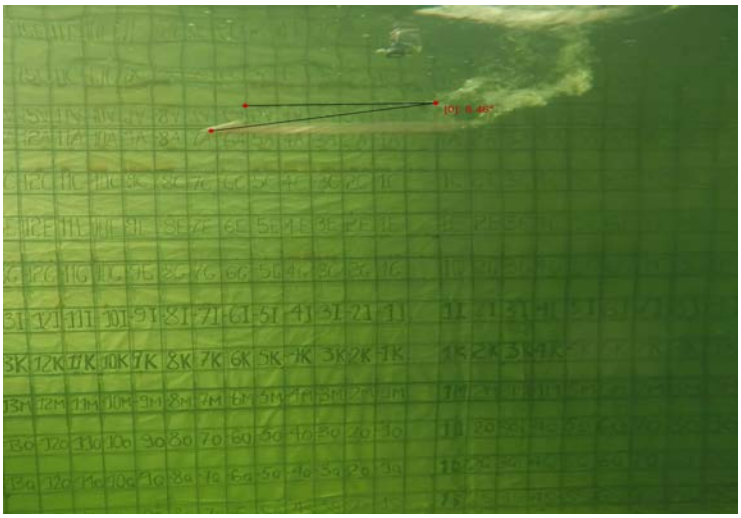

Figur 8 Measuring angle

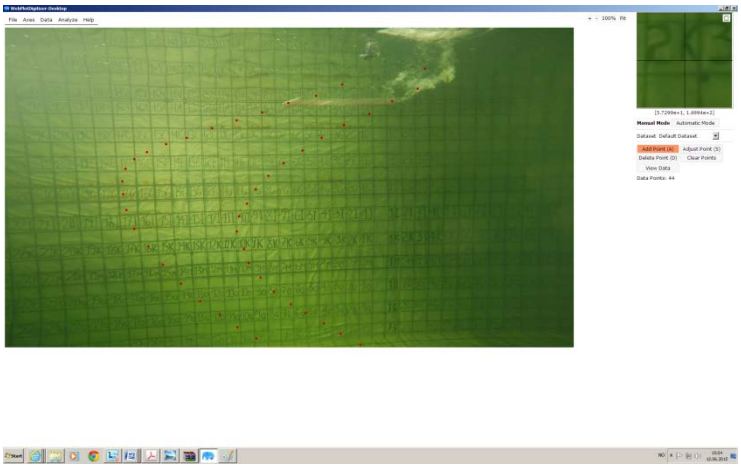

Figur 9 Path tracking 1

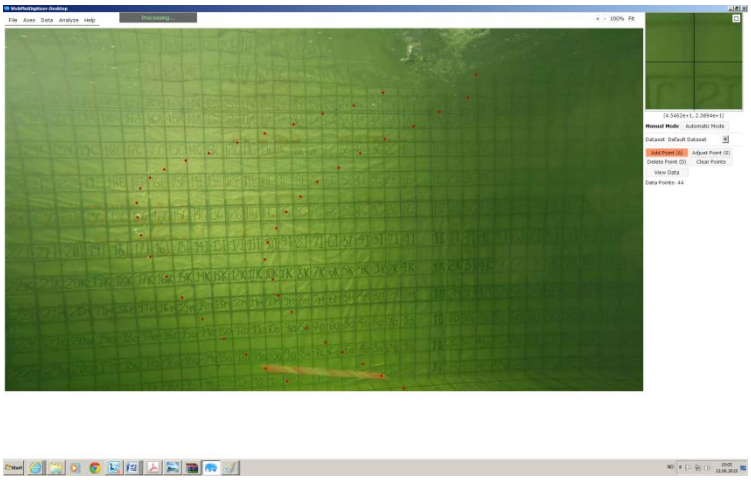

Figur 10 Path tracking 2

Chapter 5 TEST RESULT

5.1 DROP RESULT PIPE 8''

Table 14 Sea bed distribution 8'' pipe

no	Type	Test no	Angle [deg]	Scale	Maximum X excursion[1] [cm],	Mean X excursion[cm] mid point	Mean R excursion[cm] mid point	Stan-deviation R [cm]
1	8''	1,2	0	1:16,67	45,2	7	15,2	10,4
2	8''	3,4,5	30	1:16,67	34	10	26	12,4
3	8''	6,7	45	1:16,67	33	12,3	27,2	9,6
4	8''	8,9	60	1:16,67	227,7	101,4	113,4	41,9
5	8''	10,11	90	1:16,67	129,6	21,7	103,8	37
6	8''	12,13	0	1:33,3	29	3,3	17,6	7,7
7	8''	14,15	30	1:33,3	16,8	3,3	8,3	4,3
8	8''	16,17,18	45	1:33,3	76,8	44	44,3	15
9	8''	19,20,21	60	1:33,3	156	100	103,7	33
10	8''	22,23,24,25	90	1:33,3	103,8	21,2	64	29,3

[1] X axis excursion based on mid point

5.2 INTRODUCTION

Observation of videos and the digital data are processed thoroughly to come up to the above test results. These results will be discussed in section (6); the results are categorized according to pipe size. Detail result is found in the Appendix. Results were obtained as graphs of the position and direction of the pipe at the seabed.

5.3 DISTRIBUTION ON THE SEA BED (SEA BED EXCURSION) 8'' PIPE.

The results are plotted below as distribution in both X and Y axis on the sea bed. A Resultant R is taken to be the measure of the excursion radius. A ring is formed denoting R_i and R_o to show the inner radius of the mean Resultant and outer radius of the maximum resultant excursion points. The resultant radius is calculated based on the mid coordinate of each pipe. Drop point is located at (0, 0, 0). The results are numbered from 1-10 to show the distribution at each angle.

$R^2 = x^2 + y^2$; Coordinate X-Y on the seabed

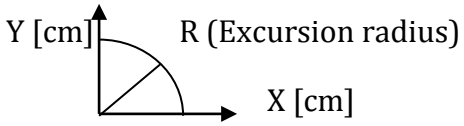

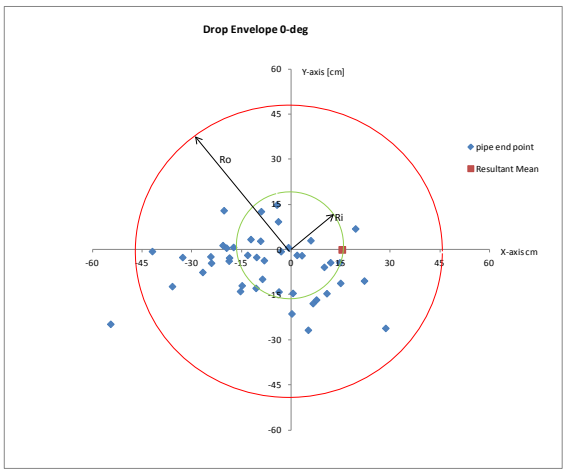

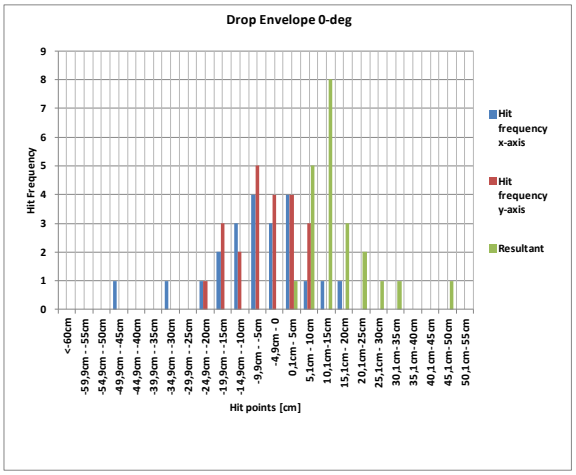

1 a) Sea bed distribution 8''-0^0 scale 1 b) Drop envelope 8''-0^0 scale 1

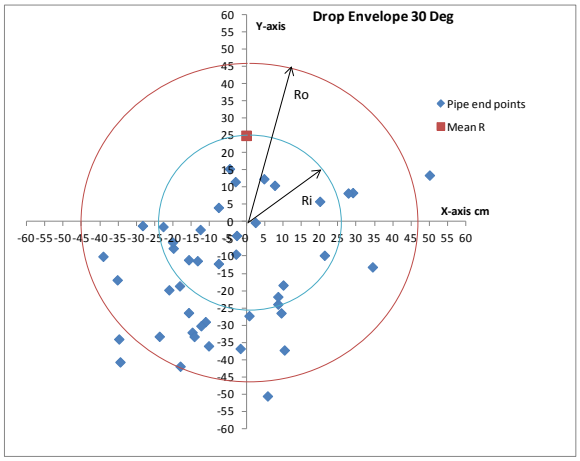

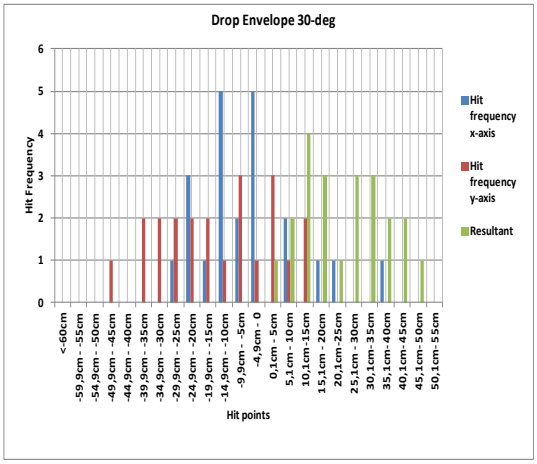

2 a) Sea bed distribution 8''-30^0 Scale1 b) Drop envelope 8''-30^0 scale 1

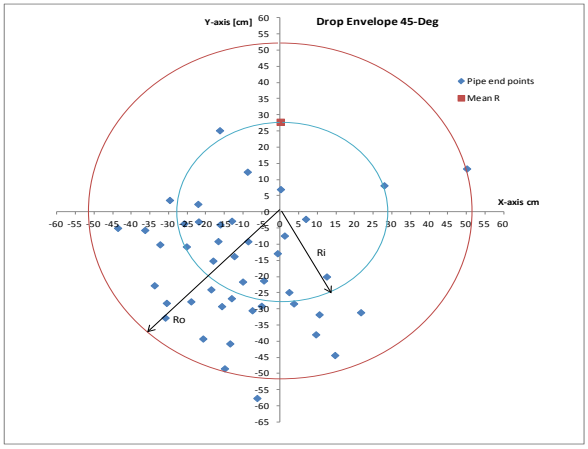

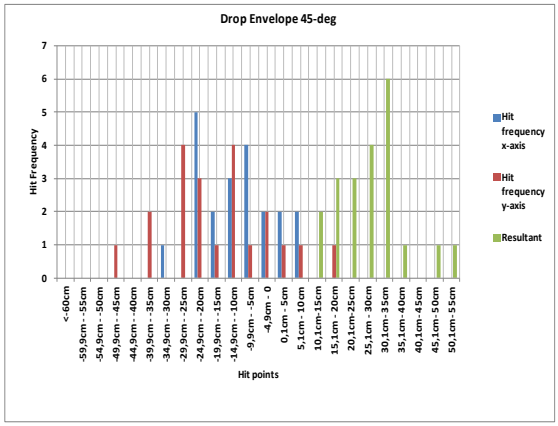

3 a) Sea bed distribution 8''-45^0 Scale 1 b) Drop envelope 8''-45^0 scale 1

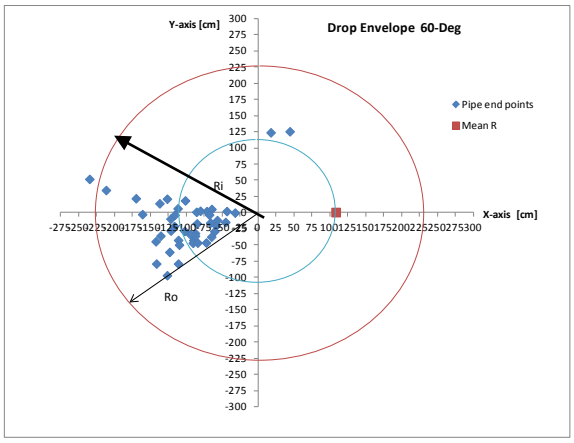

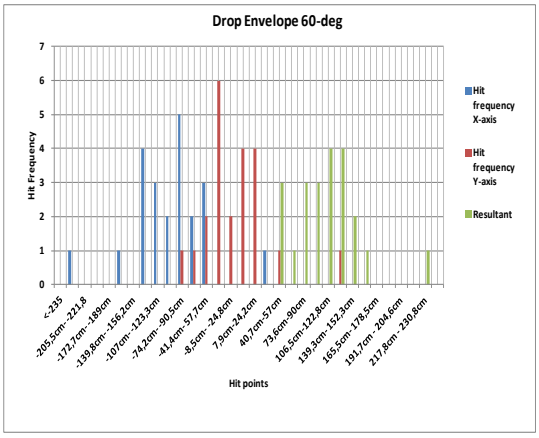

4 a) Sea bed distribution 8''-60^0 Scale 1 b) Drop envelope 8''-60^0 scale 1

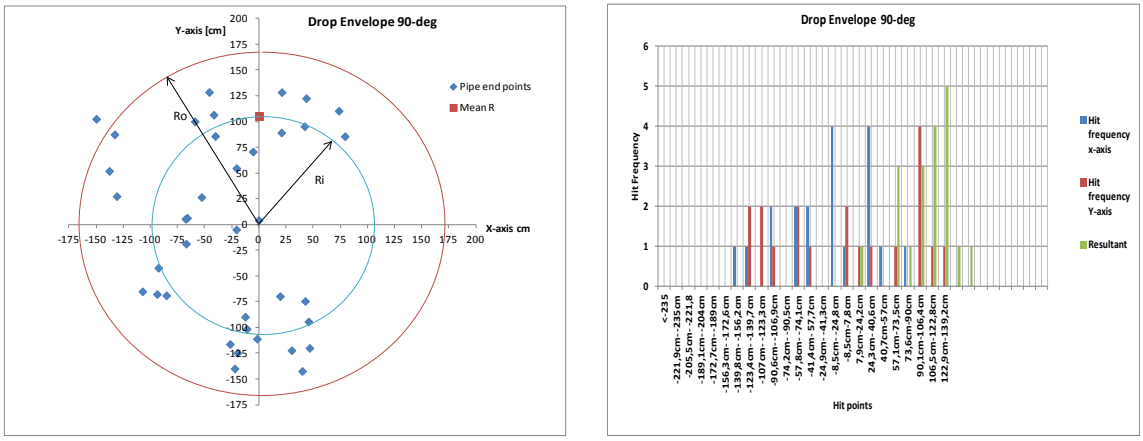

5 a) Sea bed distribution 8''-90^0 Scale 1 b) Drop envelope 8''-90^0 scale 1

Figur 11 Sea bed distribution 8'' scale 1

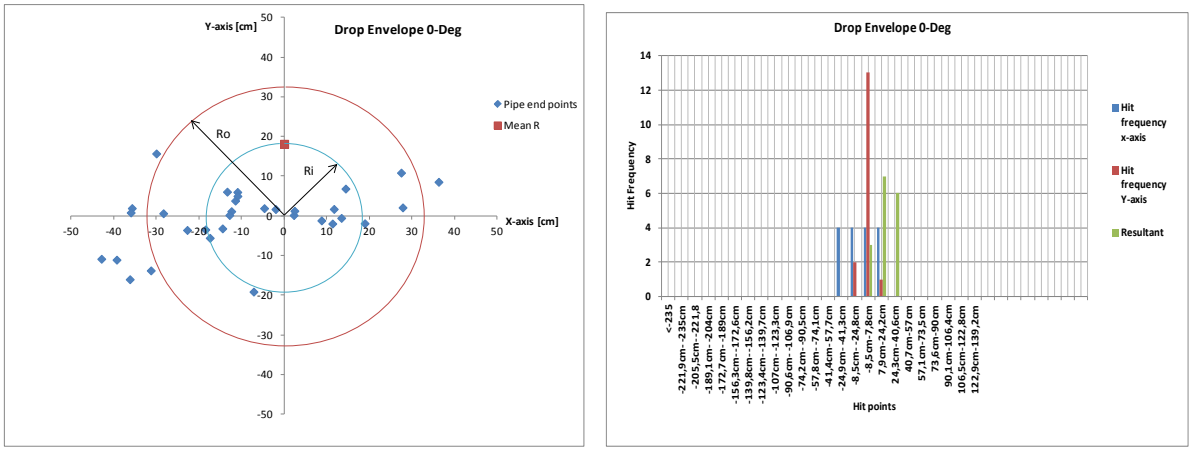

6 a) Sea bed distribution 8''-0^0 Scale 2 b) Drop envelope 8''-0^0 Scale 2

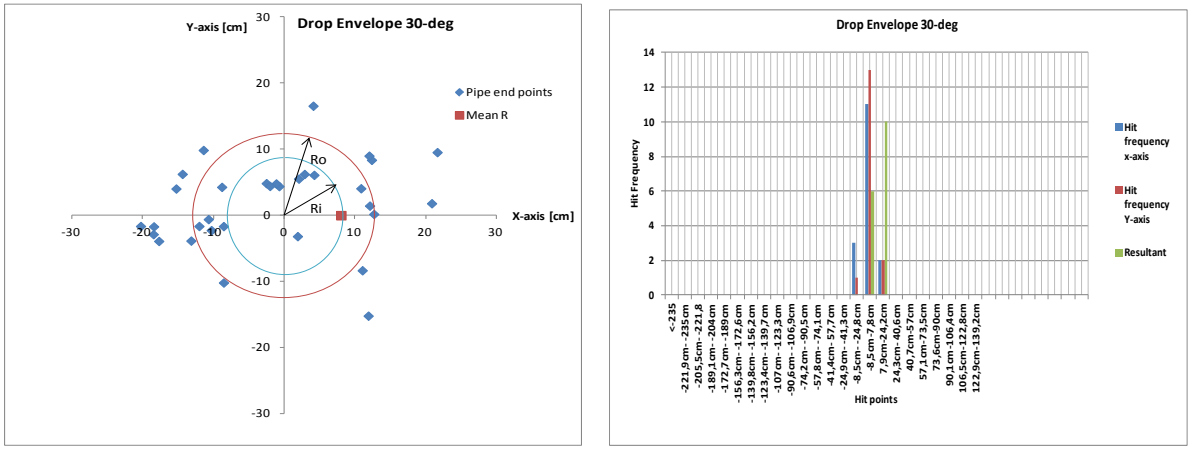

7 a) Sea bed distribution 8''-30^0 Scale 2 b) Drop envelope 8''-30^0 Scale 2

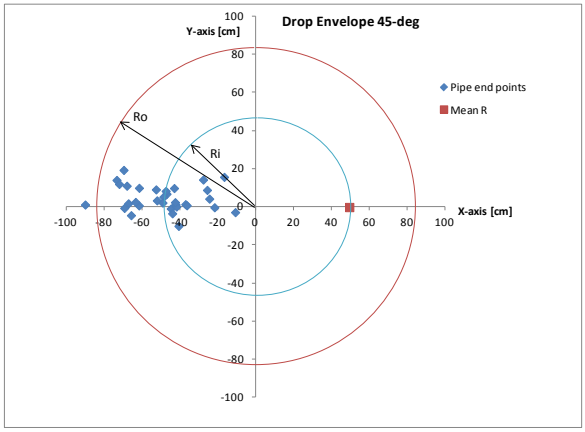

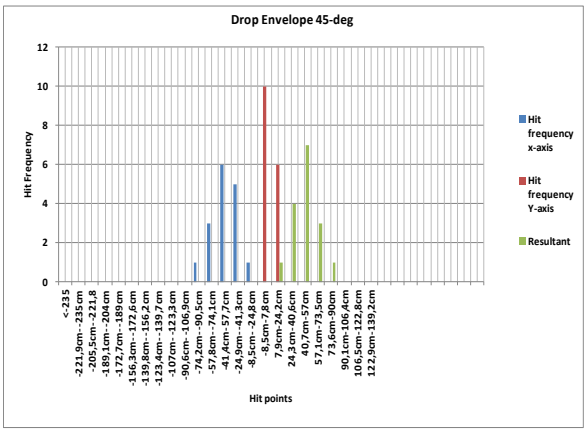

8 a) Sea bed distribution 8''-45^0 Scale 2 b) Drop envelope 8''-45^0 Scale 2

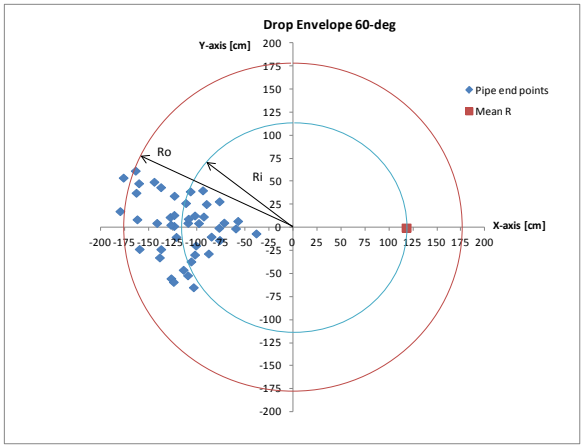

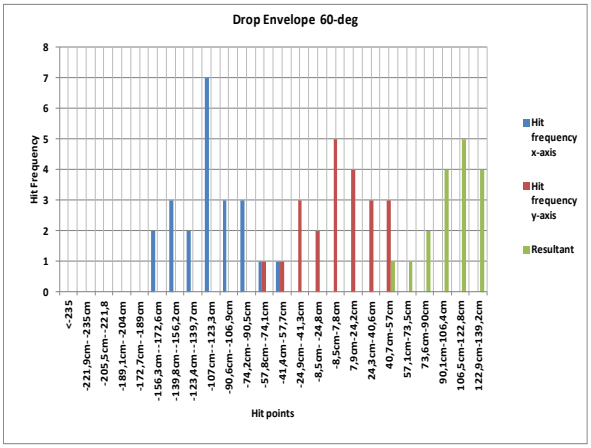

9 a)Sea bed distribution 8''-60^0 Scale 2 b) Drop envelope 8''-60^0 Scale 2

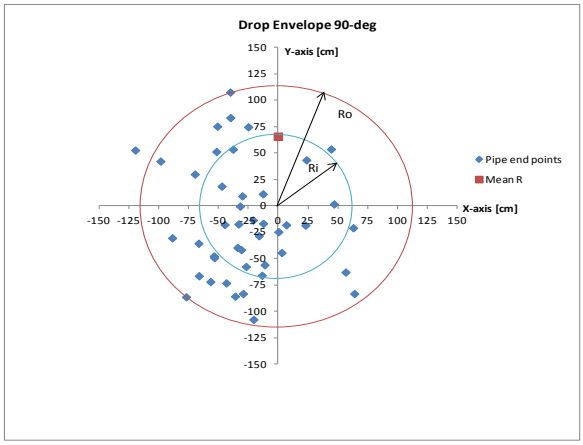

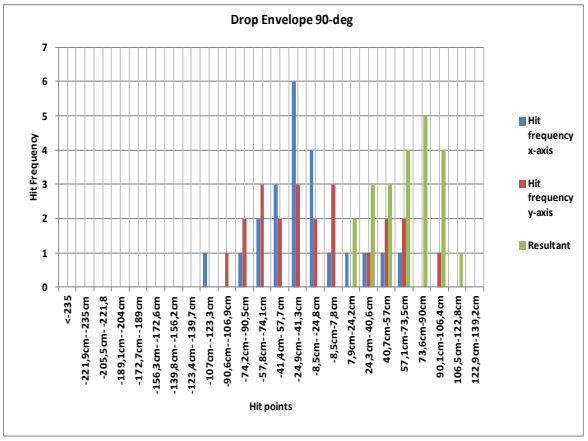

10 a) Sea bed distribution 8''-90^0 Scale 2 b) Drop envelope 8''-90^0 Scale 2

Figur 12 Sea bed distribution 8'' Scale 2

5.4 DROP RESULT 12" PIPE

Table 15 Sea bed distribution 12" pipe

no	Type	Test no	Angle	Scale	Maximum X[2]-excursion[cm]	Mean X-excursion[cm] mid point	Mean R excursion[cm] mid point	Standard Deviation R [cm]
11	12''	26,27	0	1:16,67	31,8	6,4	21,4	10,3
12	12''	28	30	1:16,67	60,4	29,8	36,2	14,7
13	12''	29	45	1:16,67	98	68,4	75,7	26
14	12'''	30,31,32	60	1:16,67	180	109,7	113,4	30,8
15	12''	33	90	1:16,67	61	21,7	34,8	17,5
16	12''	34,35	0	1:33,3	27,5	2	12,7	6,6
17	12''	36,37	30	1:33,3	49,5	34,6	35,8	13,3
18	12''	38,39	45	1:33,3	142	99	100	23
19	12''	40,41	60	1:33,3	229	176,4	178,6	28,6
20	12''	42,43	90	1:33,3	64	12,5	49,6	11,7

Similar to section 5.3, drop envelope for 12'' pipe is shown below.

[2] X-axis excursion based on mid points

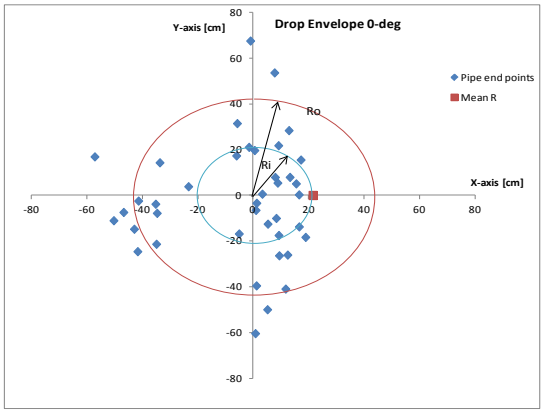

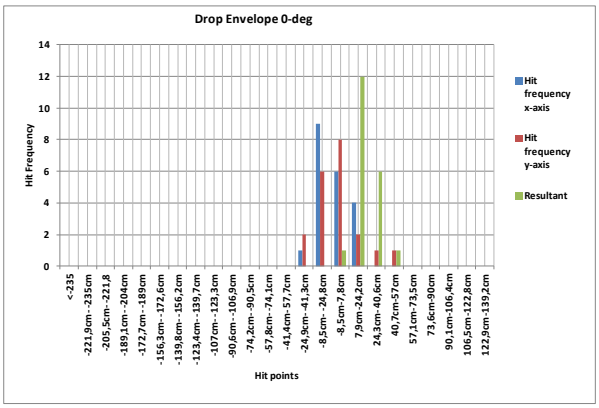

11 a) Sea bed distribution 12''-0^0 Scale 1 b) Drop envelope 12''-0^0 Scale 1

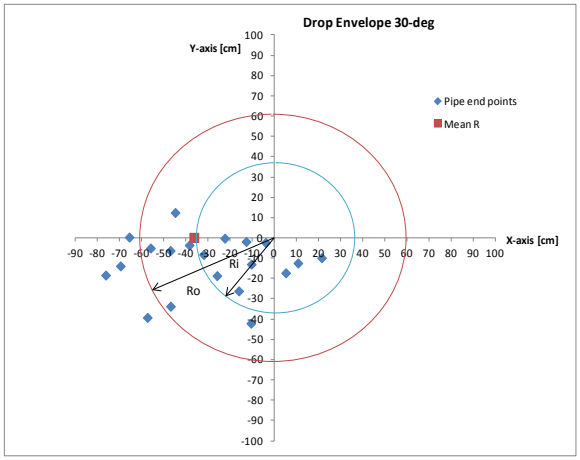

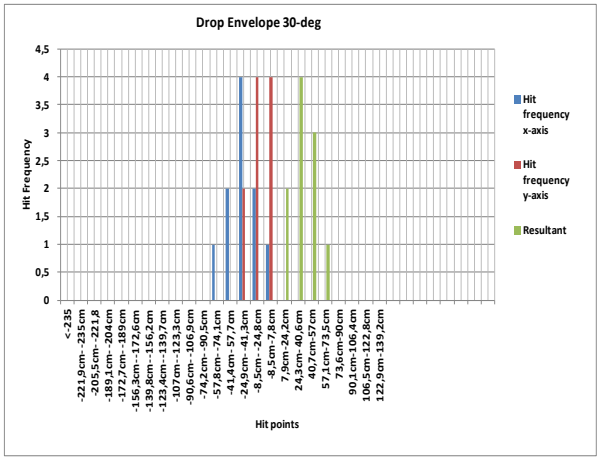

12 a) Sea bed distribution 12''-30^0 Scale 1 b) Drop envelope 12''-30^0 Scale 1

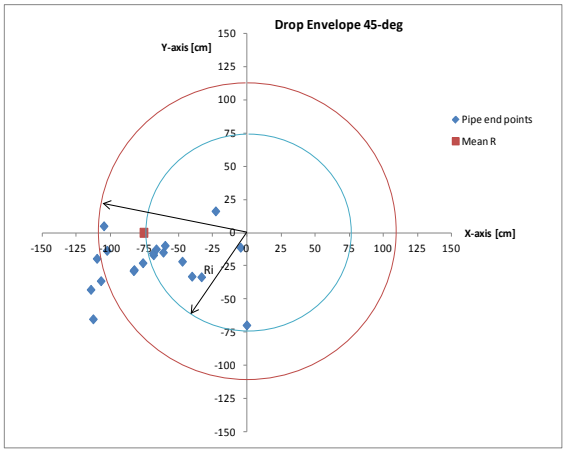

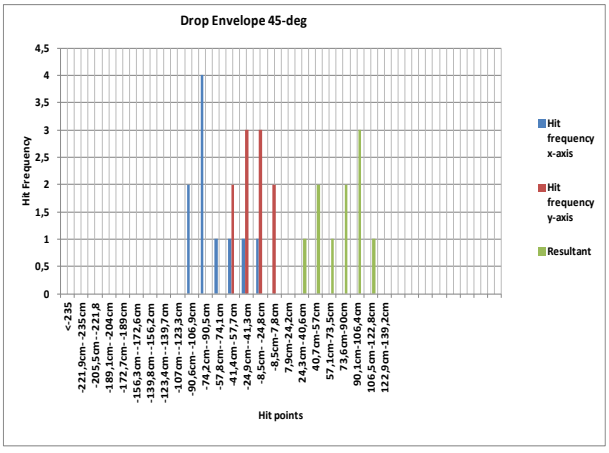

13 a) Sea bed distribution 12''-45^0 Scale b) Drop envelope 12''-45^0 Scale 1

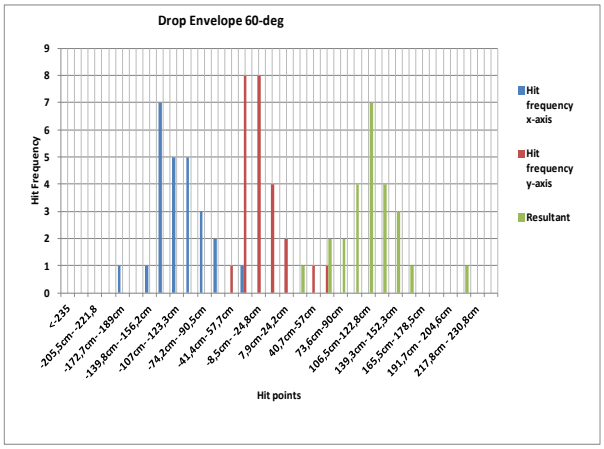

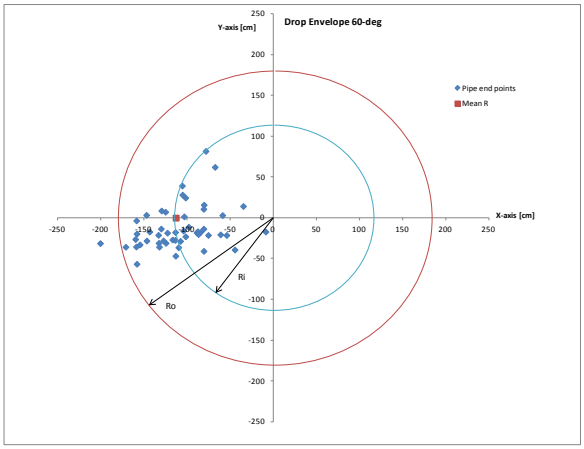

14 a) Sea bed distribution 12''-60^0 Scale 1 b) Drop envelope 12''-60^0 Scale 1

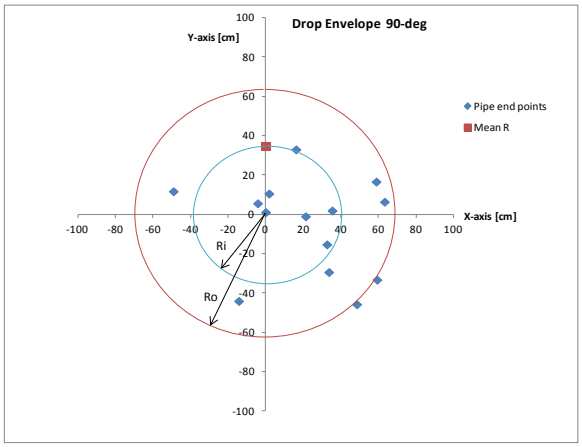

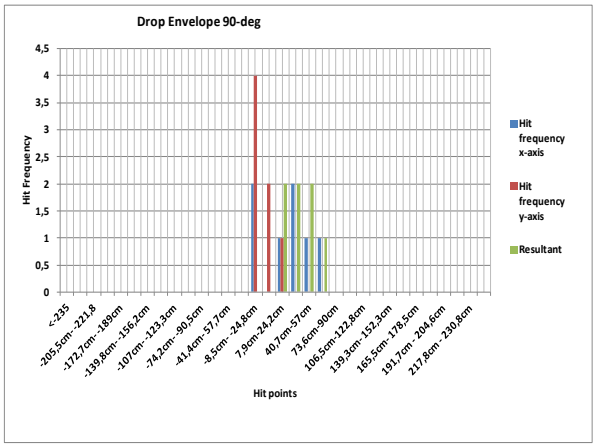

15 a) Sea bed distribution 12''-90^0 Scale 1 b) Drop envelope 12''-90^0 Scale 1

Figur 13 Sea bed distribution 12'' Scale 1

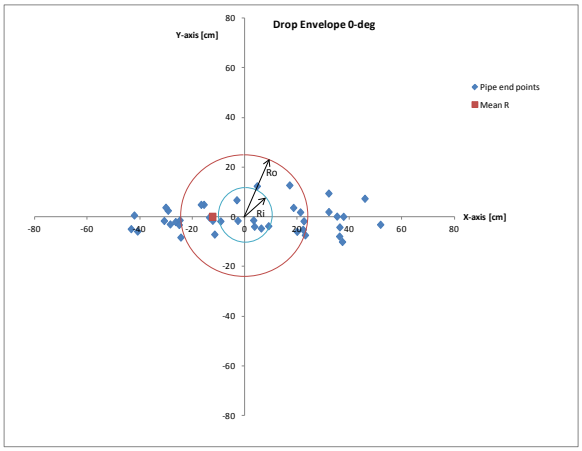

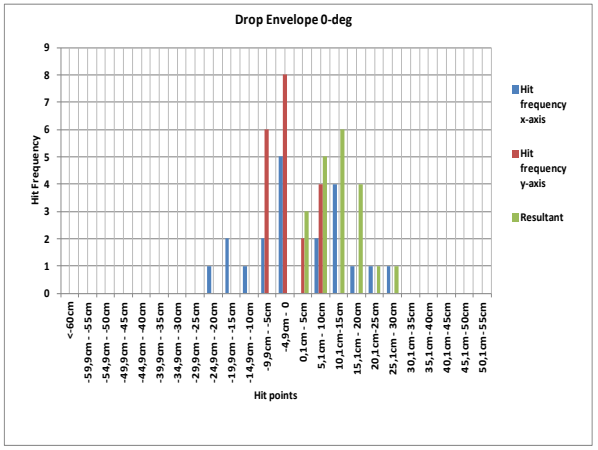

16 a) Sea bed distribution 12''-0^0 Scale 2 b) Drop envelope 12''-0^0 Scale 2

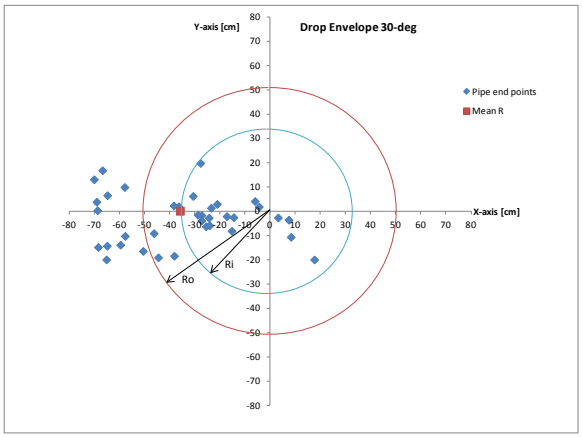

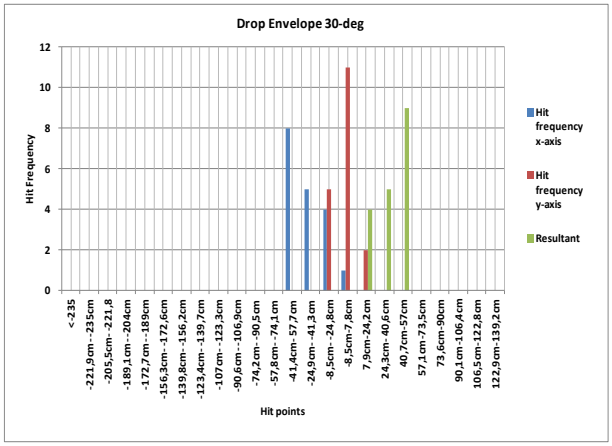

17 a) Sea bed distribution 12''-30^0 Scale 2 b) Drop envelope 12''-30^0 Scale 2

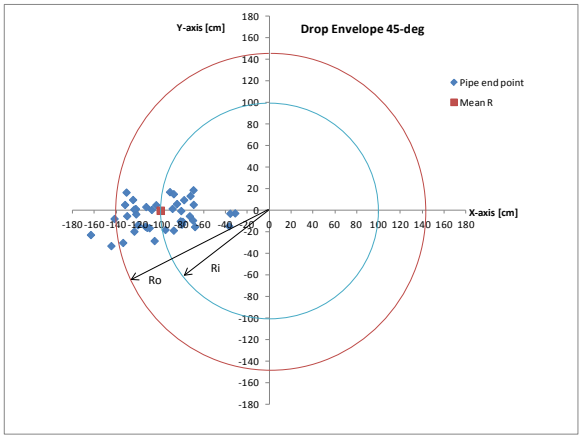

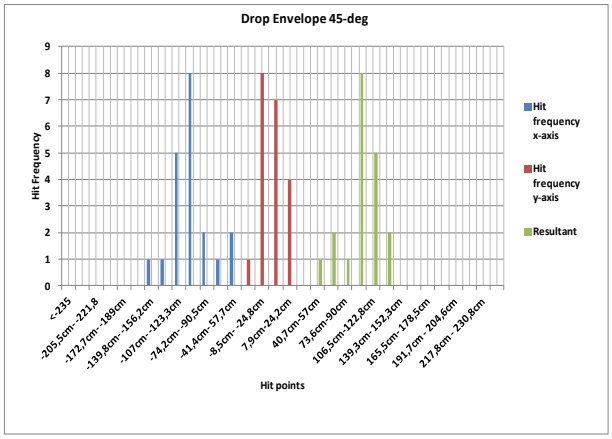

18 a) Sea bed distribution 12''-45^0 Scale 2 b) Drop envelope 12''-45^0 Scale 2

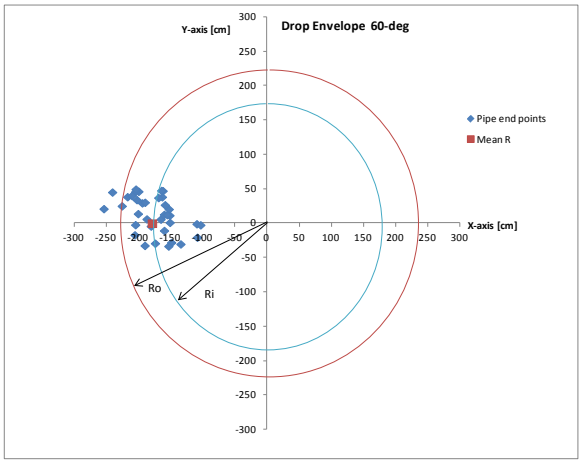

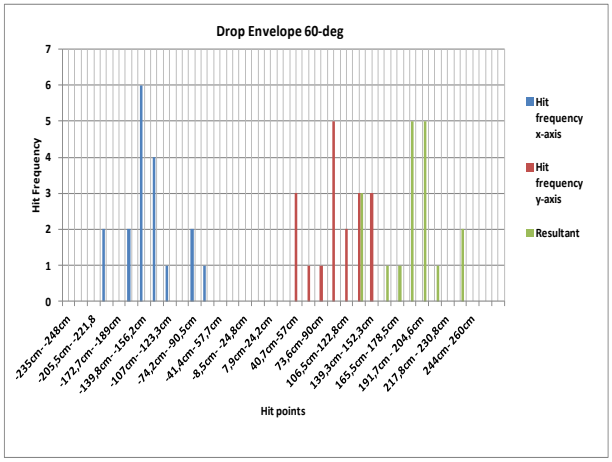

19 a) Sea bed distribution 12''-60^0 Scale 2 b) Drop envelope 12''-60^0 Scale 2

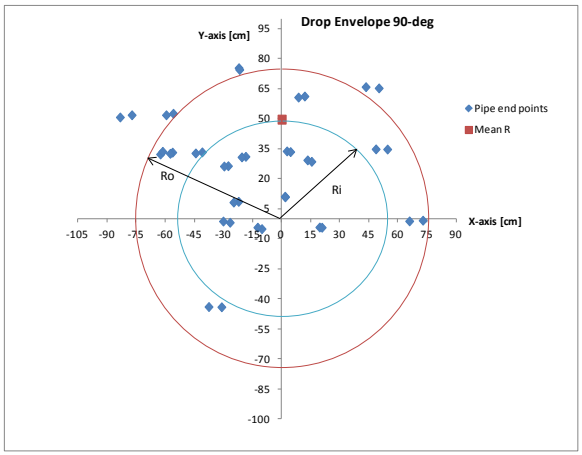

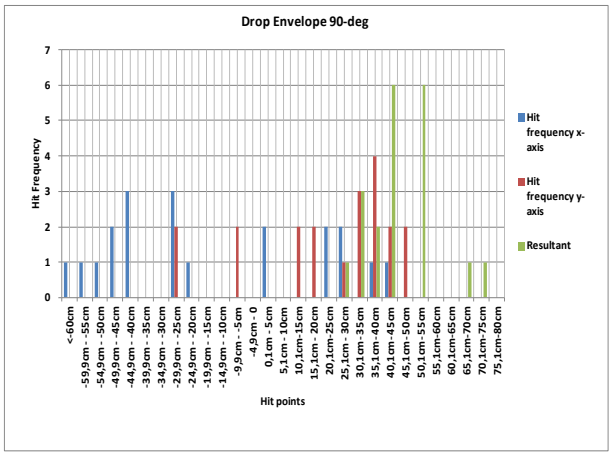

14 a) Sea bed distribution 12''-90^0 Scale 2 b) Drop envelope 12''-90^0 Scale 2

Figur 15 Sea bed distribution 12'' Scale 2

5.5 TRAJECTORY OBSERVED

5.5.1 INTRODUCTION

The paths observed from the test are attached in the Appendix, each point has been digitized and plotted in excel. The camera has been set to record 30 frames per sec initially. The method used here is to change the video data in to sequential picture frames and digitize each frame to extract the data points. The trajectory plotted match's with the animation at 30 frames per sec. Every other second frame is plotted in excel.

5.5.2 OBSERVED PATTERN IN THE EXPERMENT

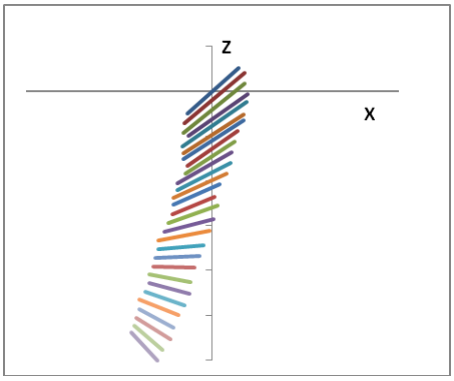

Category A

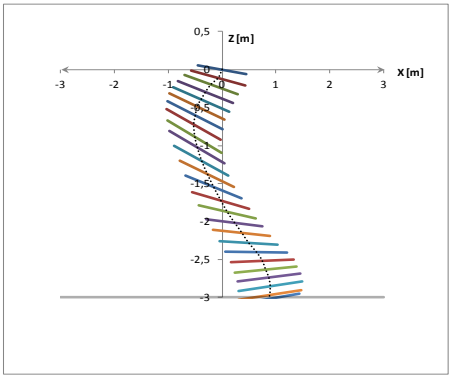

Category B

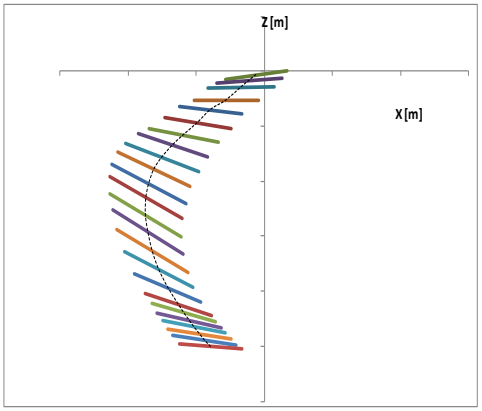

Category C

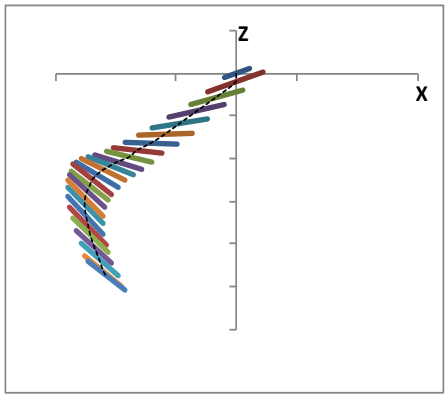

Category D

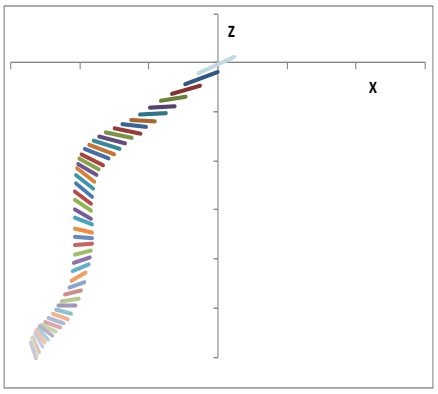

Category E

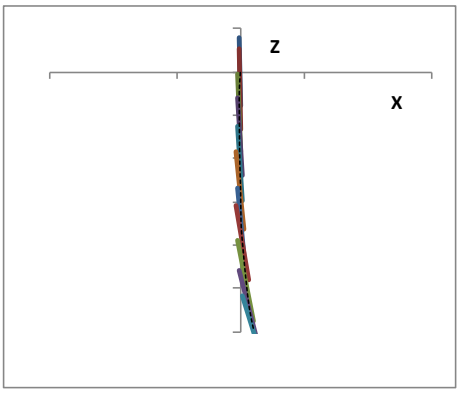

Category F

Figur 16 Observed trajectories

Chapter 6 DISCUSSION

6.1 INTRODUCTION

The dropped object analysis this paper deals is based on a parametric study of the experment conducted with an assumption that the environment as well as the object can be modelled in relatively good accuracy. The behavior can be best described using statstics to drive seabed risk contour. The amount of data gatherd is unfortunately limits a direct application of fitting the data in a known distribution.

6.2 DNV SIMPLIFIED METHOD

Dropped objects assessments are often done via a simplified method [2]. In this method, dropped objects are defined by simple shapes. An angular deviation, α is assigned based on the object's shape and weight. Based on the angular deviation, a cone angle is defined with the angular deviation serving as the standard deviation to a normal distribution for the horizontal excursions (see Figure 54).

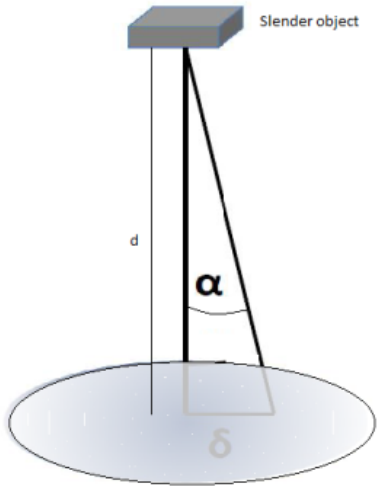

Figur 17 Simplified method

The values recommended for use in calculations of the object excursion on the seabed are listed on table 16.The object excursions on the seabed are assumed to be normal distributed with angular deviations given in Table 10 DNV, section 5.2.1. p 20 [2].

Since DNV's methedology is based on the shape and weight of the object and an assumption of a normally destrbuted angular deviation, it often end up with a very conservative or in some case's unconservative result.

Table 16 DNV recommended angular deviations

no	Description	Weight (tonnes)	Angular deviation α (deg)
1	Flat/Longed shaped	<2	15
2		2 - 8	9
3		>8	5
4	Box/round shaped	<2	10
5		2-8	5
6		>8	3
7	Box/round shaped	>>8	2

δ= d. tanα , where δ is lateral deviation, α is angular deviation , and d is the depth. For drill collar < 2t , α = 15 which assignes a lateral deviation based on the depth only.

6.3 BASE CASE STUDY 8" SCALE 1:16,67

6.3.1 SEA BED DISTRIBUTION

The two parameters that affect seabed distribution for a a specified drill pipe are , excursion angle and height h above the water level. Increasing drop height will increase impact velocity hence the excursion. In this study a fixed height ,h=1,20 m above the water level is taken representing 20m in full scale. As showen in Fig.4 .

A total no 11 test has been performed by varying each angle from 0,30,45,60,and 90. One test is droping of 10 pipes. The result found are expressed in section 5.

The distribution is made based on the following assumptions:

1- Only (open) pipes included,The objects weight is specified in table 3.

2- Uniform mass distribution has been assumed.

3- The length of the pipes is approximately 9m.

b= excursion point x-axis on the sea bed
tb= time to reach b
Test case 1 = 50 m full scale , scale 1:16,67
c= hit point y-axis
*, indicates one base case study not represent a mean for this angle
R = resultant radius

Table 17 Test result summery 8" scale 1:16,67

8''- test case 1	Mean values [cm]	Mean values[cm]	Mean time[s]	Mean[cm]
drop angle	b	c	tb [s]	R
0	2	5		15,4
30	5	15	2,47	26,3
45	12	17	2	27,2
60	101,4	14		113,4
*75	*183	*16		*193,6
90	27	2	1	104

Result in table 17 shows that the excursion at the sea bed for excursion angle α = 0^0,30^0,and even 45^0 are close to the origin. For α=60^0 , the pipes are distributed w.r.t the x-axis, and the resultant mean has a radius of 113 cm~ 1m .The seabed destribution based on mid points of the pipe (M) is illustrated below.

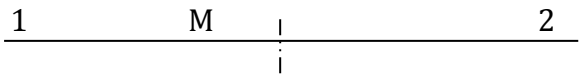

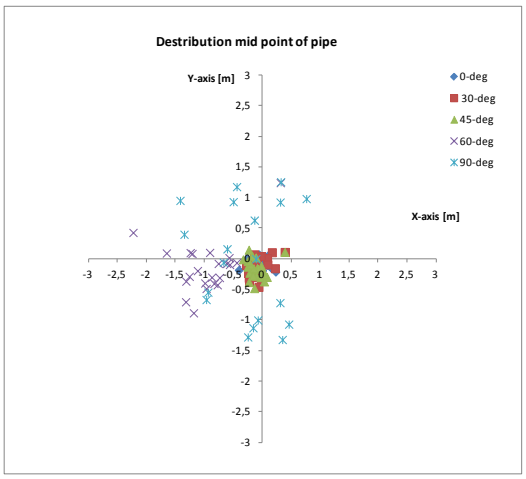

Figur 18 Distribution on the sea bed drop angle 0-90^0- 8'' Scale 1

The case is different for α=90^0, It has mean exursion radius of 1m and its distributed w.r.t both X and Y axes. It is very difficult to take the mean values of b & c as this small values

lead to wrong results cause the observed deviation is 61cm in X and 91 cm in Y coordinates.

6.3.2 COMPARISON OF DNV METHEDOLOGY WITH THE RESULT OBTAINED

According to DNV ; $\delta = d.\tan\alpha$, where δ is lateral deviation, α is angular deviation , and d is the depth. For drill collar < 2t , $\alpha = 15$; d = 3m (water depth)

$\boldsymbol{\delta} = 3.\tan(15) = 80{,}4$ cm ~ Lateral deviation

Table 18 Comparison with DNV 8" scale 1:16,67

angle	89% confidence interval	Mean R	Max R	Standard deviation R (test)	Simplified lateral deviation R
0	0cm- 46,6 cm	15,4 cm	49 cm	10,4 cm	80,4 cm
30	0cm-63,2cm	26,3 cm	47,6 cm	12,3 cm	80,4 cm
45	0cm-56cm	27,2 cm	50,2 cm	9,6 cm	80,4 cm
60	0cm-239,4cm	113,4 cm	231,6 cm	42 cm	80,4 cm
90	0cm-215cm	104 cm	166,4 cm	37 cm	80,4 cm

As it seen in tabele (18), The over-conservative results from the simplified approach comes from the simplification not accounting object-specific hydrodynamics. If the object specific hydrodynamics is not an input for the analysis , then the approach yields the same result for a general category of shapes n weights. The lateral deviation gave the same result (80,4 cm) for all angle where as the standard deviation of the test result alters with the drop angle.

Refering to Chebyshev's inequality, Atleast 89% (mean- 3d)-(mean + 3d) , 75%-(mean-2d)-(mean+2d) should fall within this range.

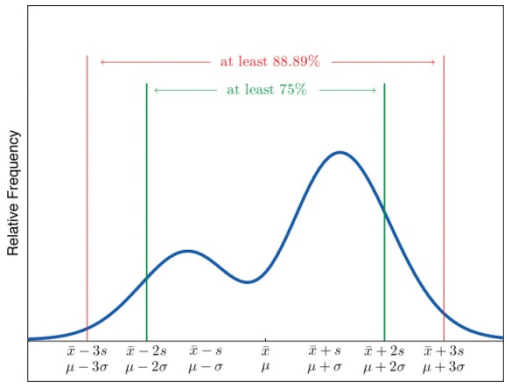

Figur 19 Chebyshev's inequality diagram

Careful attention should be given to the words "at least" at the beginning of each of the two parts. The theorem gives the *minimum* proportion of the data which must lie within a given number of standard deviations of the mean; the true proportions found within the indicated regions could be greater than what the theorem guarantees.

Case study 0 deg is given below:

Mean = 15,4 cm ; standard deviation-d = 10,4 cm

(15,4-3*10,4) – (15,4+3*10,4) → 0cm- 46,6 cm , 89% of data falles between 0cm-46,6 cm refering to chebyshev's theorem. The result for the other angles are shown in table 18. The distribution for 0^0 drop angle look like this and it matches with the frequency table in fig 61.

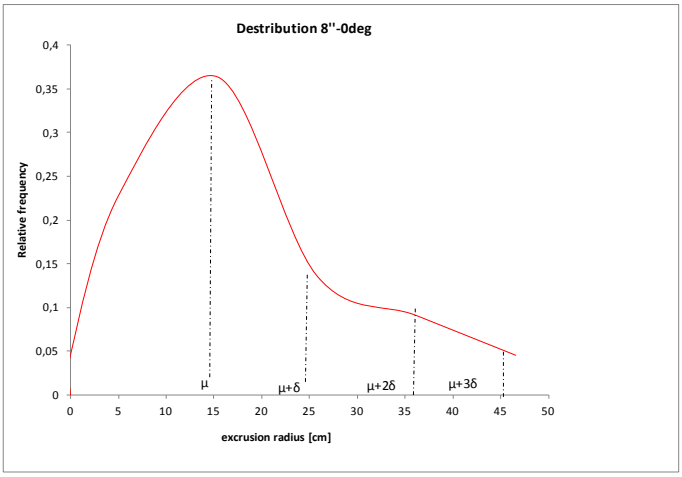

Figur 20 Distribution 8''-0^0 Scale 1

location in cm	FreQuency x	Frequency Y	Relative frequency x	% FreQuency x	Relative frequency y	% Frequency Y	Frequency R	% Frequency R
<-60cm	0	0	0	0,00 %	0	0,00 %	0	0,00 %
-59,9cm - -55cm	0	0	0	0,00 %	0	0,00 %	0	0,00 %
-54,9cm - -50cm	0	0	0	0,00 %	0	0,00 %	0	0,00 %
-49,9cm - -45cm	1	0	0,045454545	4,55 %	0	0,00 %	0	0,00 %
-44,9cm - -40cm	0	0	0	0,00 %	0	0,00 %	0	0,00 %
-39,9cm - -35cm	0	0	0	0,00 %	0	0,00 %	0	0,00 %
-34,9cm - -30cm	1	0	0,045454545	4,55 %	0	0,00 %	0	0,00 %
-29,9cm - -25cm	0	0	0	0,00 %	0	0,00 %	0	0,00 %
-24,9cm - -20cm	1	1	0,045454545	4,55 %	0,045454545	4,55 %	0	0,00 %
-19,9cm - -15cm	2	3	0,090909091	9,09 %	0,136363636	13,64 %	0	0,00 %
-14,9cm - -10cm	3	2	0,136363636	13,64 %	0,090909091	9,09 %	0	0,00 %
-9,9cm - -5cm	4	5	0,181818182	18,18 %	0,227272727	22,73 %	0	0,00 %
-4,9cm - 0	3	4	0,136363636	13,64 %	0,181818182	18,18 %	0	0,00 %
0,1cm - 5cm	4	4	0,181818182	18,18 %	0,181818182	18,18 %	1	4,55 %
5,1cm - 10cm	1	3	0,045454545	4,55 %	0,136363636	13,64 %	5	22,73 %
10,1cm-15cm	1	0	0,045454545	4,55 %	0	0,00 %	8	36,36 %
15,1cm - 20cm	1	0	0,045454545	4,55 %	0	0,00 %	3	13,64 %
20,1cm-25cm	0	0	0	0,00 %	0	0,00 %	2	9,09 %
25,1cm - 30cm	0	0	0	0,00 %	0	0,00 %	1	4,55 %
30,1cm- 35cm	0	0	0	0,00 %	0	0,00 %	1	4,55 %
35,1cm- 40cm	0	0	0	0,00 %	0	0,00 %	0	0,00 %
40,1cm- 45cm	0	0	0	0,00 %	0	0,00 %	0	0,00 %
45,1cm- 50cm	0	0	0	0,00 %	0	0,00 %	1	4,55 %
50,1cm- 55cm	0	0					0	0,00 %
sum	22	22	1	100,00 %	1	100,00 %	22	100,00 %

Figur 21 Observed frequency table 8”- 0^0 Scale1

Comparing this with DNV, the simplified method has a mean 0 , and lies slightly to the left. And it over predicts the maximum excursion for the given water depth as shown below.

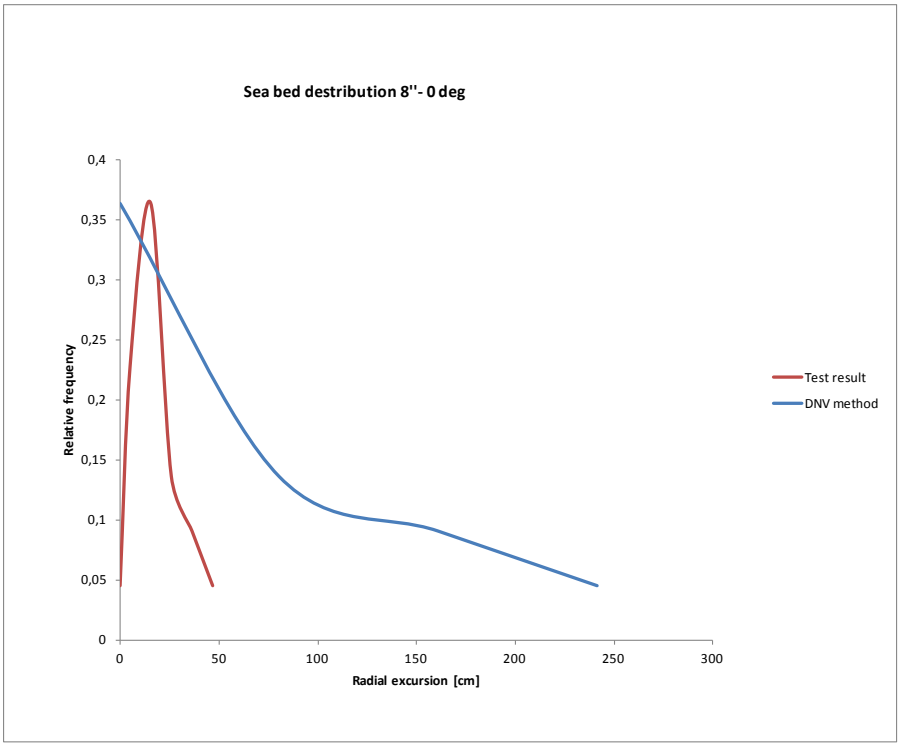

Figur 22 Test result vs. Simplified method scale 1

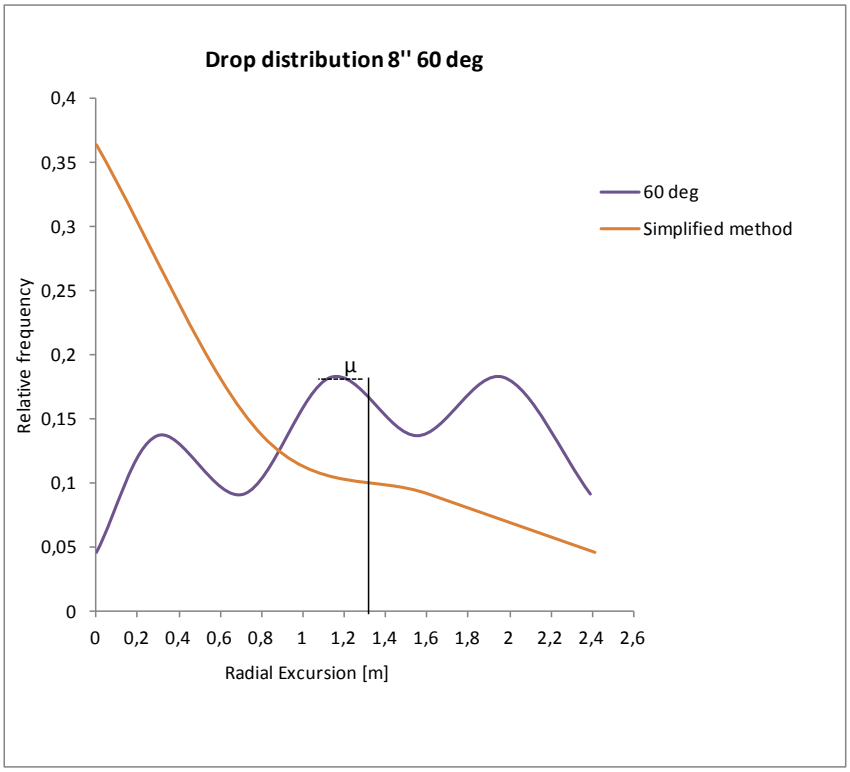

Figur 23 8'' pipe sea bed distribution scale 1- 60^0

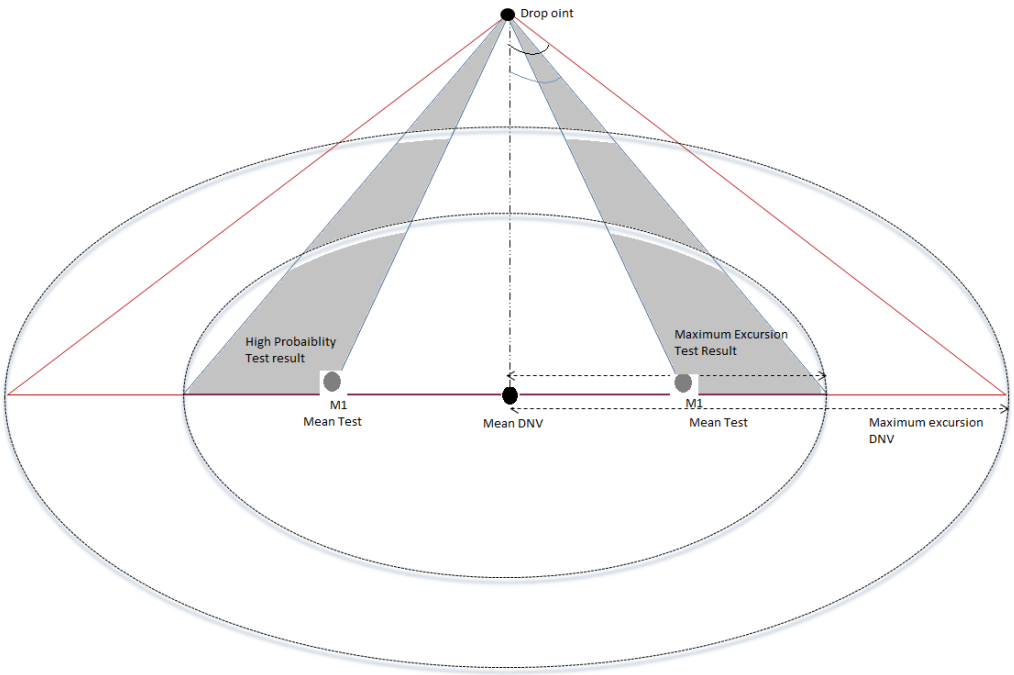

Figur 24 Comparison of 8'' test with the simplified method

Assuming we get a maximum excursion radius at 60^0 drop angle on the sea bed, and compare it with the simplified method. The mean excursion radius differs in a way that the simplified method assumes a high probability for the mean to be under the drop point, where as the test shows that there is a higher probability for the mean radius to be 1m from the drop point at 60^0 drop angle.

6.3.3 Comparison between two scales (1:33,3 and 1:16,67)

Another important observation is effect of water depth on the sea bed distribution. It's obvious that changing water depth clearly changes the hydrodynamics of the object in question. Referring to test result in table 14, comparing the two scales;

- Mean excursion on the sea bed is rationally similar for 0^0, and 60^0 drop angle.
- Increasing the scale (more water depth), the mean excursion decreases for 30^0 and 90^0, and an increases for 45^0 dropping angle.
- Maximum excursion occurs at 60-80^0 in both scales.

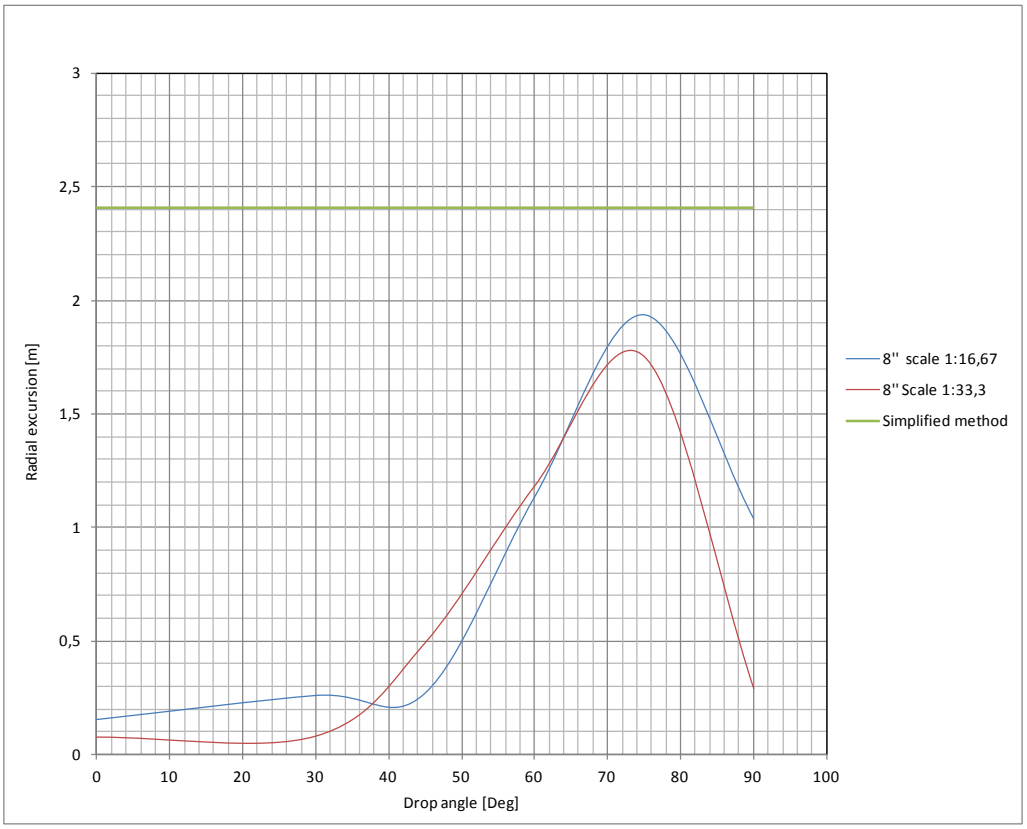

Figur 25 Drop angle and radial excursion

6.3.4 TRAJECTORY INTRODUCTION

The pipe is assumed to be dropped from the specified height with no rotation in the air in to calm water. Looking on the trajectory , α = 0-Category A,α=30-Category B,α=45 - Category C , α=60-Category D, α=75-Category E and α= 90 -Category F has been observed.

Category A :

We can observe that the motion is directionally stable between the pipe axis and vertical plane Z. The pipe gets a small rotation during the impact with water at an angle φ_1 , this angle gradualy decreases to zero since the pipe develops a returning moment. When this happenes , the pipe undergoes through a transient oscilatory motion. For small depth however the pipe hits the seabead in under purely lateral motion. The pipe hits the water perfectely horizontal at 0^0 drop angle (an ideal senario) , and no rotation initially. However, this is not usually the case, the pipe will have some rotaional inertia in the air. Hence, the angle between the cylinder axis and the free surface is the governing parameter for the motion.

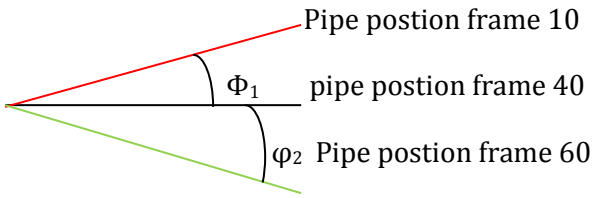

Figur 26 pipe position in frames

The pipe will oscillate between φ_1 and φ_2 due to the effect of Munk moment. The flow is assumed as near axial flow. The velocity vector (body horizontal and angular velocity) is crucial near the water surface and reduce's to a constant velocity (Body terminal velocity) as the travelling velocity stabilises. The motion is highly dependant on surface roughness , center of mass, and flow in the inner and outer cylinder if its an open cylinder. The numerical treatment of the flow will be higly dependent on choosing the right drag coefficient. Effect of current is more on the lateral motion and the total horizontal excursion on the sea bed.

Category B:

The motion is stable in the lateral direction. The axial velocity will reduced to zero at certain stage of the motion if the depth is great enough while the lateral velocity is constant. The pipe tends to turn its axis normal to the direction of motion and ocillates between φ_1 and φ_2 as shown in the Fig.60, where φ_{1max} and φ_{2max} represent the shoulder of the path. The motion is very sensetive to the hit angle and the angular velocity and angular acceleration when it hits the water surface. A similar trend has

been observed in this category which shows the consistency of the trajectory. We can further see that theortically , this can be modelled as a couple pitch-surge -heave motion.

Category C:

As the drop angle increases , the hit angle increases neglecting rotation in droping. The rotaional acceleration and velocity during impact has sginificant effect for the motion but still the hit angle are the most important parameter due to the resistance force and the rotaion it gets at impact. The axial velocity reduces gradually if greater depth considered. We can see from the shoulder of the path, that the pipe oscilates between two angles but clearly it doesn't ocillate to much as in the case of small drop angles. As the axial velocity reduces , the motion will be laterally stable.

Category D :

These pathes are observed for α=60, the motion is almost horizontal after the impact , and the axial velocity is high until it dampned by viscous force's. Hence, it travel longer in the axial direction. We can see that the pipe move axially and laterally until φ_{2max} and stabilises and the motion will be similar as to the small droping angle after wards. This shows how important the initial axial motion is for the sea bed excursion , as the excursion is further from the origin.

Category E:

This is observed in much of α=60, α=75 , the path is similar to Category D, with greater initial axial velocity , and longer shoulder than Category D.

Category F:

This trajectory is observed when α=90, it's a special category as a very small disturbance destroyes the symmetry. As observed in the path, the pipe hits the water surface vertically, but as it exits the splash zone, it develop an increasing angular deviation φ. However, the lateral motion will be constant with greater depth, and the axial velocity eventually reduces. It is observed that , φ can be in any direction between 0^0-360^0. Hence crating a circular distrbution on the sea bed. As the depth increases ,the high axial velocity reduce's and with constant lateral motion , it will be directionaly stable for a greater depth. Another important observation is that the mean can not be used as a measure of excursion for this angle , as it leads to wrong conclusion. The mean with the standard deviation can be used instead.

6.3.5 TRAJECTORY OF 8''

The trajectory followed by 0, 30, 45, and 60 in general are of category A, B, C, and D&E respectively. Looking to 90 deg dropping angle, we can see some variation due to the high axial velocity and a very little rotation during the initial impact with water.

Figur 27 8'' scale 1:33,3 90^0 path

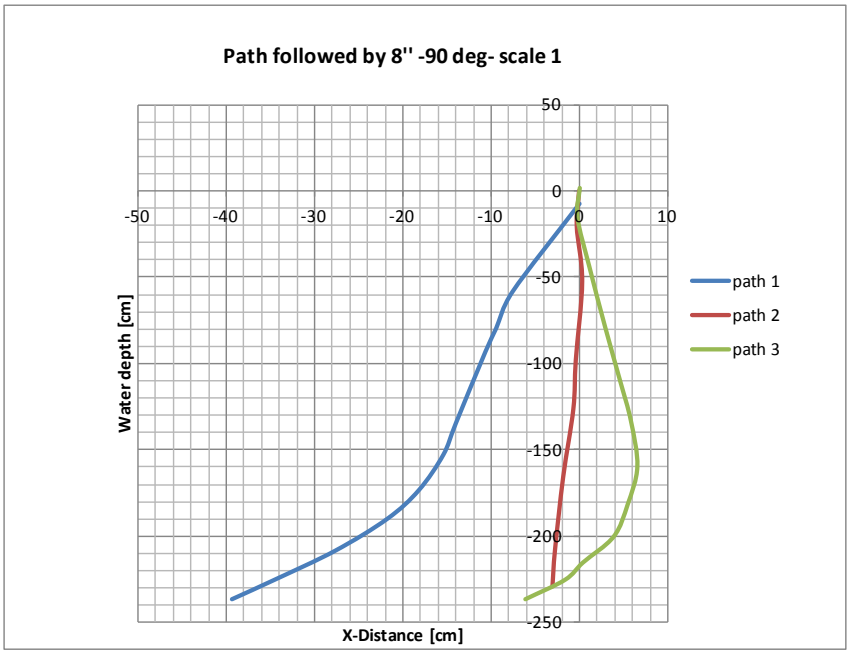

Figur 28 8'' scale 1:16,67 90^0 path

The trajectory of 90^0 droping angle for a small diameter pipe with an increasing depth is very hard to predict and it can go in any direction as observed in the test.

6.4 BASE CASE STUDY 12'' SCALE 1:33,3

6.4.1 SEABED DISTRIBUTION

Generally the distribution on the sea bed is governed by the drop angle, drop height, drop entry, impact velocity, and hydrodynamics of the object in motion. Fig 29 and Fig 30 shows the variation with drop angle.

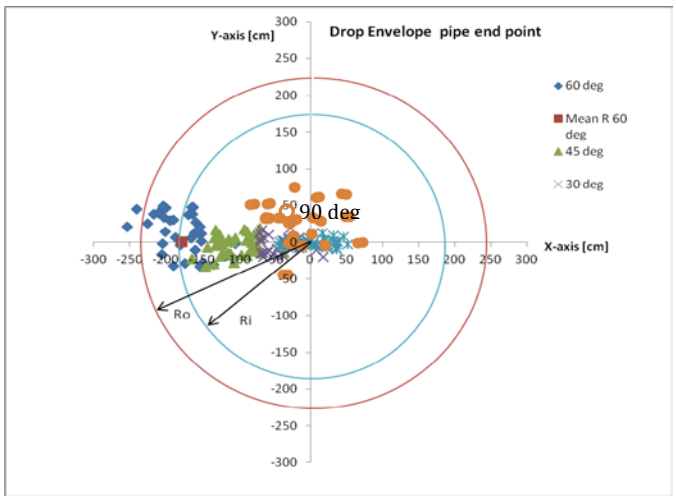

Figur 29 Distribution pipe end point

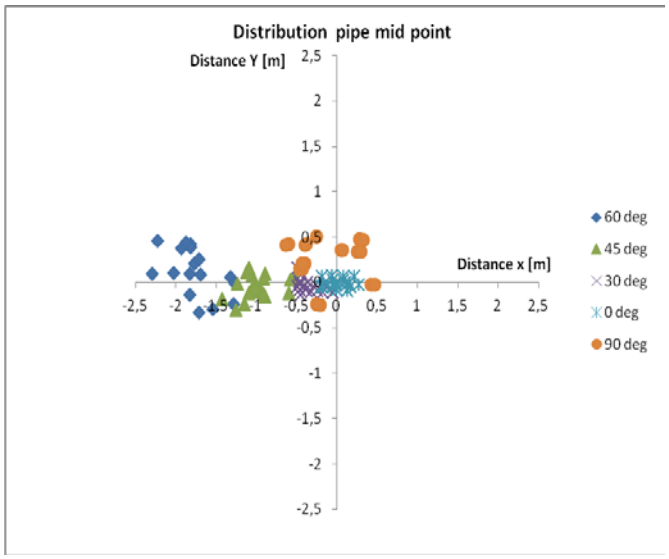

Figur 30 Distribution pipe mid point

6.4.2 COMPARISON OF DNV METHODOLOGY WITH THE RESULT OBTAINED

Table 19 Test result summery 12" scale 1:33,3

Drop angle	Mean X [cm]	Mean Y [cm]	Mean R [cm]	δ Test [cm] standard deviation	δ Simplified [cm]
0	2	1	12,4	7	47,5
30	35	3	36	13	47,5
45	99	5	100	23	47,5
60	176	13	178,6	29	47,5
90	13	26	49,6	12	47,5

We can see that at 0^0 drop angle, pipes are distributed around the x-axis in both directions close to the origin. At 30 deg, pipes are distributed around the x-axis and travelled a little bit more. As the angle increases we can see that the distribution is with respect to the x-axis and the maximum excursion occurs around $60\text{-}80^0$. At 90 deg, it is widely distributed along the y-axis in both directions. The deviation from the mean increases as the angle increases, the simplified DNV method gives an *under estimation* in this case when it comes to covering the maximum excursion radius as it doesn't consider the object specific hydrodynamic interaction.

Table 20 Comparison table 12" scale 1:33,3

Angle	75% confidence interval	Mean R radius	Max R test radius	Max R simplified radius	Standard deviation R	Lateral deviation simplified
0^0	0cm-26,4cm	12,4 cm	27,6 cm	142,5 cm	7cm	47,5cm
30^0	10cm-62cm	36 cm	51,5 cm	142,5 cm	13cm	47,5cm
45^0	54cm-146cm	100 cm	143,5 cm	142,5 cm	23cm	47,5cm
60^0	120cm-236cm	178,6 cm	229,4 cm	142,5 cm	29cm	47,5cm
90^0	25cm-73cm	49,6 cm	76,3 cm	142,5 cm	12cm	47,5cm

Case study 45^0 is shown below:

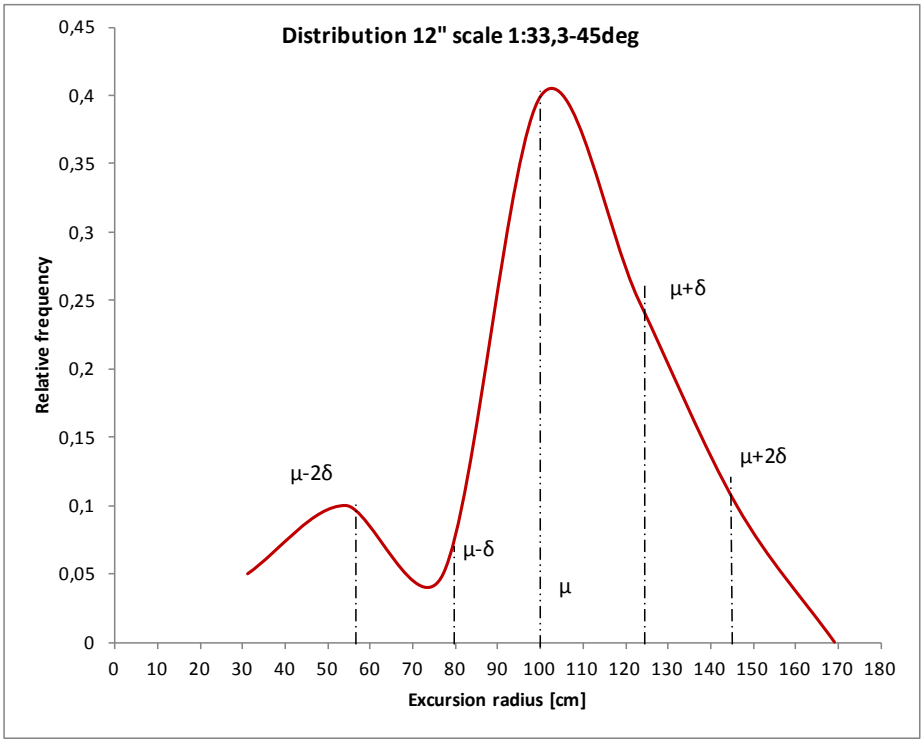

Figur 31 Sample distribution 45^0 scale 1:33,3

location in cm	FreQuency x	Frequency Y	Relative frequency x	% FreQuency x	Relative frequency y	% Frequency Y	Frequency R	%frequency R
<-235	0	0	0	0,00 %	0	0,00 %	0	0,00 %
-221,9cm- -235cm	0	0	0	0,00 %	0	0,00 %	0	0,00 %
-205,5cm- -221,8	0	0	0	0,00 %	0	0,00 %	0	0,00 %
-189,1cm- -204cm	0	0	0	0,00 %	0	0,00 %	0	0,00 %
-172,7cm- -189cm	0	0	0	0,00 %	0	0,00 %	0	0,00 %
-156,3cm- -172,6cr	0	0	0	0,00 %	0	0,00 %	0	0,00 %
-139,8cm- -156,2cr	1	0	0,05	5,00 %	0	0,00 %	0	0,00 %
-123,4cm- -139,7cr	1	0	0,05	5,00 %	0	0,00 %	0	0,00 %
-107cm- -123,3cm	5	0	0,25	25,00 %	0	0,00 %	0	0,00 %
-90,6cm- -106,9cm	8	0	0,4	40,00 %	0	0,00 %	0	0,00 %
-74,2cm- -90,5cm	2	0	0,1	10,00 %	0	0,00 %	0	0,00 %
-57,8cm- -74,1cm	1	0	0,05	5,00 %	0	0,00 %	0	0,00 %
-41,4cm- 57,7cm	2	0	0,1	10,00 %	0	0,00 %	0	0,00 %
-24,9cm- -41,3cm	0	1	0	0,00 %	0,05	5,00 %	0	0,00 %
-8,5cm- -24,8cm	0	8	0	0,00 %	0,4	40,00 %	0	0,00 %
-8,5cm-7,8cm	0	7	0	0,00 %	0,35	35,00 %	0	0,00 %
7,9cm-24,2cm	0	4	0	0,00 %	0,2	20,00 %	0	0,00 %
24,3cm- 40,6cm	0	0	0	0,00 %	0	0,00 %	0	0,00 %
40,7cm-57cm	0	0	0	0,00 %	0	0,00 %	1	5,00 %
57,1cm-73,5cm	0	0	0	0,00 %	0	0,00 %	2	10,00 %
73,6cm-90cm	0	0	0	0,00 %	0	0,00 %	1	5,00 %
90,1cm-106,4cm	0	0	0	0,00 %	0	0,00 %	8	40,00 %
106,5cm-122,8cm	0	0	0	0,00 %	0	0,00 %	5	25,00 %
122,9cm-139,2cm	0	0	0	0,00 %	0	0,00 %	2	10,00 %
139,3cm- 152,3cm	0	0	0	0,00 %	0	0,00 %	0	0,00 %
152,4cm- 165,4cm	0	0	0	0,00 %	0	0,00 %	1	5,00 %
165,5cm- 178,5cm	0	0	0	0,00 %	0	0,00 %	0	0,00 %
178,6cm- 191,6cm	0	0	0	0,00 %	0	0,00 %	0	0,00 %
191,7cm - 204,6cm	0	0	0	0,00 %	0	0,00 %	0	0,00 %
204,7cm- 217,7cm	0	0	0	0,00 %	0	0,00 %	0	0,00 %
217,8cm - 230,8cm	0	0	0	0,00 %	0	0,00 %	0	0,00 %
230,9cm - 243,9cm	0	0	0	0,00 %	0	0,00 %	0	0,00 %
sum	20	20	1	100,00 %	1	100,00 %	20	100,00 %

Figur 32 Frequency table 12'' -45^0 scale 2

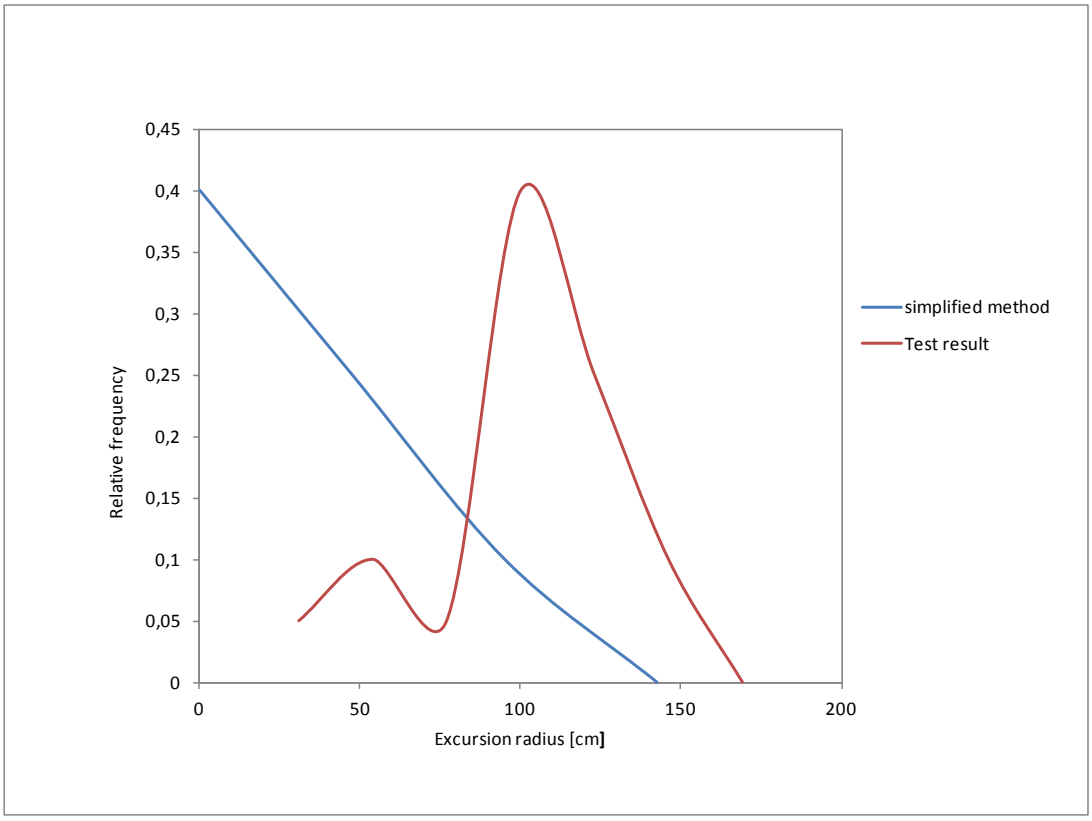

Figur 33 Normal distribution 45 deg vs. sample distribution scale 1:33,3

Comparing simplified method with the test result , the test says only 5% of the data at 45^0 drop angle falls in from 0cm- 47,5 cm. If normal distribution is assumed, 68% of the data falls in between 0cm- 47,5 cm, the present DNV recommendations says there is high probability for the mean to be zero, but as the angle increases this assumption leads to under estimation of the radial excursion for this scale.

6.4.3 COMPARISON BETWEEN TWO SCALES, 1:16, 67 AND 1:33, 3

- As the depth increases from scale 1 to scale 2, i.e. (50 m to 100 m in full scale), the excursion increases on the sea bed. That's because of the hydrodynamic forces and moments due to fluid drag changes. Coefficient of drag depends on the local Reynolds's number which itself associated with the pipe length.

- The mean radius for 30^0 drop angle, is similar in both case's indicating that the pipe follow a transient oscillatory motion in which the object appears to stall before changing to horizontal direction.

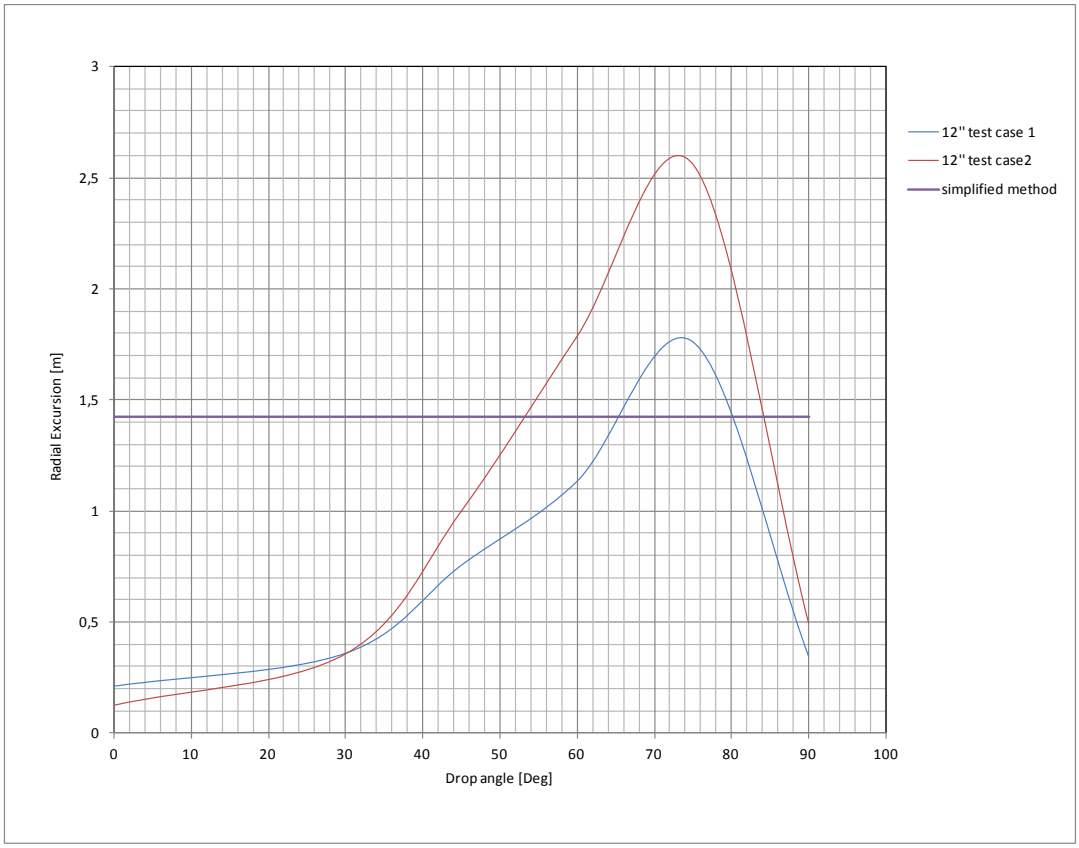

Figur 34 Drop angle and radial excursion 12" pipe

6.4.4 TRAJECTORY OF 12"

The trajectory followed by 0^0, 30^0, and 45^0 are of Category A, B, and C respectively for both scales. An interesting similarity is also seen between the two scales in drop angle 60^0 and 90^0. An illustration is given below for this two angles.

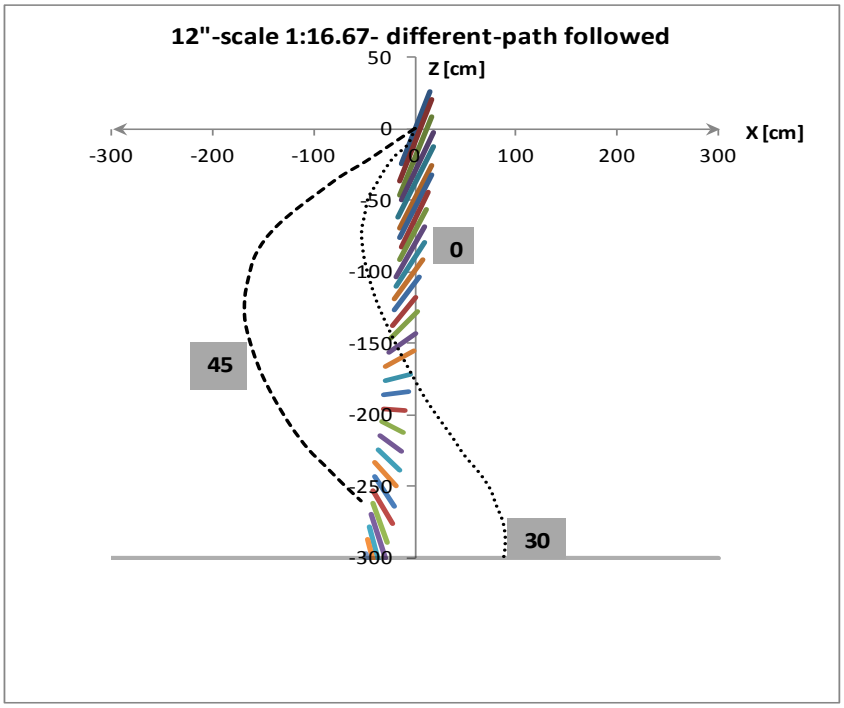

Figur 35 Drop angle vs. path for Scale 1:16,67

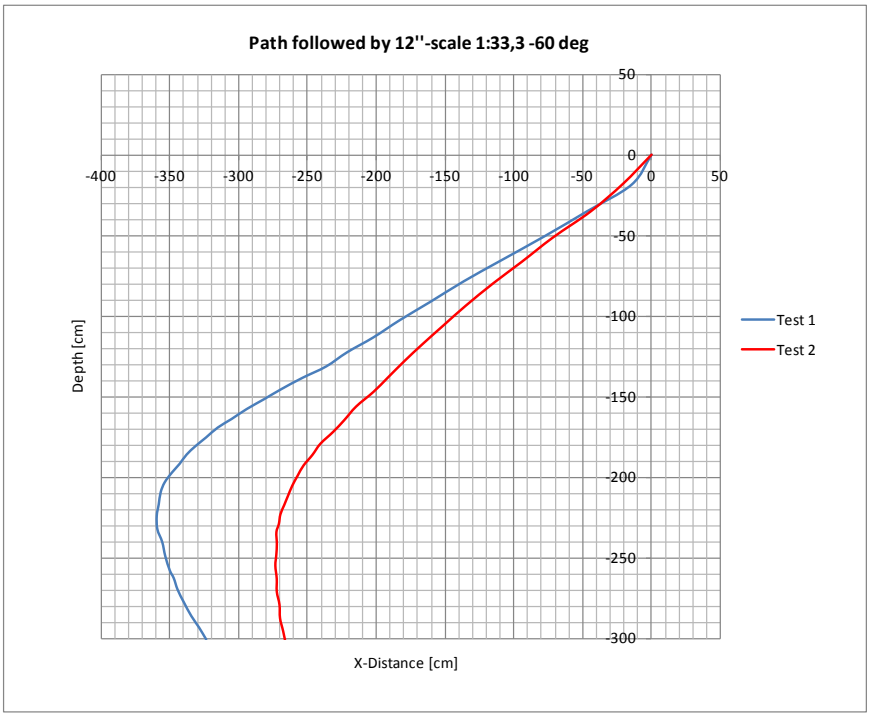

Figur 36 12” scale 1:33,3 for 60^0

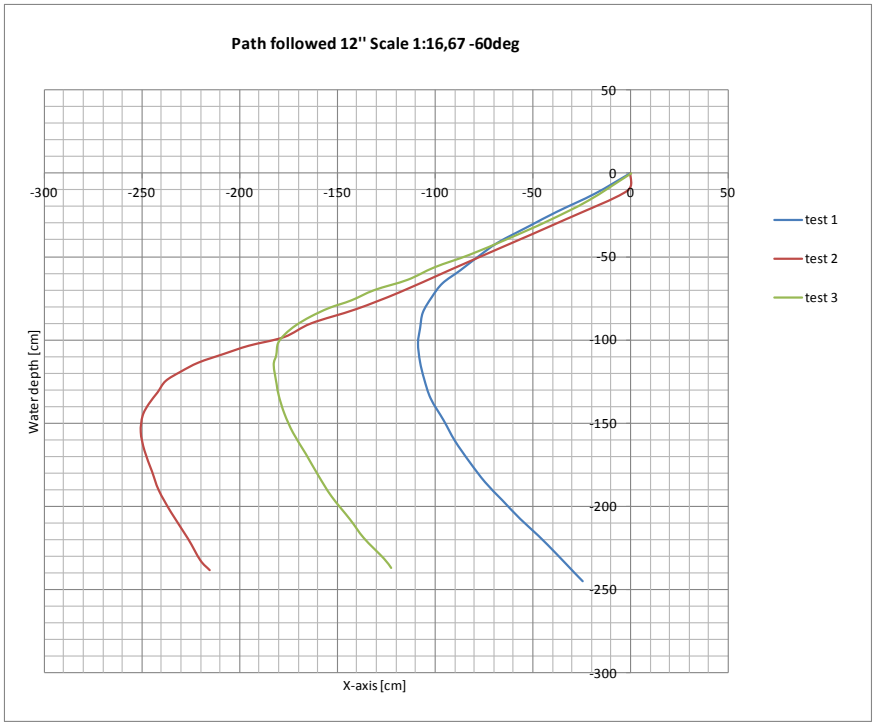

Figur 37 12" –scale 1:16,67 for 60^0

We can see from Fig (36 and 37) that scale 1:33,3 has longer shoulder comparing with scale 1:16,67. In general longer pipe with D\L ratio <<<1 has high excursion comparing with pipes which are not slender in type. Since pipe diameter length ratio (D\L) is constant, the result shows that when the depth increases, the excursion also increases at this drop angle.

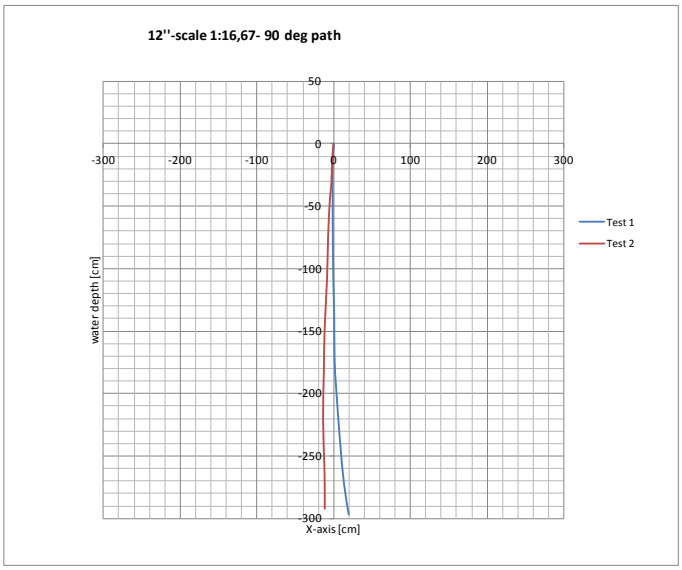

Figur 38 12" scale 1:16,67 90^0 path

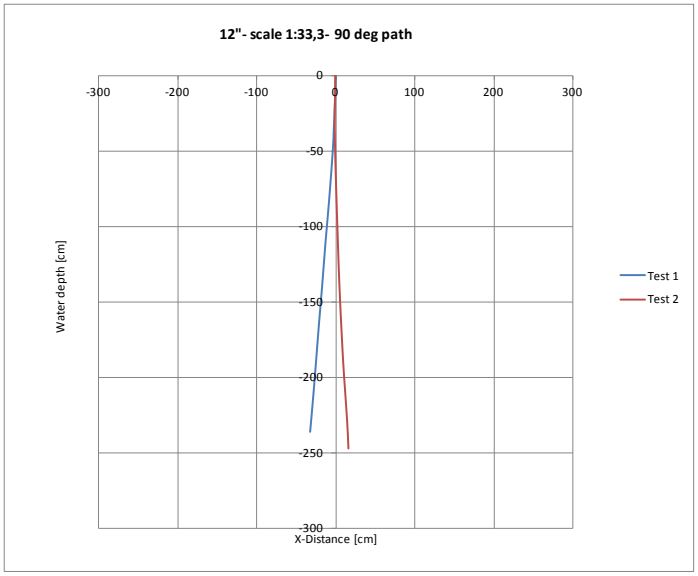

Figur 39 12'' scale 1:33,3 90^0 path

As it shown in Fig (38) and Fig (39), the 90 deg paths are with respect to the Z-axis. And the mean difference is not a lot.

6.5 FULL SCALE RESULT

6.5.1 INTRODUCTION:

Probably the difficult part of the study is changing the model scale in to full scale. Changing the result directly to full scale application might lead to erroneous conclusion if not dealt with care. This is due to several factors. To name a few limitations:

1- The depth of the tank is not big enough to study all the parameters that affect the flow.

2- Effect of current is huge when it comes to the excursion radius depending on the direction. This is not included in the experment due to resource limitation.

3- The experment performed is not supported by numerical results due to shortage of time.

4- Dropping height is crucial both in affecting impact velocity and excursion angle α. Different dropping heights have not been taken in the test.

Nevertheless, the distribution on the sea bed can be changed in to full scale for a parametric study.

Scale 1- 1:16, 67 – 50 m full scale; Scale 2- 1:33, 3 – 100m full scale

6.5.2 FULL SCALE RESULT 8'' DRILL PIPE

Table 21 Full scale test result 8"

Test no	Angle	Water depth [m]	Maximum X-excursion[m], mid point	Mean X-excursion[m] mid point	Mean R excursion[m] mid point	Standar Deviation R [m]	DNV Lateral deviation [m]
1,2	0	50	7,2	1,2	2,5	1,7	13,4
3,4,5	30	50	5,7	1,7	4,3	2	13,4
6,7	45	50	5,5	2	4,5	1,6	13,4
8,9	60	50	37,8	17	19	7	13,4
10,11	90	50	21,6	3,6	17,3	6	13,4
12,13	0	100	9,7	1	5,8	2,6	26,79
14,15	30	100	5,6	1	2,8	1,4	26,79
16,17,18	45	100	25,6	14,6	14,8	5	26,79
19,20,21	60	100	52	33,3	34,3	11	26,79
22,23,24, 25	90	100	34,6	7	21,3	9,8	15,8

6.5.3 FULL SCALE RESULT 12'' DRILL PIPE

Table 22 Full scale test result 12"

Test no	Angle	Water depth [m]	Maximum X-excursion[m], mid point	Mean X-excursion[m] mid point	Mean R excursion[m] mid point	Standar Deviation R [m]	DNV Lateral deviation [m]
26,27	0	50	5,3	1	3,6	1,7	7,9
28	30	50	10	5	6	2,5	7,9
29	45	50	16,3	11,4	12,6	4,3	7,9
30,31,32	60	50	30	18,3	19	5	7,9
33	90	50	10	3,6	5,8	3	7,9
34,35	0	100	9	0,7	4	2	15,8
36,37	30	100	16,5	11,5	12	4	15,8
38,39	45	100	47	33	33	7,7	15,8
40,41	60	100	76	58,7	59,5	9,5	15,8
42,43	90	100	21,3	4	16,5	4	15,8

6.5.4 COMPARISON OF 8'' & 12" DRILL PIPES WITH DNV IN FULL SCALE

Fig. 40 shows a comparison of 8'' pipe with 12'' pipe for a given water depth of 100m. Since we don't know at which angle the pipe hits the water surface taking the maximum excursion as the excursion radius will not be a conservative approach.

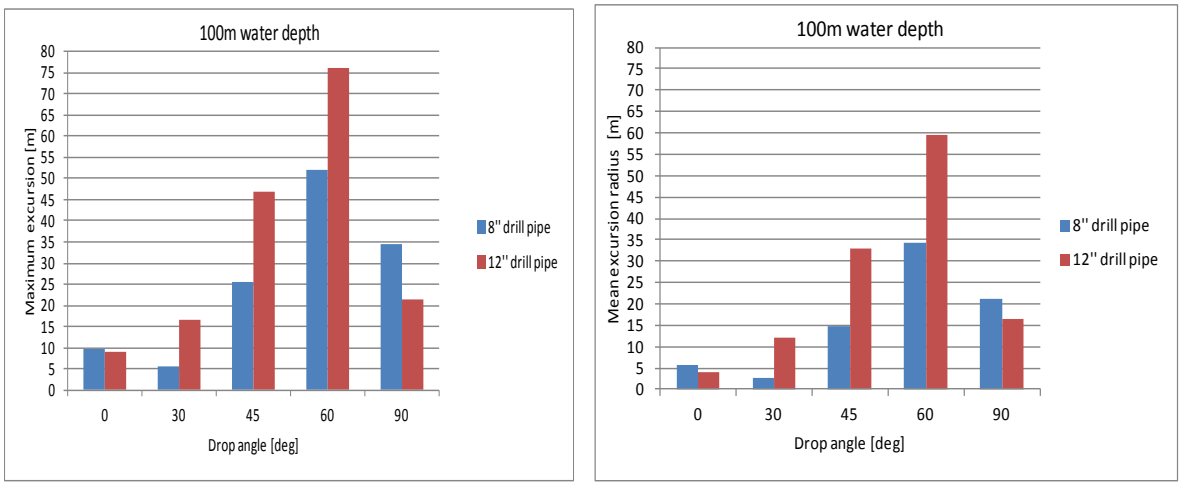

a) Maximum excursion vs. drop angle b) Mean excursion vs. drop angle

Figur 40 Variation of sea bed excursion with drop angle

The following example compares test result with the simplified method for a specified pipe diameter.

6.5.4.1 Case 1

Suppose we take the following assumption,

1- Drop points are distributed between 15m – 35m crane radius

2- A 8'' pipe is considered

3- Water depth is 100 m

4- A single drop point which is at 35m crane radius in the vertical plane is chosen

5- The crane is located at (0,0)

6- The drop angle is between 0^0-360^0 , a maximum excursion assumed to be at 60^0

7- No rotation in the air

These yields to the following result when compared with DNV approach.

DNV:

The mean lies under the drop point; hence we get 0m mean radius at the sea bottom. This indicates a high probability of the hit point to be under drop point. On the other hand the lateral deviation is 26,79m which gives us a maximum hit radius of 80m. This approach is based on the assumption that the hit points are normally distributed. We can see that DNV takes a conservative lateral deviation.

$\delta = d.\tan\alpha \rightarrow 100.\tan(15) = 26{,}79m$

$R_{Max} = mean + 3\delta$, since it is normal distribution

$R_{Max} = (0 + 3(26{,}79)) = 80{,}38m$

Test result:

The mean is further away from a drop point by 34m; the deviation is 11m which is smaller than what is expected by a simplified method. The mean radius is reasonable unlike the DNV methodology. The maximum hit point is smaller by 23% compared with DNV.

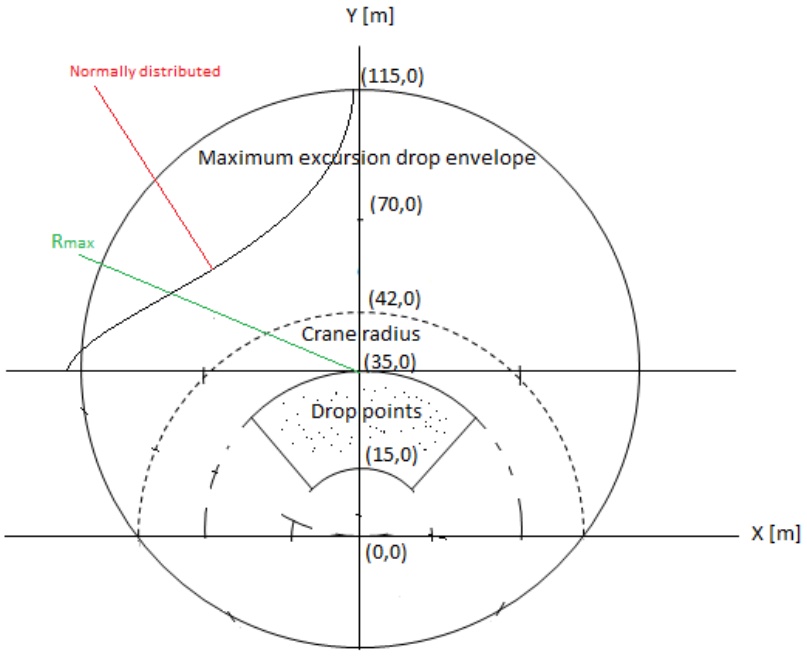

Figur 41 8'' Full scale DNV 100m case 1

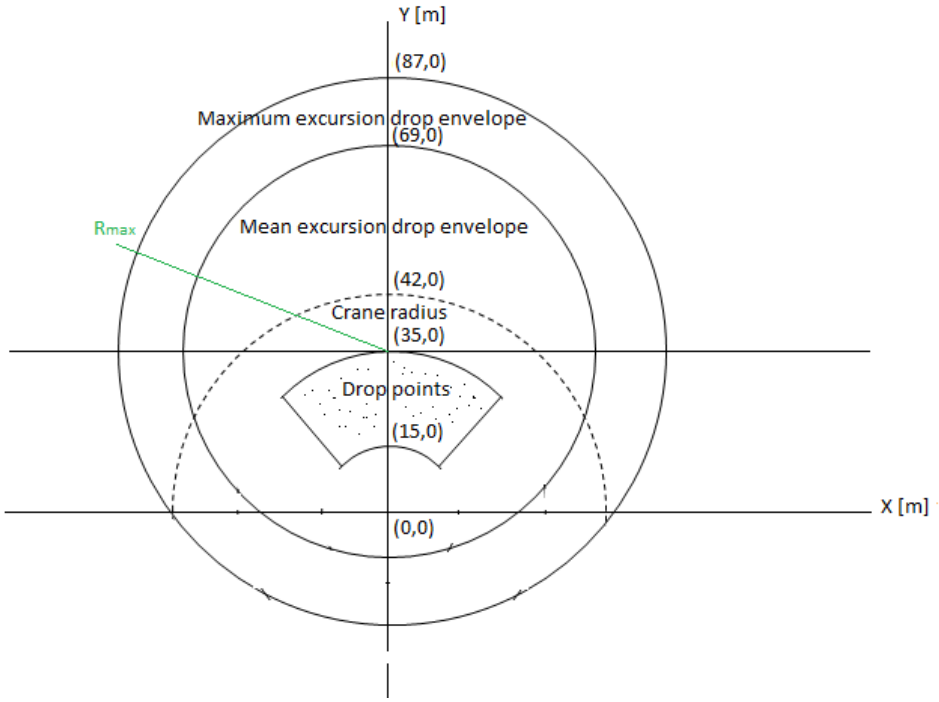

Figur 42 8'' Full scale test Drop envelope 100m

6.5.4.2 Case 2

Suppose we take the following assumption,

1- Drop points are distributed between 15m – 35m crane radius

2- A 12'' pipe is considered

3- Water depth is 100 m

4- A single drop point which is at 35m crane radius in the vertical plane is chosen

5- The crane is located at (0,0)

6- The drop angle is between 0^0-360^0 , a maximum excursion assumed to be at 60^0

7- No rotation in the air

These yields to the following result when compared with DNV approach.

DNV:

The mean lies under the drop point; hence we get 0m mean radius at the sea bottom. This indicates a high probability of the hit point to be under drop point. On the other hand the lateral deviation is 15,8m which gives us a maximum hit radius of 47m. This approach is based on the assumption that the hit points are normally distributed. We can see that DNV takes a conservative lateral deviation but it doesn't cover the possible maximum hit points on the sea bed compared with the test conducted.

Test result:

The mean is further away from a drop point by 59,5m; the deviation is 9,5m which is smaller than what is expected by a simplified method. The mean radius is reasonable unlike the DNV methodology. The maximum hit point is larger by26% compared with DNV

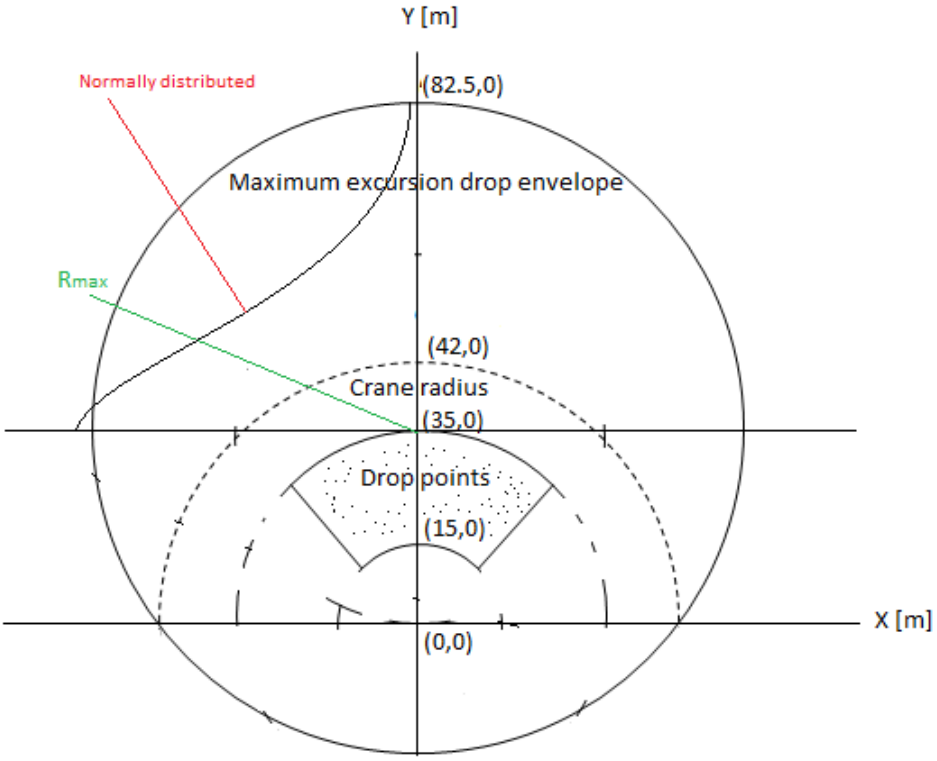

Figur 43 12" full scale DNV 100m case 2

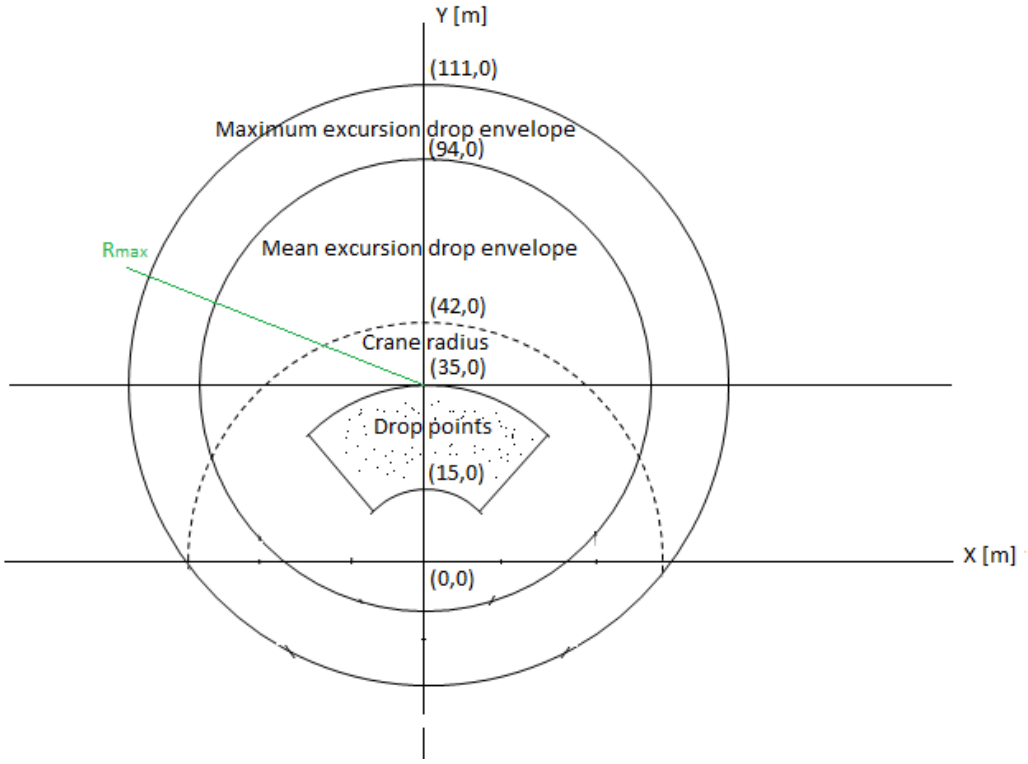

Figur 44 12" full scale 100m Test result case 2

6.6 CONTAINERS

6.6.1 INTRODUCTION:

Type of container in this test used is 40'' shipping container-see section (3.2.3). It represents baskets for offshore operations. While most of the containers are picked up with a ship while floating, the study conducted here is to see the motion under water for a sinking container. The study shows a consistency in the distribution.

These objects will in general fall like the compact objects after they are filled with water. With great depth the trajectory might be oscillatory for closed containers. The container starts to sink when 80% is filled with water depending on the weight distribution. The center of mass will rule the trajectory since there is an initial rotation before it sinks.

6.6.2 SEABED DISTRIBUTION:

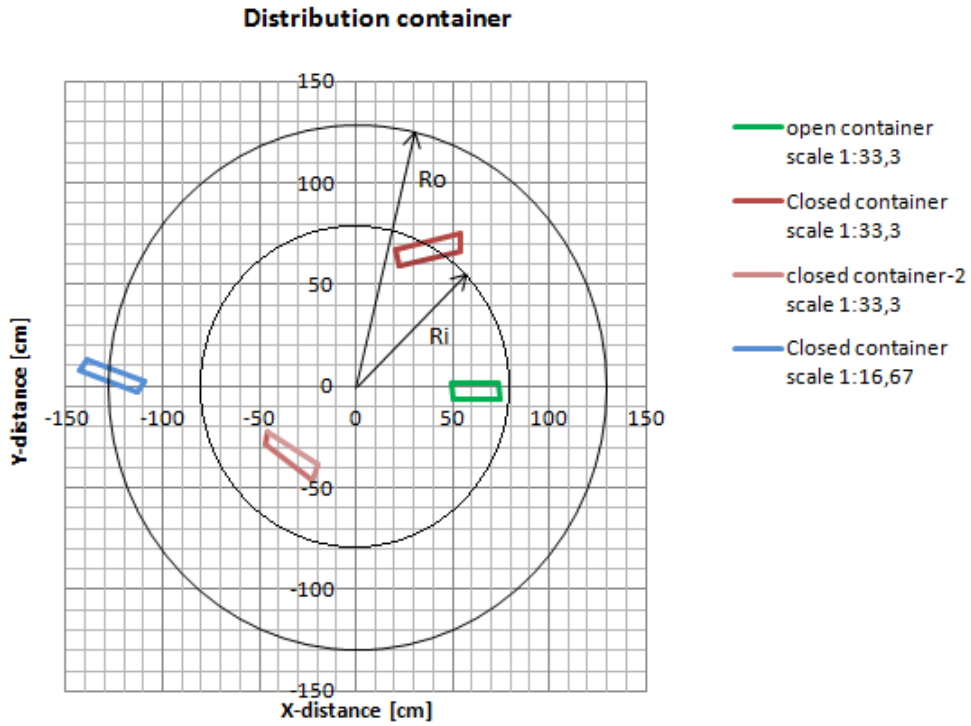

Figur 45 Scale 1:33,3

Open container: Radius of excursion 62 cm; Scale 1:33, 3 → 21m full scale for a 100m water depth.

Closed container: Radius excursion R_i = 77cm; Scale 1:33, 3 → 25,6m in full scale for a 100m water depth.

Closed container: Radius 126,5cm; Scale 1:16, 67 → 21m in full scale for a 50 m water depth.

6.6.3 TRAJECTORY

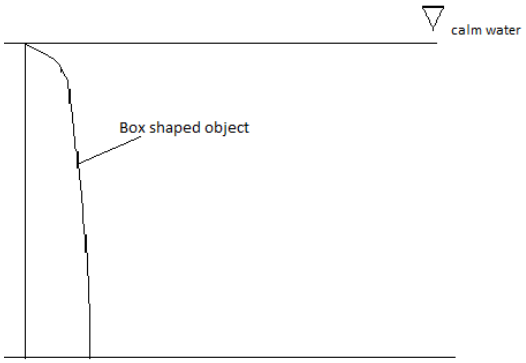

Figur 46 A typical trajectory for a container

Closed containers need longer time before they sink depending on the leak points and mass distribution. The excursion will give an angle of spread varying with depth; the maximum spread suggested is 3^0 from sinking point to sea bed [15]. The total spread angle φ can then be calculated. x- drift (Excursion) ϵ (0, 40), the maximum drift is assumed to be 40m for containers < 1t.

$\Phi_{total} = \tan^{-1}(\tan 3^0.(H+x))/H$

H- Depth ϵ (0, 1000)

Observed path in the test:

Figur 47 a) Trajectory closed container: 3D b) Trajectory open container: 3D

Chapter 7 CONCLUSION AND RECOMMENDATION

7.1 INTRODUCTION

A model test has been performed to investigate the trajectory and seabed distribution of a falling drill pipe and a container. The result obtained somehow describes the event from dropping point to the bottom of the tank. This test result can be used to support numerical results obtained by modeling and simulating programs since there are only few available data in literature. The digital camera used to record the trajectory and distribution on the sea bed in combination with the available digitizing program to retrieve the data helps in avoiding error comparing with analog observation. The amount of data collected from the test can be used for further analysis, or for the use of statistics.

If numerical modeling has been done for the test, the recorded time, and horizontal excursion at the maximum, intermediate and at the bottom can be used as an input together with hydrodynamic loading to calculate the velocity in each time step. The maximum excursion points and the seabed hitting points are plotted. (Appendix B).

The maximum possible horizontal excursion can be calculated or predicted knowing the parameters that affect the motion combining experimental results with numerical modeling. A danger zone can be marked around the platform with a radius R, as probability distribution function of the drop angle and drop height. The present recommended methodology for use of calculation by DNV is generally conservative and in some case's not conservative at all. The simplified method gives the initial estimate since it's based on a general category rather than a specific object hydrodynamics. Application of numerical tools in combination with experimental data promotes further development in preventing potential dropped/ falling objects.

7.2 MAJOR FINDINGS FROM THE TEST

1- Comparing 8'' drill pipe with 12 "pipe, we can see that at drop angle 90^0 the mean excursion radius decreases as the diameter increases. This is probably due the viscous upward pressure force distribution in the pipe, and moment of inertia of the body. As the diameter and mass increase's, the resistance to rotation also increase's. Hence the pipe travels close to a straight line in early stage of the path. This changes of course as the depth increases and the pipe will develop a rotational moment perpendicular to its axis due to an increasing angular deviation along its axis. However, as the diameter decreases with an increase water depth, the trajectory is difficult to predict as it can go in any direction.

2- As the diameter of the pipe increases for a drop angle 60, and 45 deg- the excursion radius increases. This is due to the combination of an increase in mass and tangential velocity at the early stage of the path and apparently this will dampened by viscous forces in the later stage. The simplified method underestimates the maximum excursion for 12'' pipe.

3- As the diameter of the pipe increases, for a drop angle 30 deg, the mean excursion radius increases by significant amount when great depth.

4- As the diameter of the pipe increases, for a drop angle 0 deg, the mean excursion radius increases , however if great depth is considered , the mean excursion radius reduce since the pipe will undergo from purely lateral motion in to a transient oscillatory motion due to the Munk moment.

5- The present simplified DNV methodology is way over predicting the drop envelope for 8'' pipe < 2t, as it doesn't consider specific hydrodynamic interaction.

6- The simplified method under predicts the drop envelope for 12'' pipe > 2t. The safety factor is almost twice the value obtained in both cases.

7- If δ is lateral deviation, and α is angular deviation;

   $\alpha = 8^0$-10^0 is found to be reasonable for 8'' pipe < 2t ;

   $\alpha = 6^0$ is found to be reasonable for 12'' pipe >2t

8- Open containers have the tendency of transient oscillatory motion while closed containers follow a trajectory of compact objects.

7.3 RECOMMENDATION

If the test is performed in much bigger scale with a known coefficient of drag and sensors to record the instantaneous acceleration and velocity of the trajectory, detail analysis can be done. The use of slender theory has its own limits and its application in deep water might not be reliable. Impact loads at the splash zone, effect of current, axial rotation of the cylinder, arbitrary mass distribution should be included in further study.

1- A larger tank experment where current and rotation of the body in the air is included

2- Numerical treatment of the experment conducted in this paper, developing a model to do: Monte Carlo simulation, simulating the path, finding the maximum velocity, acceleration, and distribution on the sea bed using the data as an input.

7 REFERENCE'S

1- Dropped Objects Register of Incidents & Statistics. (2011). Hentet 2015 fra http://dropsonline.org/assets/documents/DORIS-Presentation.pdf

2- Veritas, D. N. (2010, october). Recommended practice DNV-RP-F107.

3- V.Aanesland. (1984). *Expermental And Numerical Investigation of Accidental Drops of Drilling Tubes.* Trondheim: NTNF.

4- J.N.Newman. (1977). *Marine Hydrodynamics.* The Massachusetts Institute of Technology.

5- I.C.Browen, & RY, S. (1989). The assessment of impact damage caused by dropped objects on concrete offshore structures. *OTH 87 240.* London: H.M.S.O.

6- A.Santhakumaran. (u.d.). Mathimatical Modelling on motion of free falling objects.

7- Yonghwan, K., Yuming, L., & Dick, K. Y. *Motion Dynamics of three-dimentional bodies falling through water.* Cambridge.

8- ESDU. (1980). *Mean forces, pressure and flow field velocities for a circular cylinder structure.* Hentet 2015 fra https://www.esdu.com/cgi-bin/ps.pl?sess=unlicensed_1150615120016gtc&t=doc&p=esdu_80025c

9- Y.Luo, & J.Davis. (1992). Motion simulation and hazard assessment of dropped objects. London.

10- Apslay, D. (2013). *Dimentional Analysis* .

11- TMR7. *Expermental Methods in Marine Hydrodynamics.* Trondheim: NTNU.

12- ANSI/ASME B36 10M-1995; http://www.wes.ir/files/797832605piptub.pdf

13- ISO 4200

14- Katteland, L. H., & Øygarden, B. (1995). *Risk Analysis Of Dropped Objects For Deep Water Development.* Stavanger: OMAE.

15- Rohatgi, A. (2014). *Web Plot Digitizer*. Hentet 2015 fra http//arohatgi.info/WebPlotDigitizer

APPENDIX A

SEA BED DISTRIBUTION 8'' PIPE

The entire Dimension in both X- Y axis are expressed is in [cm], only selected number of tests are included in the appendix. Each grid is 15cm x 15 cm.

Scale 1 – 1:16,67 → 50m in full scale

Scale 2- 1:33,3 → 100m in full scale

TEST 2

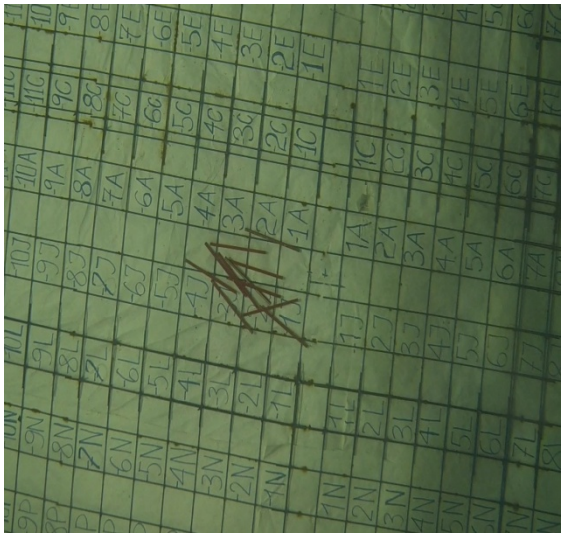

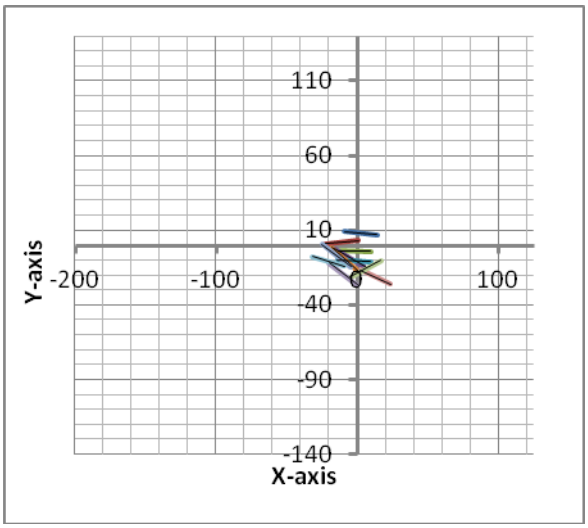

8''- Scale 1- 0^0 original picture

8''-Scale 1- 0^0 digitized version [cm]

TEST 3

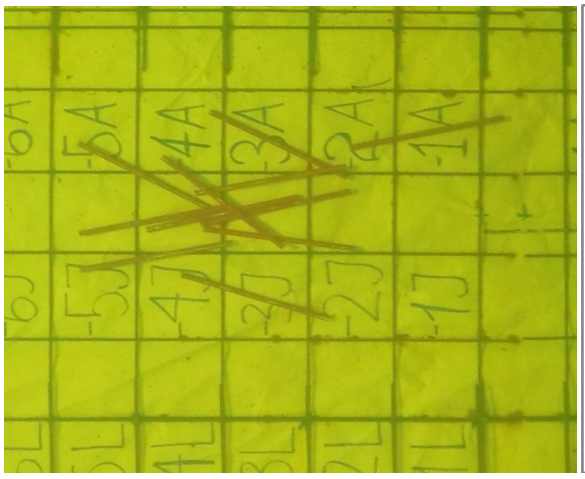

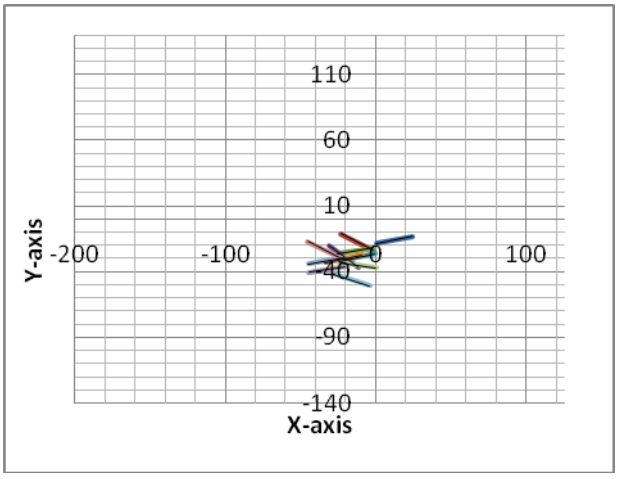

8''- Scale 1- 30^0 original picture

8''-Scale 1-30^0 digitized version [cm]

TEST 6

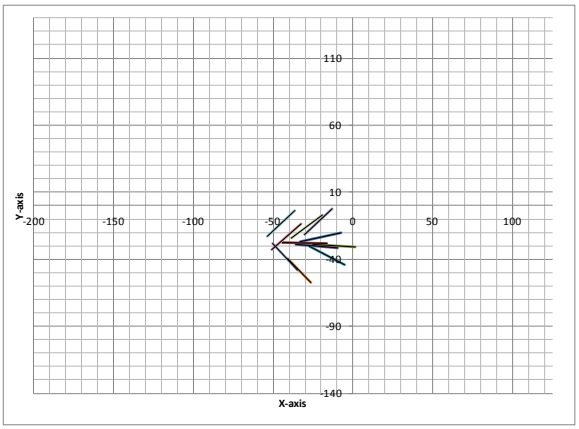

8''- Scale 1- 45^0 original picture

8''-Scale 1-45^0 digitized version [cm]

TEST 9

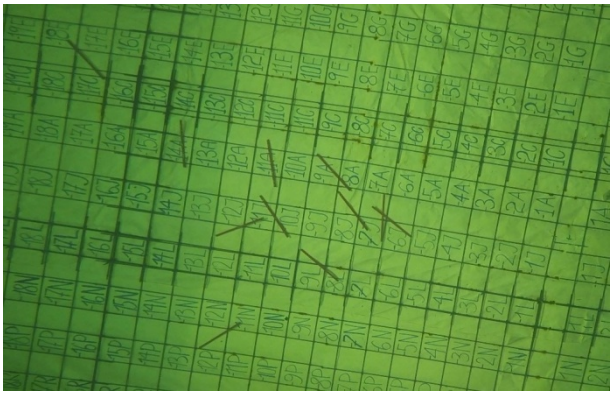

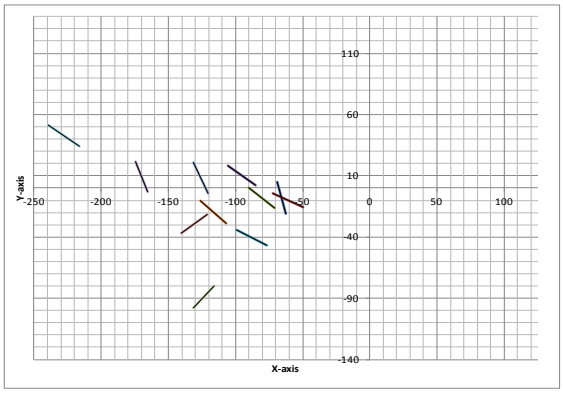

8''- Scale 1- 60^0 original picture

8''-Scale 1-60^0 digitized version [cm]

TEST 11

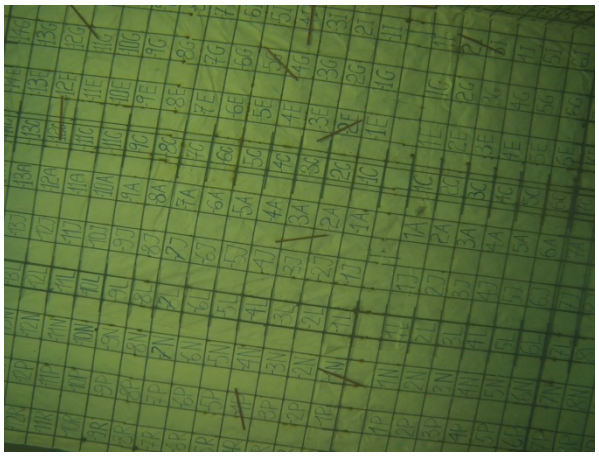

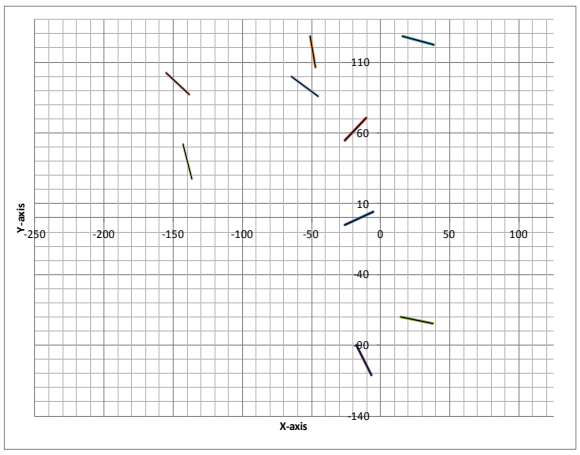

8''- Scale 1- 90^0 original picture

8''-Scale 1-90^0 digitized version [cm]

TEST 13

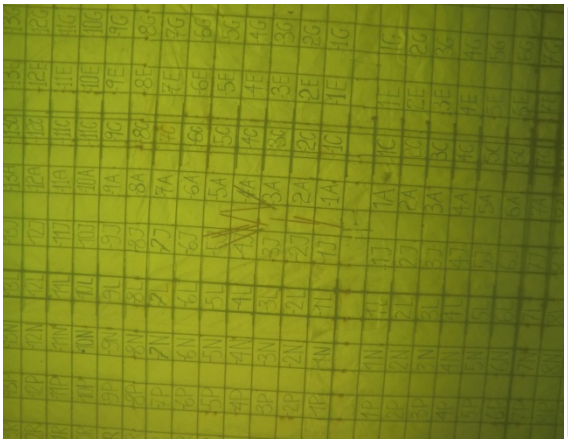

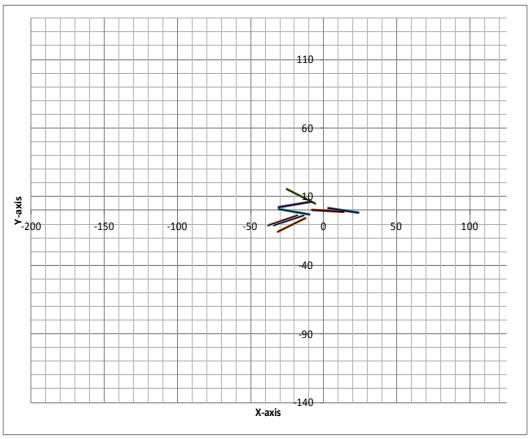

8''- Scale 2- 0^0 original picture 8''-Scale 2-0^0 digitized version [cm]

TEST 14

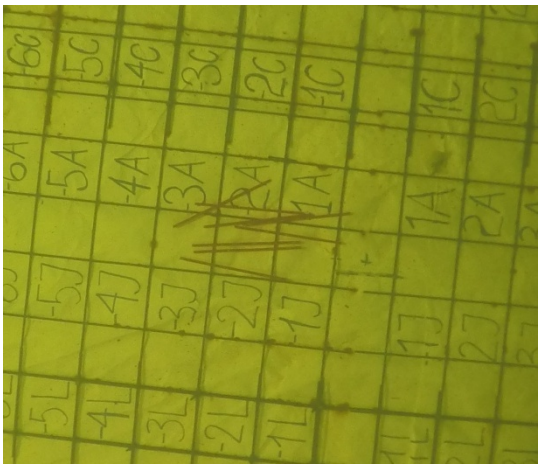

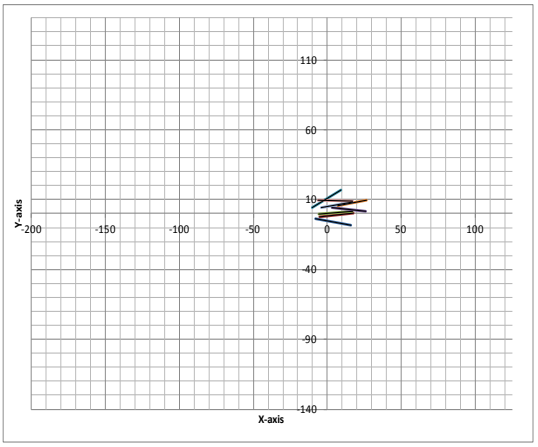

8''- Scale 2- 30^0 original picture 8''-Scale 2-30^0 digitized version [cm]

TEST 16

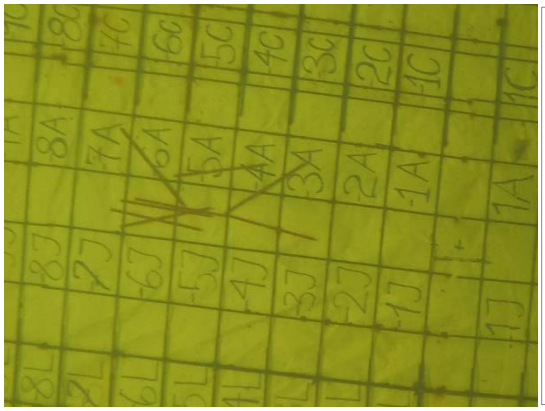

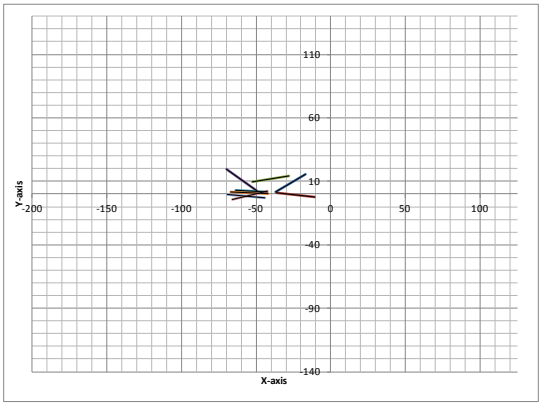

8''- Scale 2- 45^0 original picture 8''-Scale 2-45^0 digitized version [cm]

TEST 19

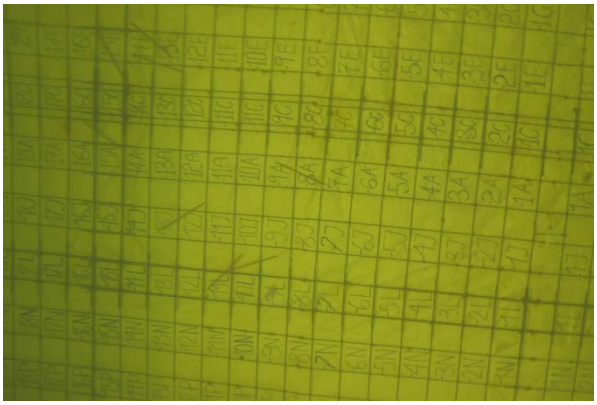

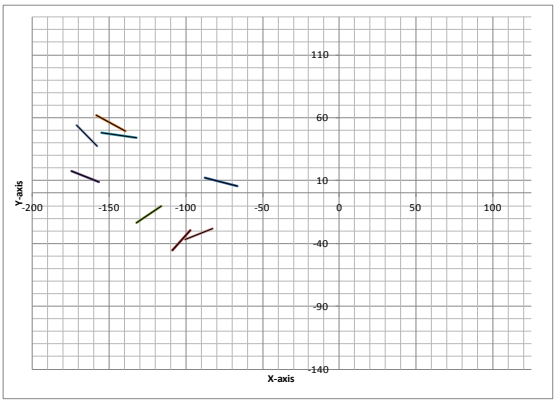

8''- Scale 2- 60^0 original picture

8''-Scale 2-60^0 digitized version [cm]

TEST 24

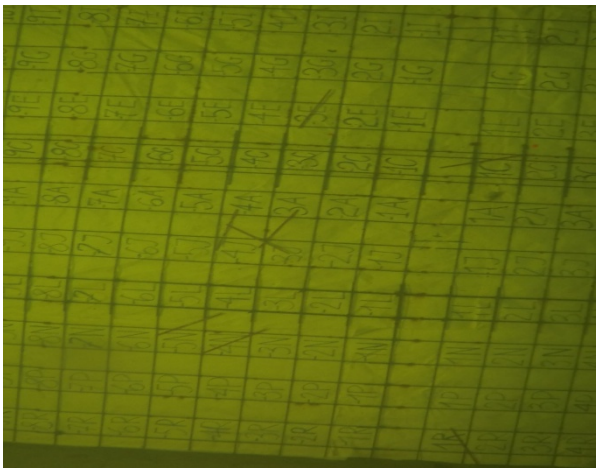

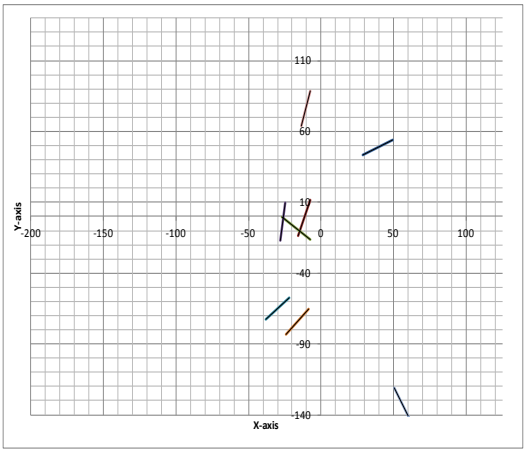

8''- Scale 2- 90^0 original picture

8''-Scale 2-90^0 digitized version [cm]

SEA BED DISTRIBUTION 12'' PIPE

TEST 26

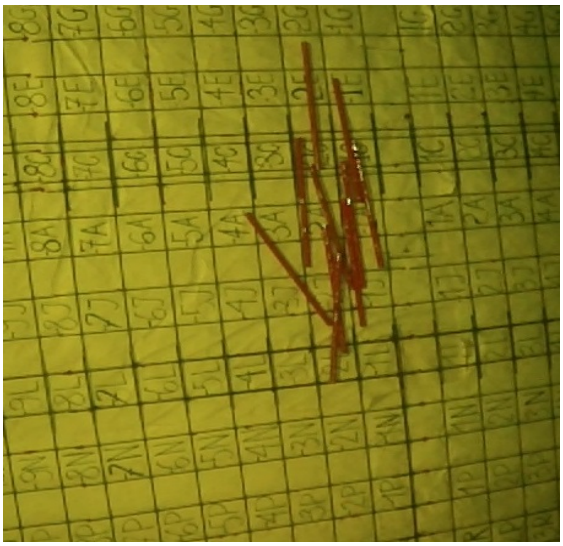

12''- Scale 1- 0^0 original picture

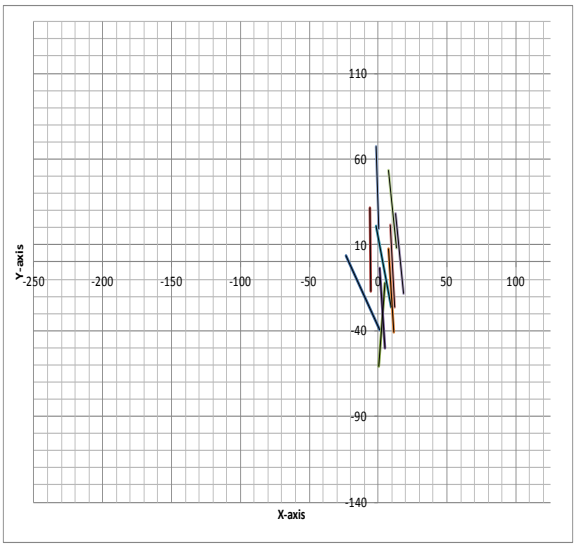

12''-Scale 1-0^0 digitized version [cm]

TEST 28

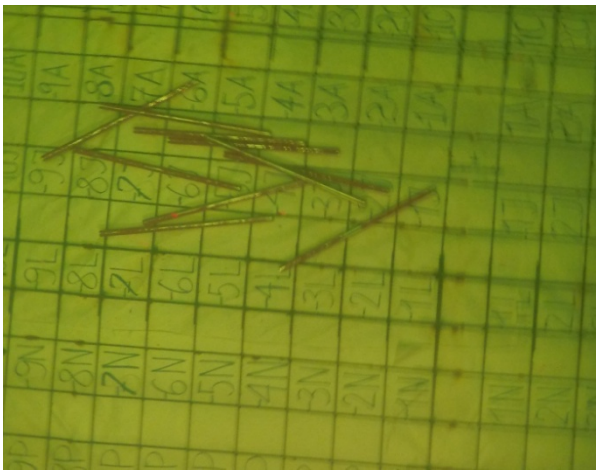

12''- Scale 1- 30^0 original picture

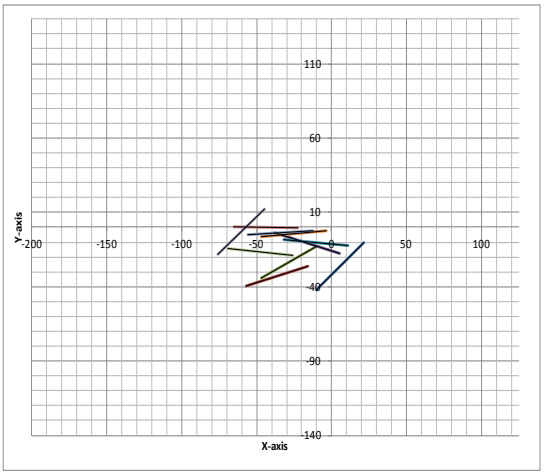

12''-Scale 1-30^0 digitized version [cm]

TEST 29

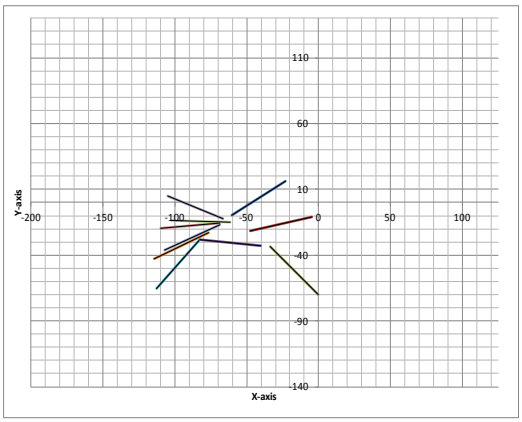

12''- Scale 1- 45^0 original picture 12''-Scale 1-45^0 digitized version

TEST 30

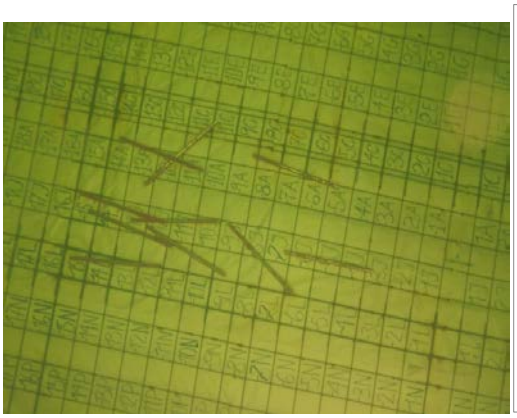

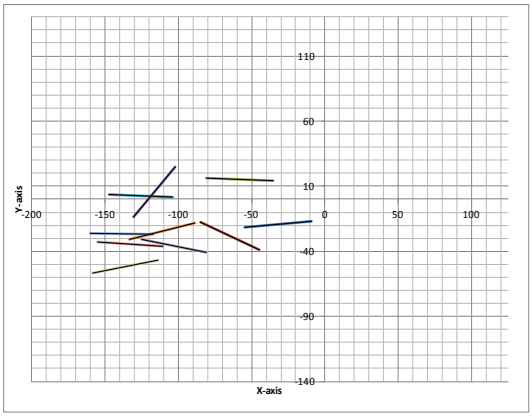

12''- Scale 1- 60^0 original picture 12''-Scale 1-60^0 digitized version [cm]

TEST 33

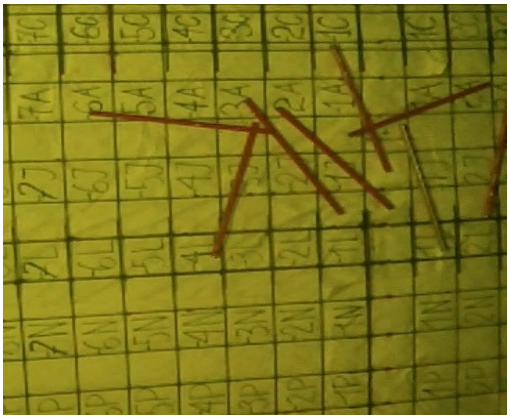

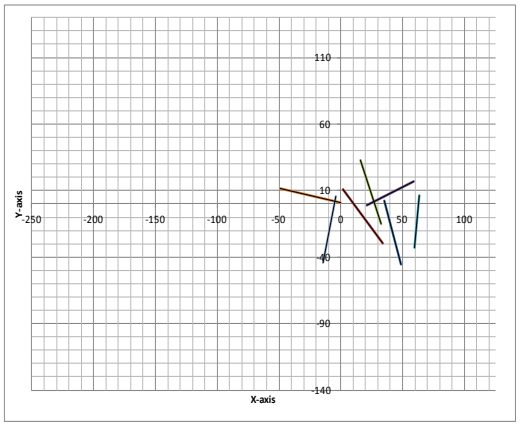

12''- Scale 1- 90^0 original picture 12''-Scale 1-90^0 digitized version [cm]

TEST 34

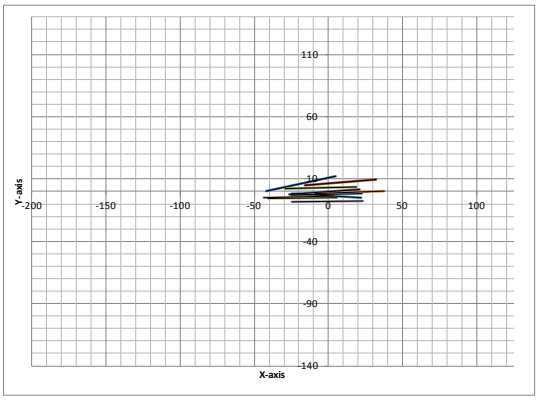

12''- Scale 2- 0^0 original picture 12''-Scale 2-0^0 digitized version [cm]

TEST 37

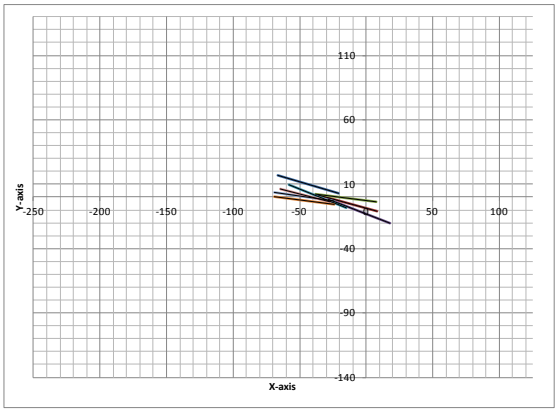

12''- Scale 2- 30^0 original picture 12''-Scale 2- 30^0 digitized version [cm]

TEST 39

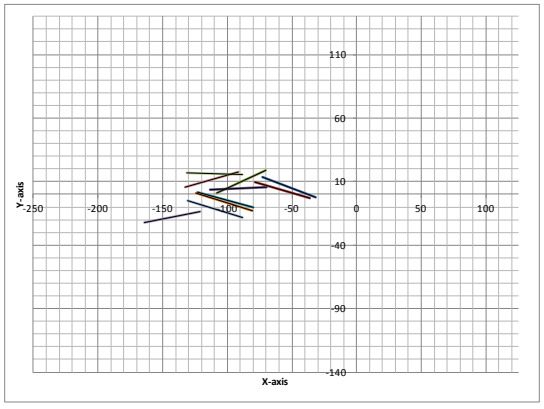

12''- Scale 2- 45^0 original picture 12''-Scale 2- 45^0 digitized version [cm]

TEST 41

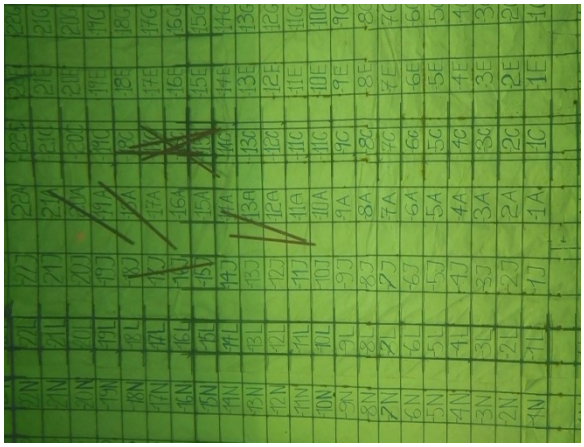

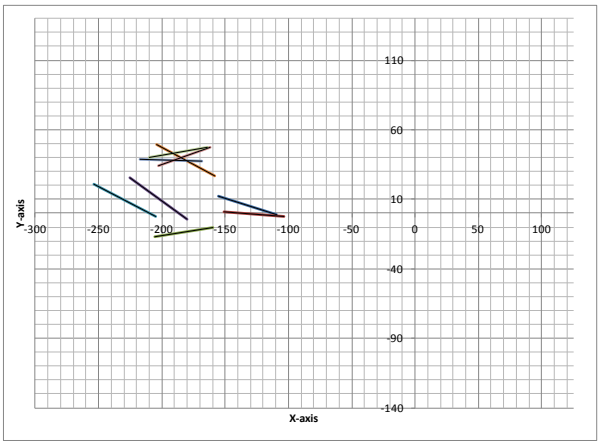

12''- Scale 2- 60^0 original picture

12''-Scale 2- 60^0 digitized version [cm]

TEST 43

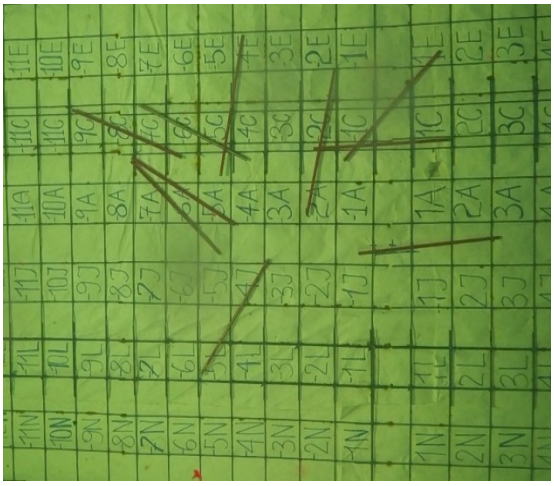

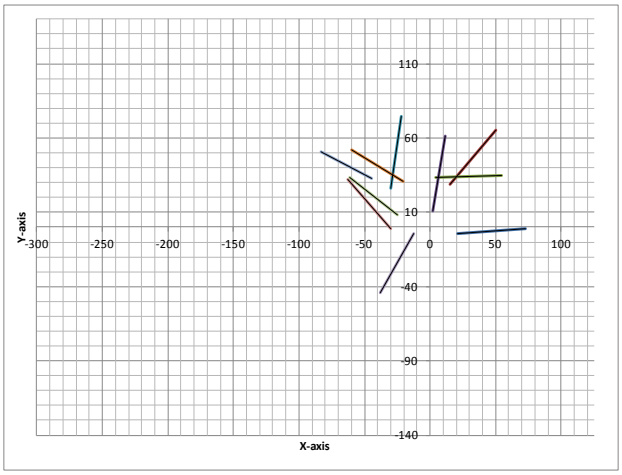

12''- Scale 2- 90^0 original picture

12''-Scale 2- 90^0 digitized version [cm]

APPENDIX B

TRAJECTORY 8'' PIPE

Only selected trajectories are included in the appendix.

PATH 2

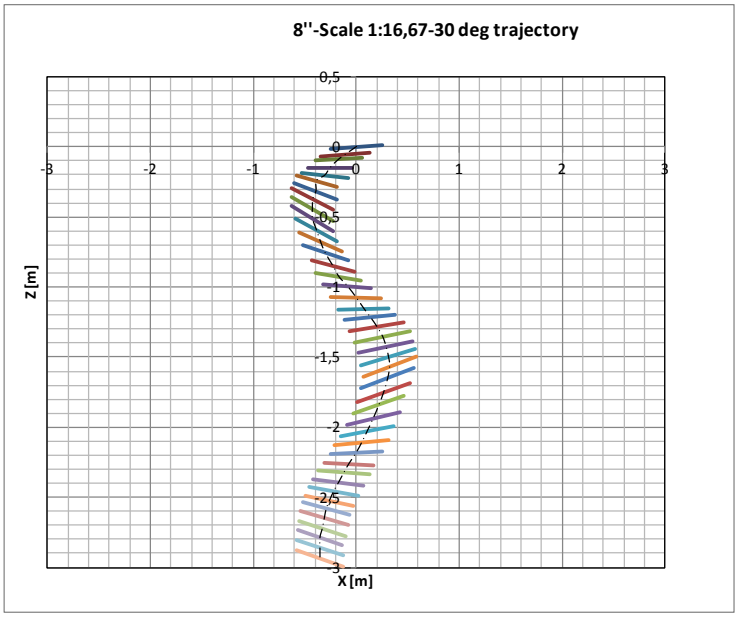

8'' Scale 1- 30^0 trajectory followed

PATH 3

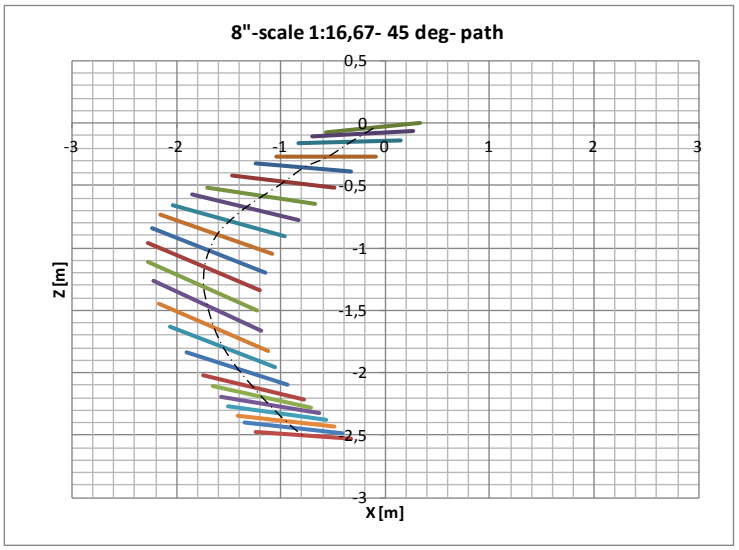

8'' Scale 1- 45^0 trajectory followed

PATH 4

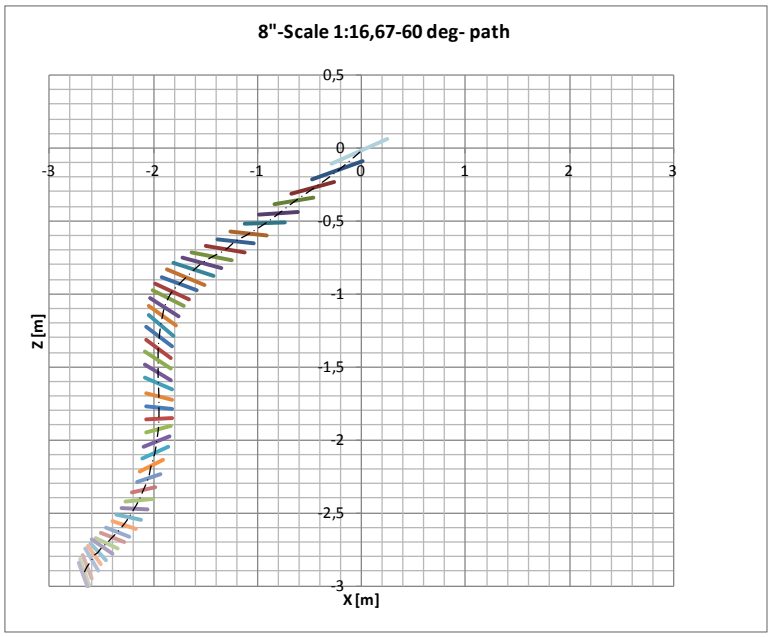

8'' Scale 1- 60^0 trajectory followed

PATH 5

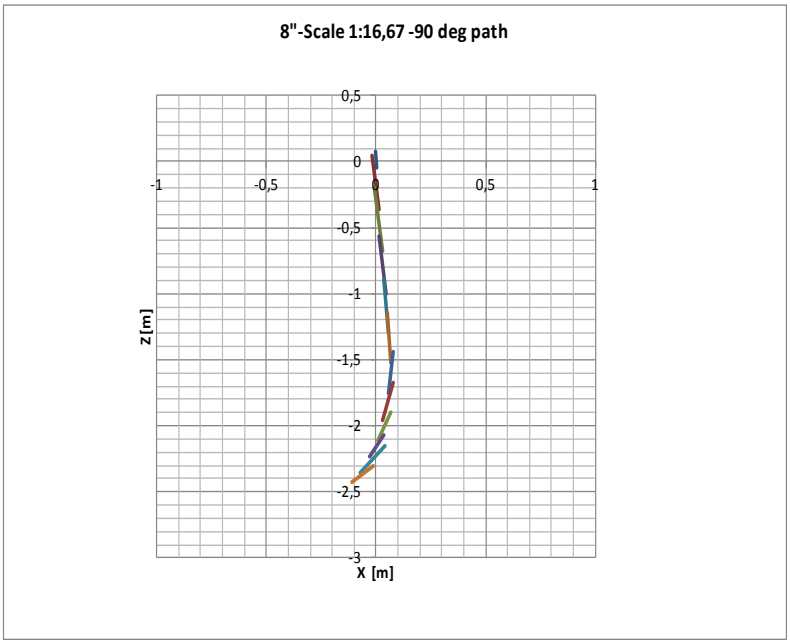

8'' Scale 1- 90^0 trajectory followed 1

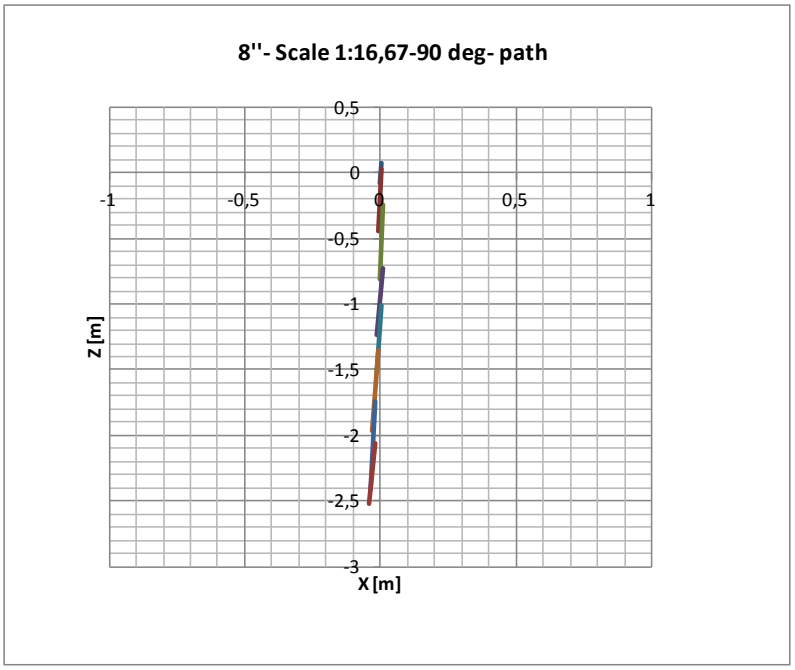

8'' Scale 1- 90^0 trajectory followed 2

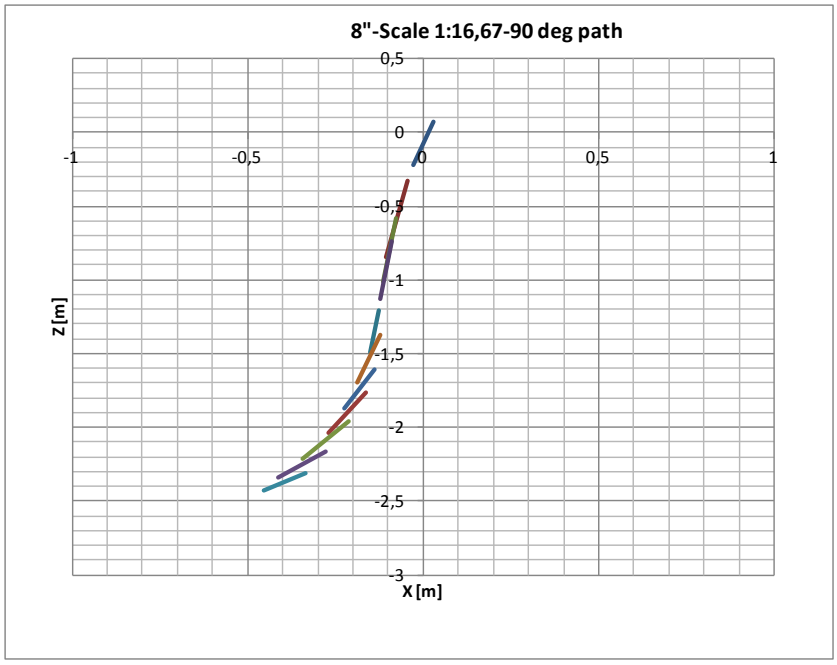

8'' Scale 1- 90^0 trajectory followed 3

PATH 7

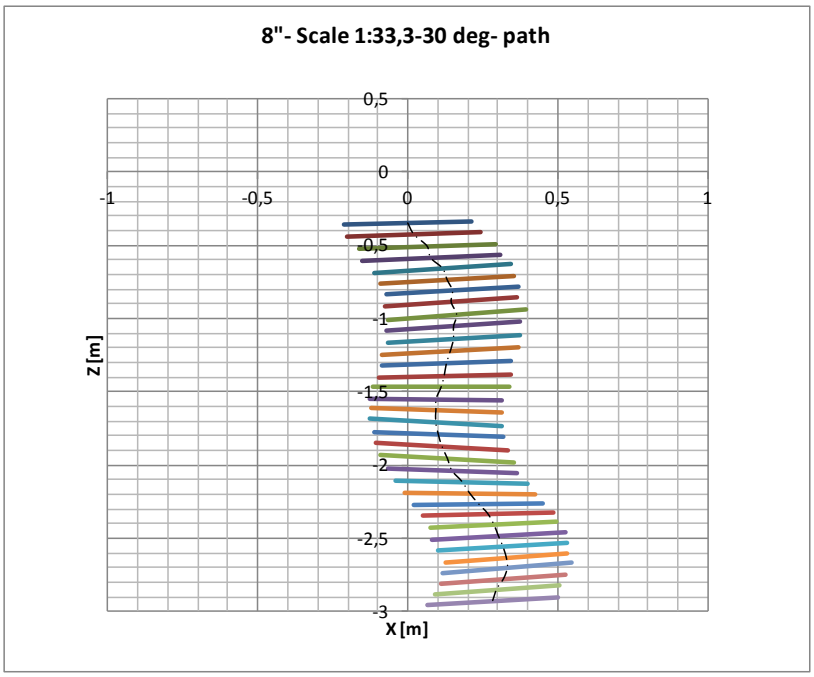

8'' Scale 2- 30^0 trajectory followed

PATH 8

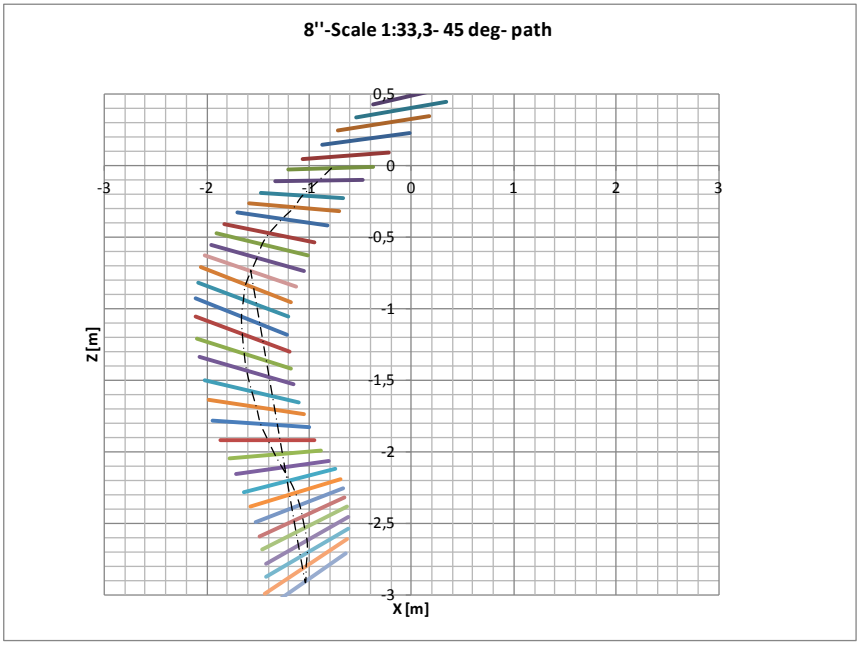

8'' Scale 2- 45^0 trajectory followed

PATH 9

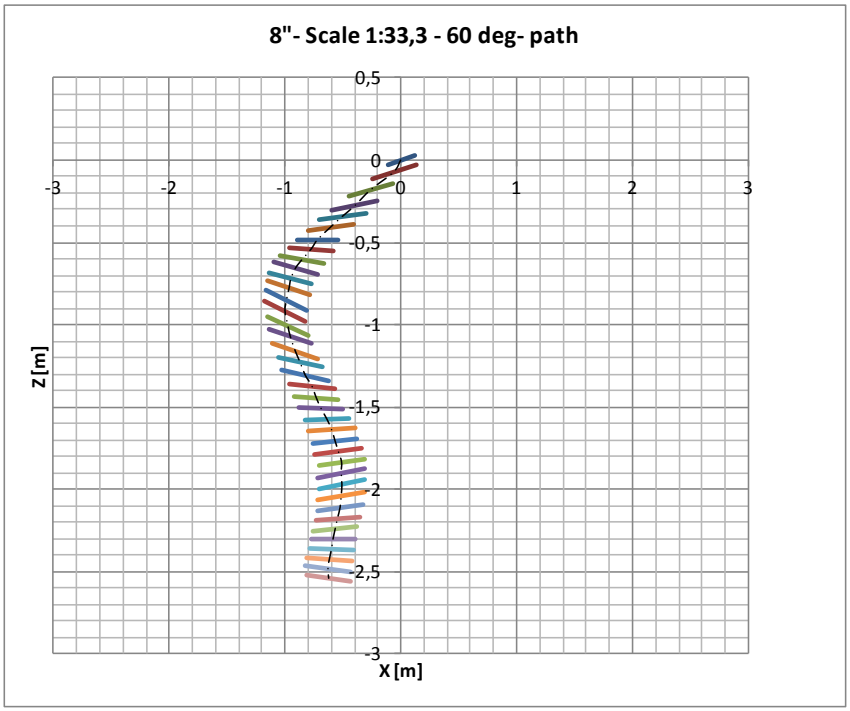

8'' Scale 2- 60^0 trajectory followed

PATH 10

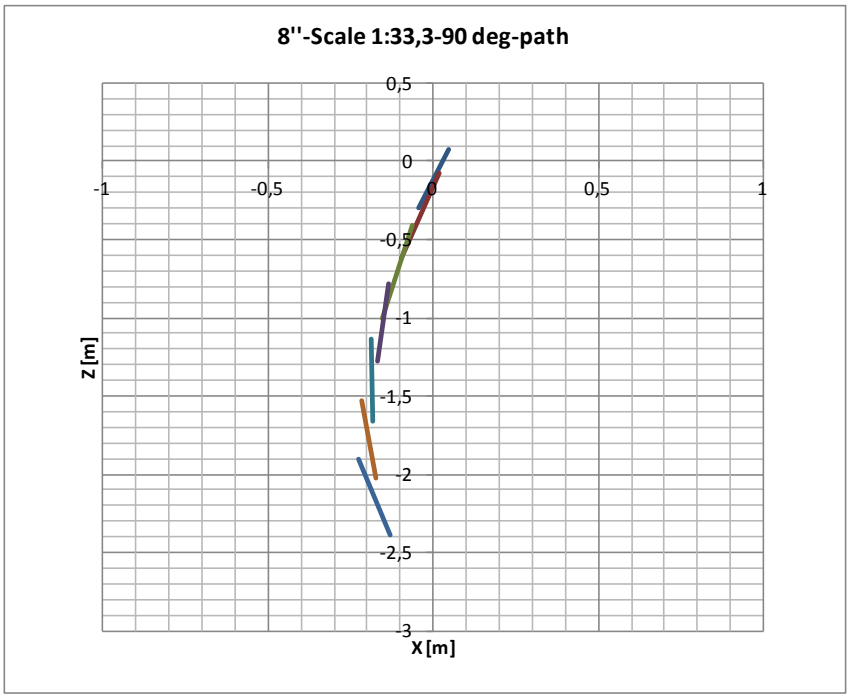

8'' Scale 2- 90^0 trajectory followed 1

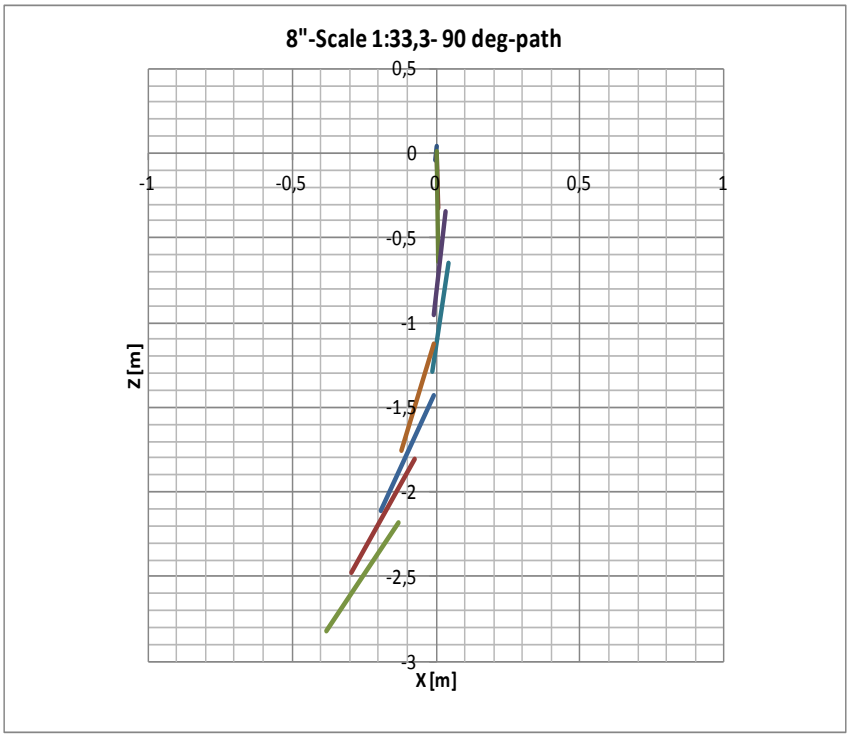

8'' Scale 2- 90^0 trajectory followed 2

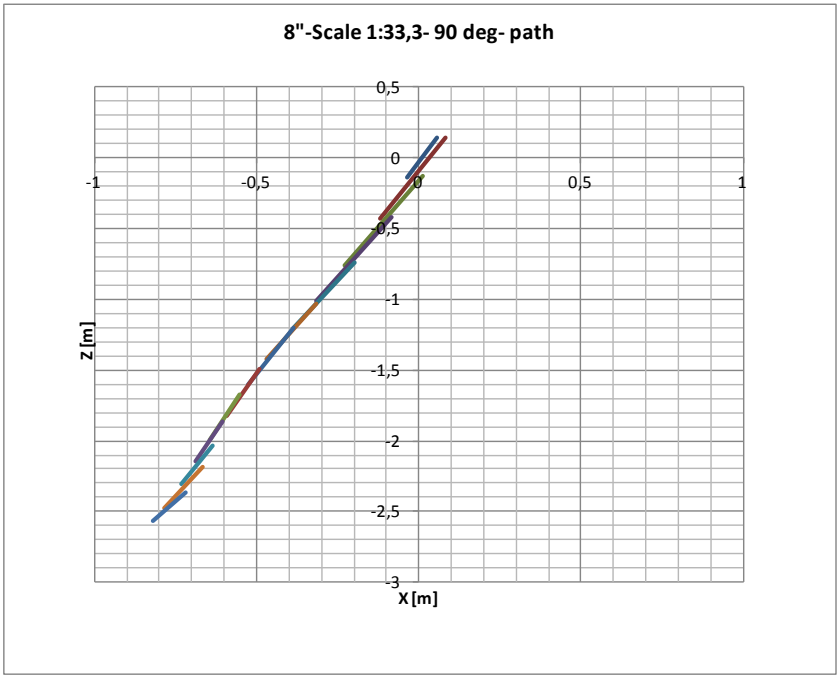

8'' Scale 2- 90^0 trajectory followed 3

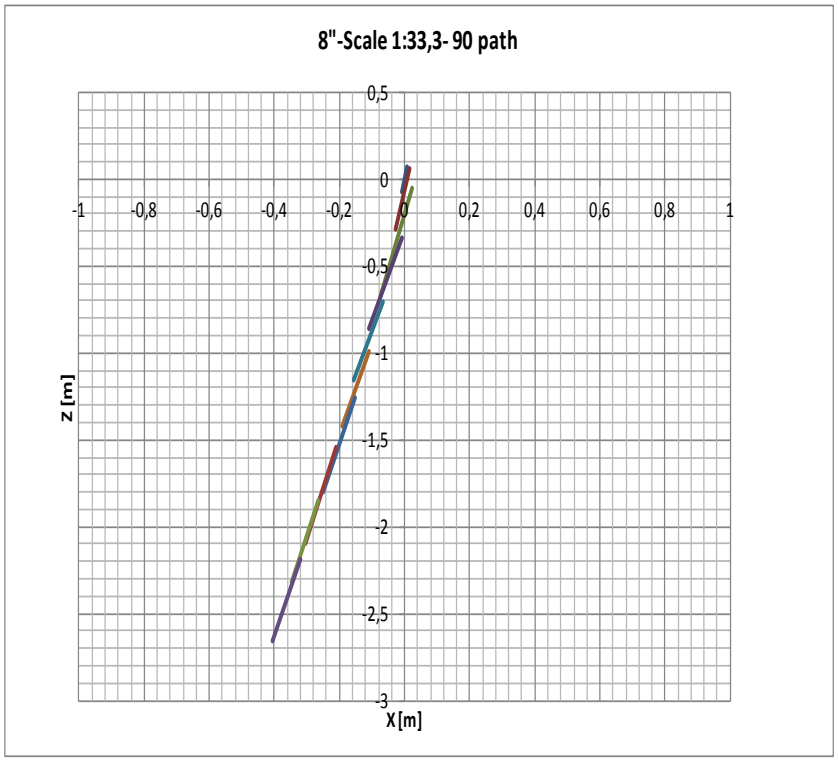

8'' Scale 2- 90^0 trajectory followed 4

TRAJECTORY 12 ''

PATH 11

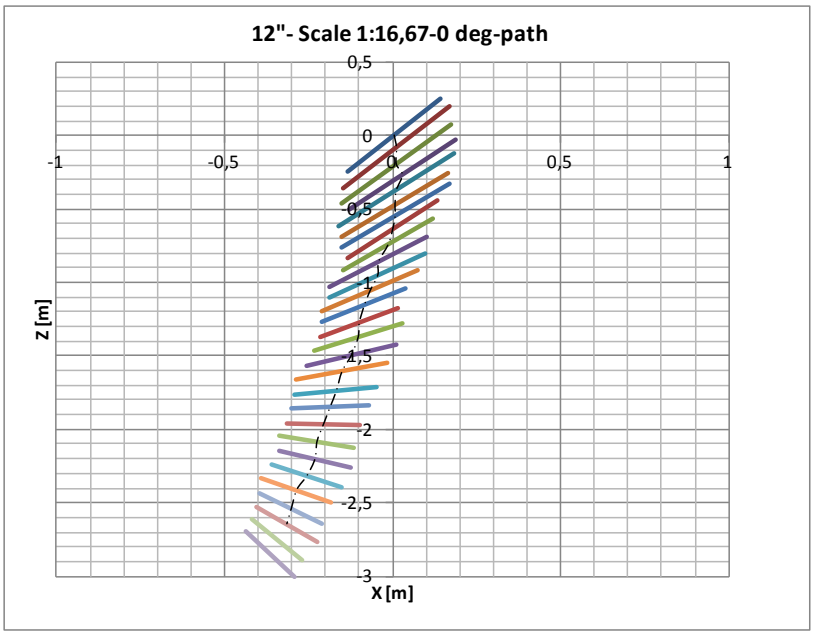

12" Scale 1 – 0^0 trajectory followed

PATH 12

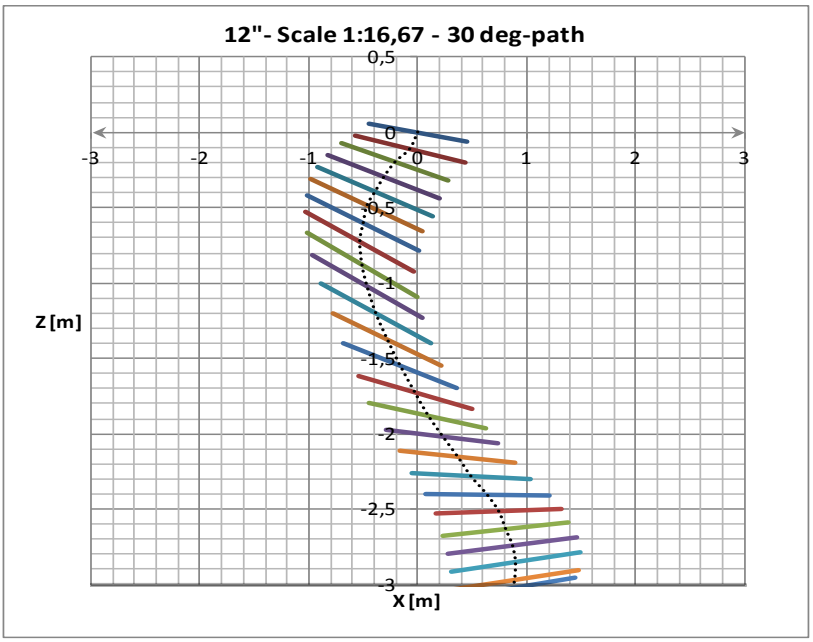

12" Scale 1 – 30^0 trajectory followed

PATH 13

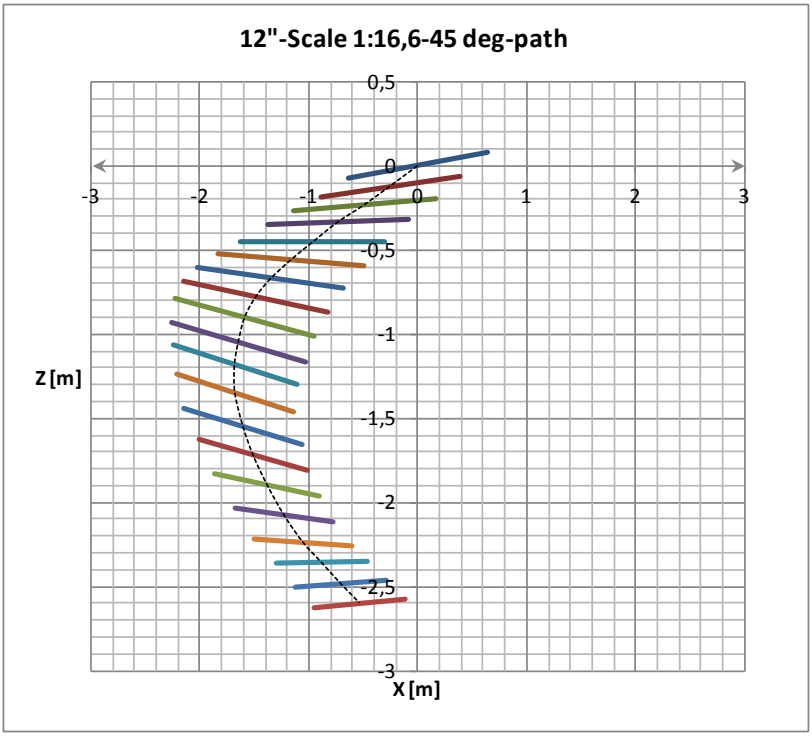

12" Scale 1 – 45^0 trajectory followed

PATH 14

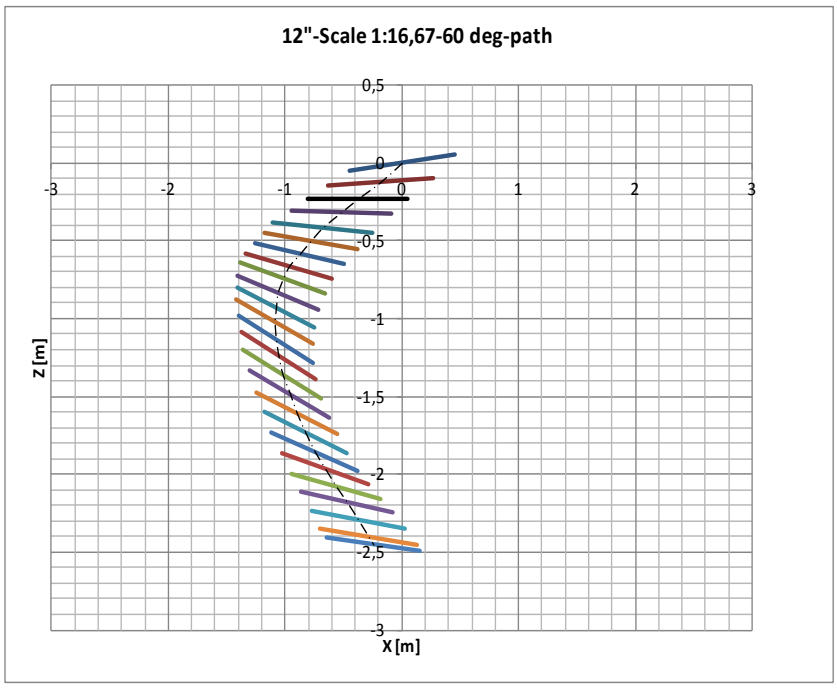

12" Scale 1 – 60^0 trajectory followed 1

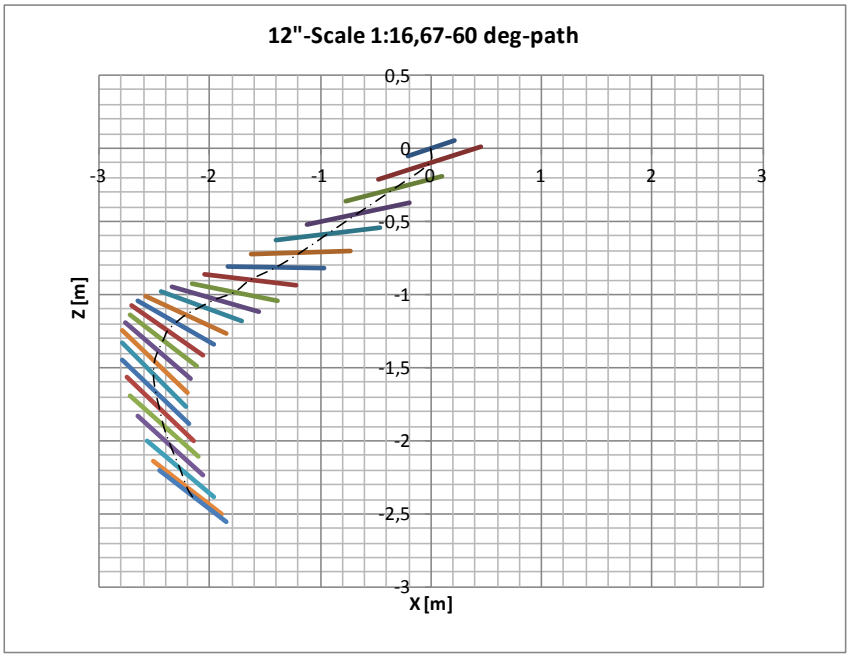

12” Scale 1 – 60^0 trajectory followed 2

PATH 15

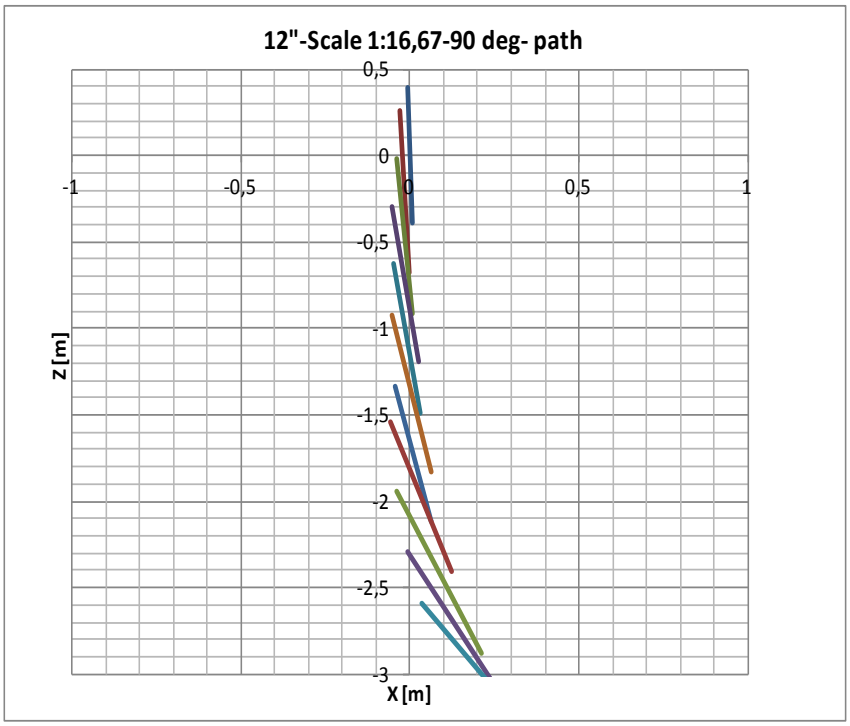

12” Scale 1 – 90^0 trajectory followed 1

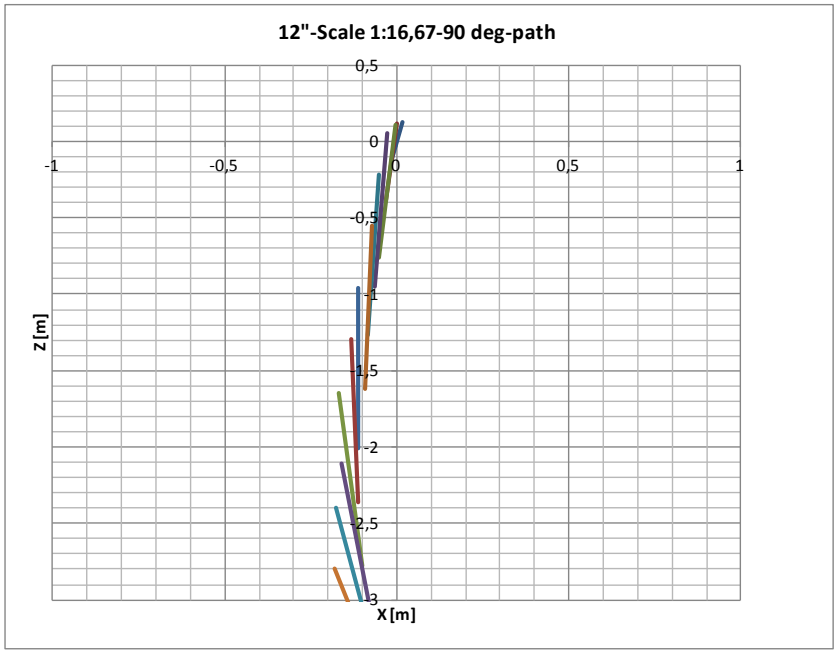

12" Scale 1 – 90^0 trajectory followed 2

PATH 16

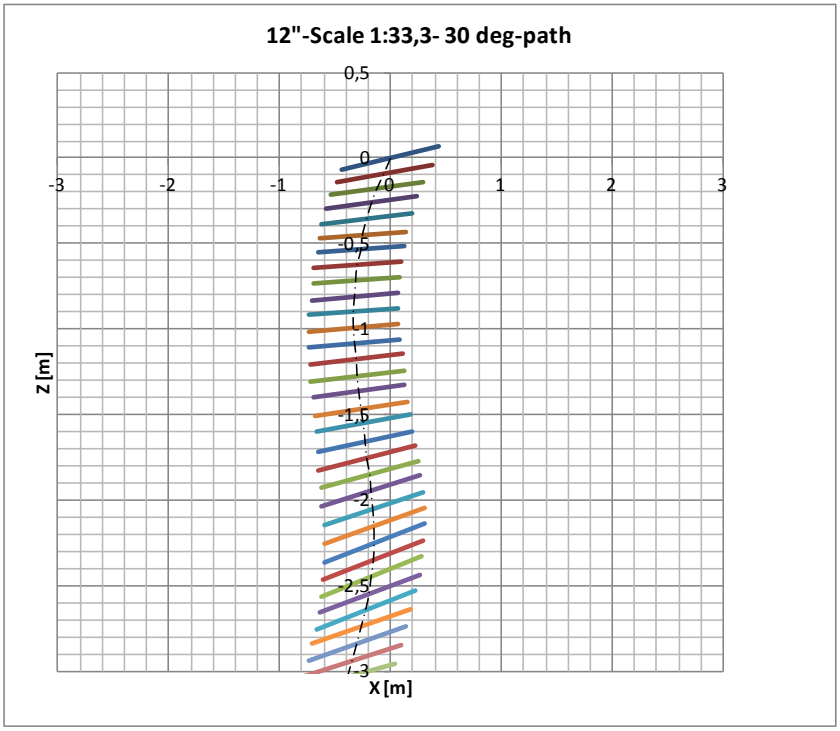

12" Scale 2 – 30^0 trajectory followed

PATH 17

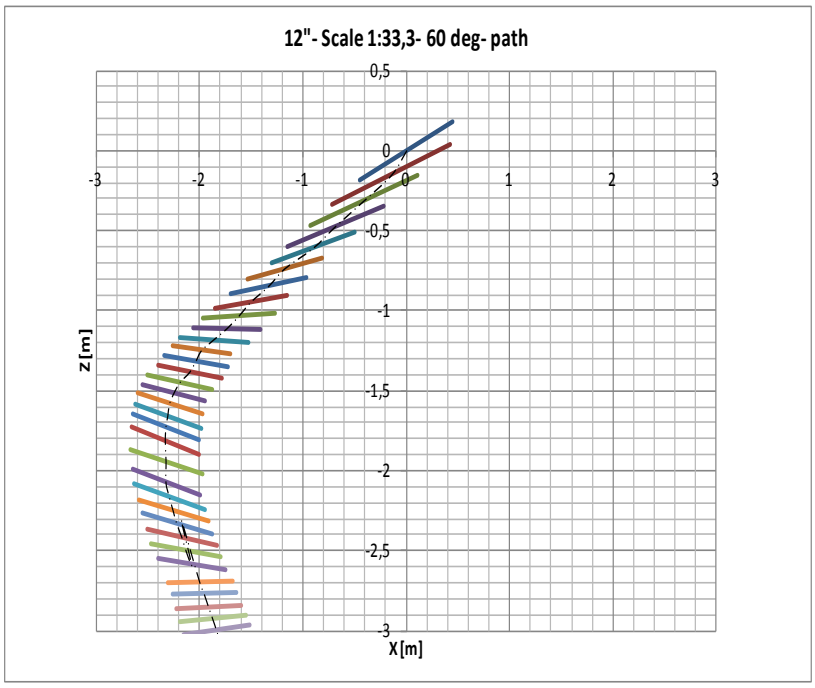

12” Scale 2 – 60^0 trajectory followed 1

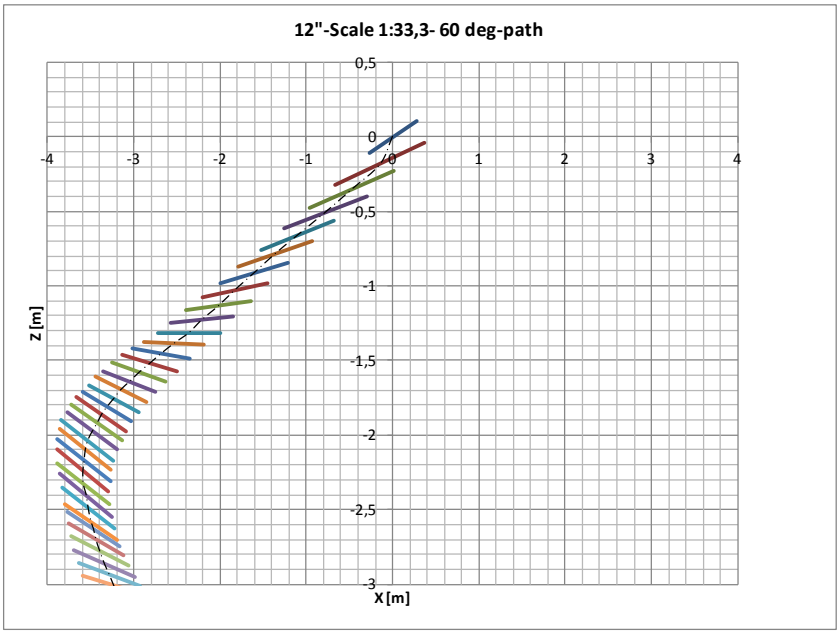

12” Scale 2 – 60^0 trajectory followed 2

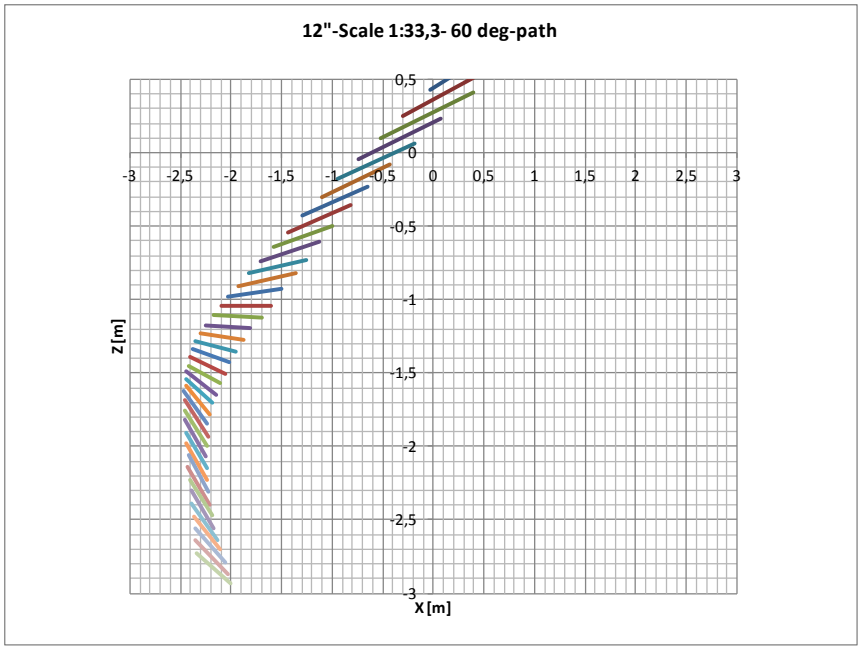

12” Scale 2 – 60^0 trajectory followed 3

PATH 18

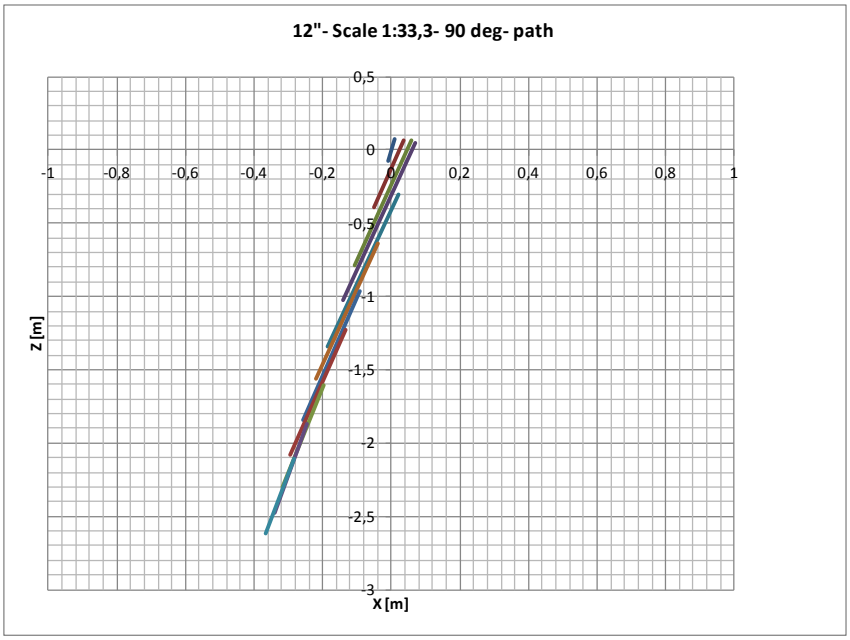

12” Scale 2 – 90^0 trajectory followed 1

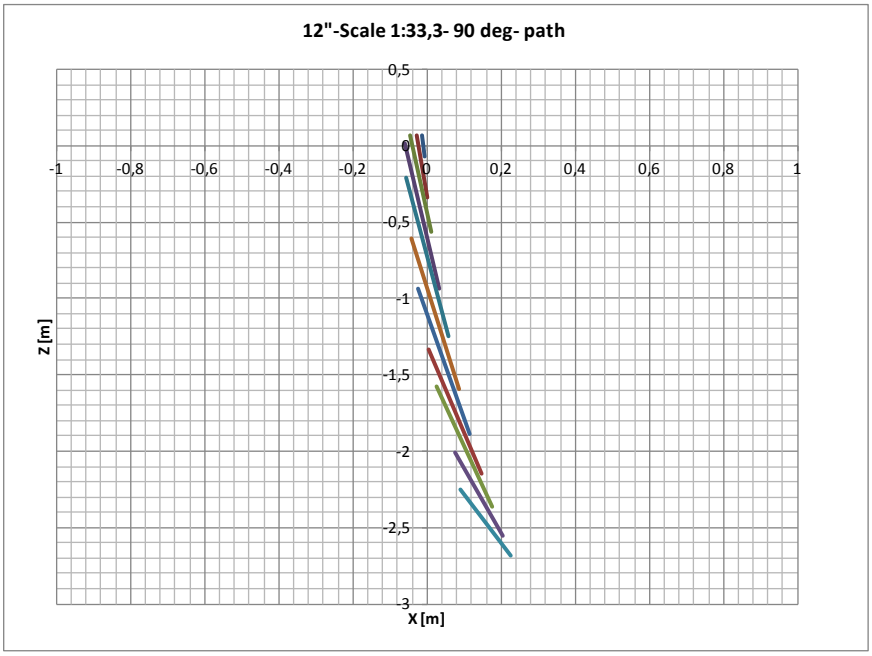

12” Scale 2 – 90^0 trajectory followed 2